Electromagnetic Compatibility

Principles and Applications

Second Edition, Revised and Expanded

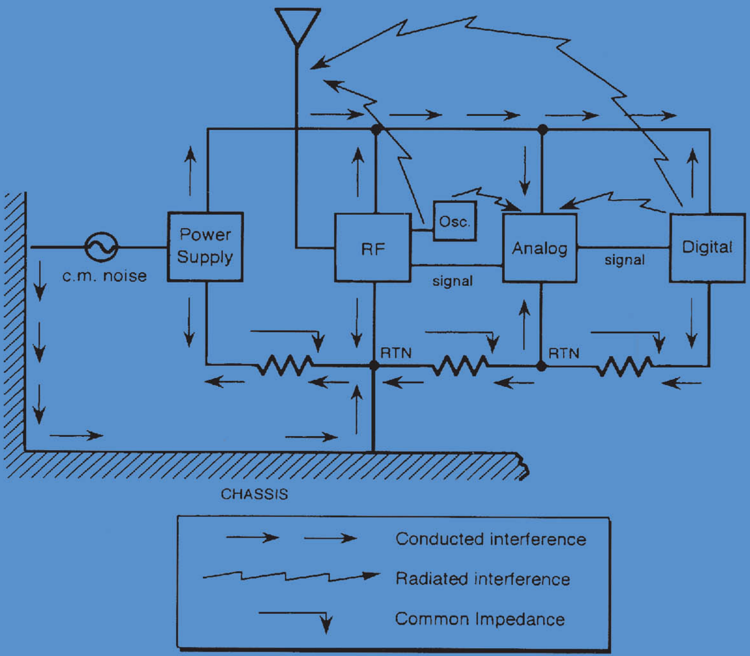

David A. Weston

Electromagnetic Compatibility

ELECTRICAL AND COMPUTER ENGINEERING

A Series of Reference Books and Textbooks

FOUNDING EDITOR

Marlin O. Thurston
Department of Electrical Engineering
The Ohio State University
Columbus, Ohio

1. Rational Fault Analysis, *edited by Richard Saeks and S. R. Liberty*
2. Nonparametric Methods in Communications, *edited by P. Papantoni-Kazakos and Dimitri Kazakos*
3. Interactive Pattern Recognition, *Yi-tzuu Chien*
4. Solid-State Electronics, *Lawrence E. Murr*
5. Electronic, Magnetic, and Thermal Properties of Solid Materials, *Klaus Schröder*
6. Magnetic-Bubble Memory Technology, *Hsu Chang*
7. Transformer and Inductor Design Handbook, *Colonel Wm. T. McLyman*
8. Electromagnetics: Classical and Modern Theory and Applications, *Samuel Seely and Alexander D. Poularikas*
9. One-Dimensional Digital Signal Processing, *Chi-Tsong Chen*
10. Interconnected Dynamical Systems, *Raymond A. DeCarlo and Richard Saeks*
11. Modern Digital Control Systems, *Raymond G. Jacquot*
12. Hybrid Circuit Design and Manufacture, *Roydn D. Jones*
13. Magnetic Core Selection for Transformers and Inductors: A User's Guide to Practice and Specification, *Colonel Wm. T. McLyman*
14. Static and Rotating Electromagnetic Devices, *Richard H. Engelmann*
15. Energy-Efficient Electric Motors: Selection and Application, *John C. Andreas*
16. Electromagnetic Compossibility, *Heinz M. Schlicke*
17. Electronics: Models, Analysis, and Systems, *James G. Gottling*
18. Digital Filter Design Handbook, *Fred J. Taylor*
19. Multivariable Control: An Introduction, *P. K. Sinha*
20. Flexible Circuits: Design and Applications, *Steve Gurley, with contributions by Carl A. Edstrom, Jr., Ray D. Greenway, and William P. Kelly*
21. Circuit Interruption: Theory and Techniques, *Thomas E. Browne, Jr.*
22. Switch Mode Power Conversion: Basic Theory and Design, *K. Kit Sum*
23. Pattern Recognition: Applications to Large Data-Set Problems, *Sing-Tze Bow*

24. Custom-Specific Integrated Circuits: Design and Fabrication, *Stanley L. Hurst*
25. Digital Circuits: Logic and Design, *Ronald C. Emery*
26. Large-Scale Control Systems: Theories and Techniques, *Magdi S. Mahmoud, Mohamed F. Hassan, and Mohamed G. Darwish*
27. Microprocessor Software Project Management, *Eli T. Fathi and Cedric V. W. Armstrong (Sponsored by Ontario Centre for Microelectronics)*
28. Low Frequency Electromagnetic Design, *Michael P. Perry*
29. Multidimensional Systems: Techniques and Applications, *edited by Spyros G. Tzafestas*
30. AC Motors for High-Performance Applications: Analysis and Control, *Sakae Yamamura*
31. Ceramic Motors for Electronics: Processing, Properties, and Applications, *edited by Relva C. Buchanan*
32. Microcomputer Bus Structures and Bus Interface Design, *Arthur L. Dexter*
33. End User's Guide to Innovative Flexible Circuit Packaging, *Jay J. Miniet*
34. Reliability Engineering for Electronic Design, *Norman B. Fuqua*
35. Design Fundamentals for Low-Voltage Distribution and Control, *Frank W. Kussy and Jack L. Warren*
36. Encapsulation of Electronic Devices and Components, *Edward R. Salmon*
37. Protective Relaying: Principles and Applications, *J. Lewis Blackburn*
38. Testing Active and Passive Electronic Components, *Richard F. Powell*
39. Adaptive Control Systems: Techniques and Applications, *V. V. Chalam*
40. Computer-Aided Analysis of Power Electronic Systems, *Venkatachari Rajagopalan*
41. Integrated Circuit Quality and Reliability, *Eugene R. Hnatek*
42. Systolic Signal Processing Systems, *edited by Earl E. Swartzlander, Jr.*
43. Adaptive Digital Filters and Signal Analysis, *Maurice G. Bellanger*
44. Electronic Ceramics: Properties, Configuration, and Applications, *edited by Lionel M. Levinson*
45. Computer Systems Engineering Management, *Robert S. Alford*
46. Systems Modeling and Computer Simulation, *edited by Naim A. Kheir*
47. Rigid-Flex Printed Wiring Design for Production Readiness, *Walter S. Rigling*
48. Analog Methods for Computer-Aided Circuit Analysis and Diagnosis, *edited by Takao Ozawa*
49. Transformer and Inductor Design Handbook: Second Edition, Revised and Expanded, *Colonel Wm. T. McLyman*
50. Power System Grounding and Transients: An Introduction, *A. P. Sakis Meliopoulos*
51. Signal Processing Handbook, *edited by C. H. Chen*
52. Electronic Product Design for Automated Manufacturing, *H. Richard Stillwell*
53. Dynamic Models and Discrete Event Simulation, *William Delaney and Erminia Vaccari*
54. FET Technology and Application: An Introduction, *Edwin S. Oxner*

55. Digital Speech Processing, Synthesis, and Recognition, *Sadaoki Furui*
56. VLSI RISC Architecture and Organization, *Stephen B. Furber*
57. Surface Mount and Related Technologies, *Gerald Ginsberg*
58. Uninterruptible Power Supplies: Power Conditioners for Critical Equipment, *David C. Griffith*
59. Polyphase Induction Motors: Analysis, Design, and Application, *Paul L. Cochran*
60. Battery Technology Handbook, *edited by H. A. Kiehne*
61. Network Modeling, Simulation, and Analysis, *edited by Ricardo F. Garzia and Mario R. Garzia*
62. Linear Circuits, Systems, and Signal Processing: Advanced Theory and Applications, *edited by Nobuo Nagai*
63. High-Voltage Engineering: Theory and Practice, *edited by M. Khalifa*
64. Large-Scale Systems Control and Decision Making, *edited by Hiroyuki Tamura and Tsuneo Yoshikawa*
65. Industrial Power Distribution and Illuminating Systems, *Kao Chen*
66. Distributed Computer Control for Industrial Automation, *Dobrivoje Popovic and Vijay P. Bhatkar*
67. Computer-Aided Analysis of Active Circuits, *Adrian Ioinovici*
68. Designing with Analog Switches, *Steve Moore*
69. Contamination Effects on Electronic Products, *Carl J. Tautscher*
70. Computer-Operated Systems Control, *Magdi S. Mahmoud*
71. Integrated Microwave Circuits, *edited by Yoshihiro Konishi*
72. Ceramic Materials for Electronics: Processing, Properties, and Applications, Second Edition, Revised and Expanded, *edited by Relva C. Buchanan*
73. Electromagnetic Compatibility: Principles and Applications, *David A. Weston*
74. Intelligent Robotic Systems, *edited by Spyros G. Tzafestas*
75. Switching Phenomena in High-Voltage Circuit Breakers, *edited by Kunio Nakanishi*
76. Advances in Speech Signal Processing, *edited by Sadaoki Furui and M. Mohan Sondhi*
77. Pattern Recognition and Image Preprocessing, *Sing-Tze Bow*
78. Energy-Efficient Electric Motors: Selection and Application, Second Edition, *John C. Andreas*
79. Stochastic Large-Scale Engineering Systems, *edited by Spyros G. Tzafestas and Keigo Watanabe*
80. Two-Dimensional Digital Filters, *Wu-Sheng Lu and Andreas Antoniou*
81. Computer-Aided Analysis and Design of Switch-Mode Power Supplies, *Yim-Shu Lee*
82. Placement and Routing of Electronic Modules, *edited by Michael Pecht*
83. Applied Control: Current Trends and Modern Methodologies, *edited by Spyros G. Tzafestas*
84. Algorithms for Computer-Aided Design of Multivariable Control Systems, *Stanoje Bingulac and Hugh F. VanLandingham*
85. Symmetrical Components for Power Systems Engineering, *J. Lewis Blackburn*
86. Advanced Digital Signal Processing: Theory and Applications, *Glenn Zelniker and Fred J. Taylor*

87. Neural Networks and Simulation Methods, *Jian-Kang Wu*
88. Power Distribution Engineering: Fundamentals and Applications, *James J. Burke*
89. Modern Digital Control Systems: Second Edition, *Raymond G. Jacquot*
90. Adaptive IIR Filtering in Signal Processing and Control, *Phillip A. Regalia*
91. Integrated Circuit Quality and Reliability: Second Edition, Revised and Expanded, *Eugene R. Hnatek*
92. Handbook of Electric Motors, *edited by Richard H. Engelmann and William H. Middendorf*
93. Power-Switching Converters, *Simon S. Ang*
94. Systems Modeling and Computer Simulation: Second Edition, *Naim A. Kheir*
95. EMI Filter Design, *Richard Lee Ozenbaugh*
96. Power Hybrid Circuit Design and Manufacture, *Haim Taraseiskey*
97. Robust Control System Design: Advanced State Space Techniques, *Chia-Chi Tsui*
98. Spatial Electric Load Forecasting, *H. Lee Willis*
99. Permanent Magnet Motor Technology: Design and Applications, *Jacek F. Gieras and Mitchell Wing*
100. High Voltage Circuit Breakers: Design and Applications, *Ruben D. Garzon*
101. Integrating Electrical Heating Elements in Appliance Design, *Thor Hegbom*
102. Magnetic Core Selection for Transformers and Inductors: A User's Guide to Practice and Specification, Second Edition, *Colonel Wm. T. McLyman*
103. Statistical Methods in Control and Signal Processing, *edited by Tohru Katayama and Sueo Sugimoto*
104. Radio Receiver Design, *Robert C. Dixon*
105. Electrical Contacts: Principles and Applications, *edited by Paul G. Slade*
106. Handbook of Electrical Engineering Calculations, *edited by Arun G. Phadke*
107. Reliability Control for Electronic Systems, *Donald J. LaCombe*
108. Embedded Systems Design with 8051 Microcontrollers: Hardware and Software, *Zdravko Karakehayov, Knud Smed Christensen, and Ole Winther*
109. Pilot Protective Relaying, *edited by Walter A. Elmore*
110. High-Voltage Engineering: Theory and Practice, Second Edition, Revised and Expanded, *Mazen Abdel-Salam, Hussein Anis, Ahdab El-Morshedy, and Roshdy Radwan*
111. EMI Filter Design: Second Edition, Revised and Expanded, *Richard Lee Ozenbaugh*
112. Electromagnetic Compatibility: Principles and Applications, Second Edition, Revised and Expanded, *David A. Weston*

Additional Volumes in Preparation

Electromagnetic Compatibility

Principles and Applications

Second Edition, Revised and Expanded

David A. Weston
EMC Consulting Inc.
Merrickville, Ontario, Canada

MARCEL DEKKER, INC. NEW YORK • BASEL

Library of Congress Cataloging-in-Publication Data

Weston, David A.
Electromagnetic compatibility : principles and applications / David A. Weston.—2nd ed., rev. and expanded.
p. cm.—(Electrical and computer engineering ; 112)
Includes bibliographical references and index.
ISBN 0-8247-8889-3 (alk. paper)
1. Electromagnetic compatibility. 2. Electronic apparatus and appliances—Design and construction. I. Title. II. Electrical engineering and electronics ; 112.

TK7867.2.W46 2000
621.382'24—dc21

00-047591

This book is printed on acid-free paper.

Headquarters
Marcel Dekker, Inc.
270 Madison Avenue, New York, NY 10016
tel: 212-696-9000; fax: 212-685-4540

Eastern Hemisphere Distribution
Marcel Dekker AG
Hutgasse 4, Postfach 812, CH-4001 Basel, Switzerland
tel: 41-61-261-8482; fax: 41-61-261-8896

World Wide Web
http://www.dekker.com

The publisher offers discounts on this book when ordered in bulk quantities. For more information, write to Special Sales/Professional Marketing at the headquarters address above.

Current printing (last digit):
10 9 8 7 6 5 4 3

PRINTED IN THE UNITED STATES OF AMERICA

Preface

This second, revised and updated, edition of the book contains approximately 65% more information than the first edition. This includes a review of computer modeling programs, a new chapter on PCB layout, and additional commercial and military EMI test methods. New data on cable radiation and coupling to cables is included, extending out to 12 GHz, and on EMI enclosure shielding.

All electronic and electrical equipment is a potential source of electromagnetic interference (EMI). Similarly, such equipment will not function as designed at some level of electromagnetic ambient. The problems associated with EMI can range from simple annoyance (e.g., static on telecommunications equipment or increased bit error rates on digital equipment) to catastrophe (e.g., inadvertent detonation of explosive devices).

Electromagnetic compatibility (EMC) can be achieved by evaluating the electromagnetic environment (often characterized by standards or requirements) to which equipment/systems is exposed and then designing and building equipment/systems to function correctly in the operational environment without itself creating EMI.

This book is written for the design/systems engineer, technologist, technician, or engineering manager who designs, maintains, or specifies equipment either to meet an electromagnetic compatibility requirement specification or to function safely in a given electromagnetic environment.

Many engineers do not have, or need, radio frequency (RF) experience. However, in operation, digital control or switching power equipment functions as an RF system. Therefore, an understanding of the high-frequency characteristics of components, simple radiators, and wave theory is imperative in achieving an understanding of EMC.

One aim of the book is to teach EMI prediction and enable the reader to build EMC into equipment and systems without overdesign. By achieving EMC, the designer averts the program delay and additional cost of fixing EMI after the equipment is built. With the recognition that EMI problems exist, we present EMI diagnostic techniques and cost effective solutions with practical implementation and options.

The book discusses typical sources of EMI and characteristics of the radiated and conducted emissions that might be expected in a given electromagnetic environment and reviews ways of decreasing electromagnetic emissions as well as the susceptibility of equipment to EMI. Some books on EMI/EMC contain equations that are theoretically sound but may not be useful in practical EMI/EMC problems. All equations in this book have been found to be invaluable in EMI prediction and EMC design. In most instances, theory is substantiated by measured data, and where anomalies exist most probable reasons are offered. Where the reader may wish to pursue a given subject area further, numerous references are provided. Worked examples of the equations are given in predictions and case studies throughout the book. Physical geometry and frequency limitations exist in the application of all wave or circuit theory, including the effect of parasitic components, and these limits are discussed.

The apparent anomalies that have given EMC a reputation for "black magic" are explained. For example, the case where the addition of shielding, a filter, or grounding increases either the level of EMI emissions or the susceptibility during EMC tests is examined. The major reason these results are apparently inexplicable is that the underlying theory is not well understood. The approach used in the book is to provide an understanding of the theory with an emphasis on its applicability in the practical realization of EMC design and EMI solutions, including implementation and maintenance.

The intent is that information contained herein have a practical application or be required for an understanding of the principles of EMC. For example, calculated or published data on attenuation or shielding effectiveness is of little use unless its application is explained. Therefore, it must be used in conjunction with the worst-case levels of radiated or conducted noise that may be expected in a given environment. Any practical limitation on the achievable attenuation or shielding must then be accounted for, after which the noise levels applied to the system or circuit and its immunity may be predicted. The aim has been to avoid the overly simplistic cookbook approach with its inherent errors, and yet to limit the mathematics to that used by the practicing engineer or technician.

Simple measurement techniques that are possible with standard electronic measurement equipment are described. These are useful for EMI diagnostic measurements as well as a "quick look" at equipment that must meet EMC requirements such as the commercial FCC, DO-160, VCE, and EN, and the military/aerospace MIL-STD-461. Also, the correct measurement techniques and possible errors encountered using more sophisticated equipment required for certification and qualification EMC testing are introduced.

The book is based on experience gained in EMC consulting and on the course notes of one- to four-day EMC seminars presented over a 12-year period. Many questions posed by attendees of the seminars and clients have been answered in this book.

I am very grateful to David Viljoen, who made a significant contribution to the preparation of the contents of the first edition of the book (i.e., the layout of the book, drafting the majority of the figures, editing Chapters 1 to 5, and writing the computer programs). Without the attention to detail, hard work, and high-quality effort of Mr. Viljoen, this book would not have been possible in its present form.

I am also indebted to the late Mr. Jabez Whelpton, of Canadian Astronautics Ltd., who was of great assistance in reading and correcting the content of those chapters that contain information on wave theory and antennas.

For the second edition of the book I wish to thank Mr. Chris Ceelen, who made many of the additional EMI measurements, and Ms. Lianne Boulet, who helped prepare the text and figures.

Finally, I wish to thank the organizations specifically acknowledged beneath figures and in the text, especially the Canadian Space Agency.

David A. Weston

Contents

Electromagnetic Compatibility

1
Introduction to EMI and the Electromagnetic Environment

1.1 INTRODUCTION TO ELECTROMAGNETIC INTERFERENCE (EMI)

This chapter introduces a few of the important coupling modes involved in electromagnetic interference (EMI) as well as some EMI regulations. Both of these topics will be addressed in more detail in subsequent chapters. In addition, this chapter presents data on average and worst-case electromagnetic emissions found in the environment. This data is useful in evaluating the severity of a given electromagnetic environment and in predicting electromagnetic compatibility (EMC) for equipment operated in these environments.

1.1.1 Effects of Electromagnetic Interference

The effects of EMI are extremely variable in character and magnitude, ranging from simple annoyance to catastrophe. Some examples of the potential effects of EMI are

- Interference to television and radio reception
- Loss of data in digital systems or in transmission of data
- Delays in production of equipment exhibiting intraunit, subsystem, or system-level EMI
- Malfunction of medical electronic equipment (e.g., neonatal monitor, heart pacemaker)
- Malfunction of automotive microprocessor control systems (e.g., braking or truck anti-jackknife systems)
- Malfunction of navigation equipment
- Inadvertent detonation of explosive devices
- Malfunction of critical process-control functions (e.g., oil or chemical industry)

To correct EMI problems that occur after equipment is designed and in production is usually expensive and results in program delays, which may adversely affect the acceptance of a new product. It is preferable to follow good EMC engineering practice during the equipment design and development phases. Our goal should be to produce equipment capable of functioning in the predicted or specified electromagnetic environment and that does not interfere with other equipment or unduly pollute the environment—that is, to achieve EMC.

The techniques of EMC prediction described in subsequent chapters will aid in meeting the goal of EMC when applied at the design stage. These same techniques of analysis and modeling are applicable to EMI control and problem solving or in the location of out-of-specification emissions. It is in the area of emission reduction where analysis is most likely to be supplemented by measurement and diagnostic intervention. However, the value of simple EMI

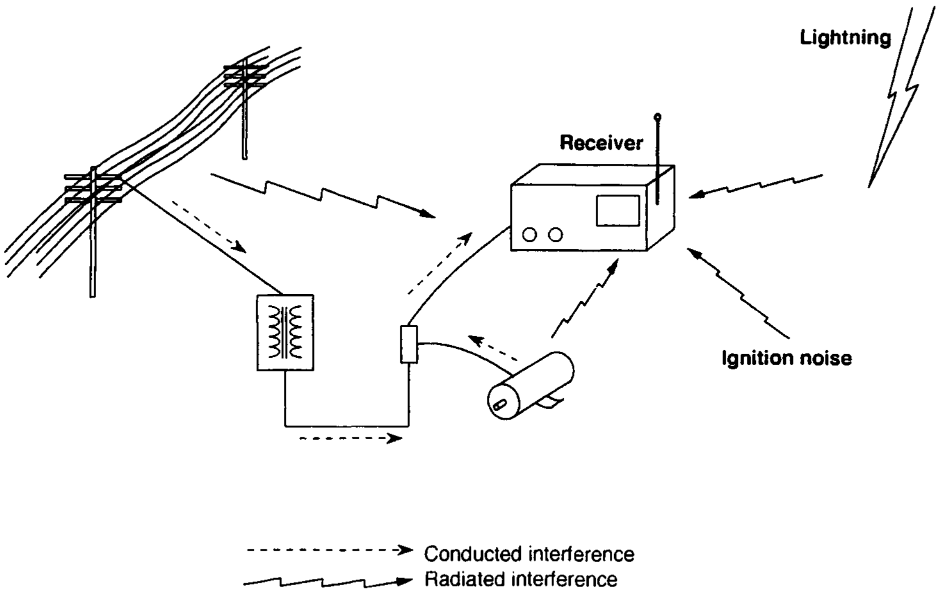

Figure 1.1 Possible sources of ambient noise and how they may be coupled into a receiver.

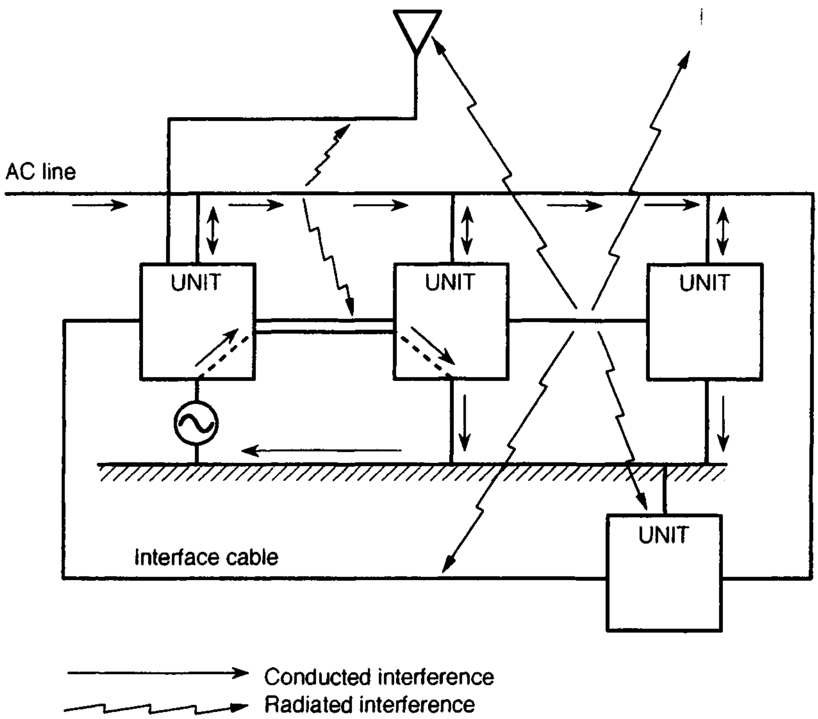

Figure 1.2 Some of the possible interference coupling modes within a system.

measurements made as early as feasible in the design, breadboard, and prototype phases cannot be emphasized enough.

1.1.2 Electromagnetic Interference Coupling Modes

For EMI to exist there must be a source of emission, a path for the coupling of the emission, and a circuit, unit, or system sensitive to the received noise. Figures 1.1–1.3 illustrate that two modes of coupling, radiated and conducted, can exist. In the near field, the radiated coupling may be either a predominantly magnetic (H) field coupling or an electric (E) field coupling, whereas the coupling in the far field will be via electromagnetic waves exhibiting a fixed ratio of the E to H field strengths. A more rigorous definition of near and far field is presented in Section 2.2.1. Suffice it to say here that the near field is in close proximity to a source and the far field is beyond some determined distance from the source.

For circuits and conductors in close proximity we consider the coupling, or crosstalk, to be via mutual inductance and intercircuit capacitance, although one of these modes usually predominates. The source of noise may be power lines, signal lines, logic (especially clocks and data lines), or current-carrying ground connections. The conducted path may be resistive or contain inductance or capacitance, intentional or otherwise, and it is often a combination of these. The reactive components often result in resonances, with their concomitant increase or decrease in current at the resonant frequencies.

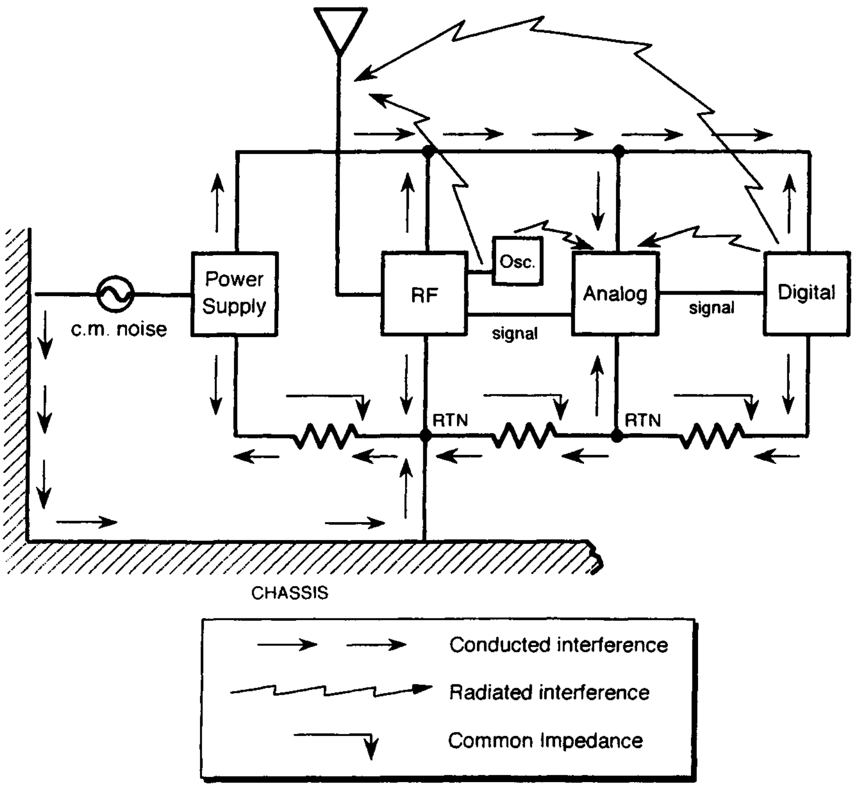

Figure 1.3 A few of the intraequipment (unit) coupling modes.

1.2 INTRODUCTION TO ELECTROMAGNETIC INTERFERENCE REGULATIONS

The level of immunity built into equipment depends on how critical the correct functioning of the equipment is and on the electromagnetic environment in which it is designed to operate. Many EMI requirements take the criticality and environment into account by classifying equipment and by imposing different susceptibility test levels on the different classes.

EMI can be considered a form of environmental pollution; in order to reduce the impact of this pollution, some control on the environmental level of conducted and radiated emissions of noise is necessary.

Many countries impose commercial regulations on the emissions from data-processing equipment; industrial, scientific, and medical (ISM) equipment; vehicles; appliances; etc. In some instances standards are developed by a nongovernmental agency, such as the Society of Automotive Engineers (SAE), and are not necessarily mandatory. The majority of military regulations and standards, and some commercial specifications, also require that equipment be demonstrated immune to susceptibility test levels.

Chapter 9 describes the typical EMI regulations and requirements and EMI measurement techniques.

1.2.1 Military Regulations

The options are limited for manufacturers of equipment that must meet specified requirements. The military requirements are intended to be tailored to the specific electromagnetic environment by the procuring agency; however, this is seldom implemented. Should equipment fail specified military requirements and, after analysis or measurement, the environment be found more benign than the specified levels indicate, then the possibility exists for the procuring agency to grant a waiver on the specification limit. A more satisfactory approach is to specify realistic limits in the first place. The difficulty here is that the requirements are location dependent. That is, the proximity of equipment to transmitting antennas or other equipment or the number of units connected to the same power supply varies from case to case. Where equipment is intended for operation in a known location, the limits may be readily tailored to the environment.

1.2.2 Commercial Regulations

The manufacturers of equipment that must meet commercial requirements are seldom if ever awarded a waiver, and the limits are inflexible. To date only the countries of the European Union (EU) require immunity testing. Some manufacturers who want to market in non-EU countries may consider this an advantage until the equipment is found to be susceptible in a typical environment.

1.2.3 Unregulated Equipment

For the manufacturers of equipment to which no regulations apply but who want to achieve EMC either for the sake of customer satisfaction or safety or to minimize the risk of a lawsuit, the choice is either to design for a realistic worst-case environment or to define the environment with an existing EMI standard. We define a realistic worst case as either a measured maximum environment in a large sample of similar environments or a predicted maximum where all the mitigating factors have been considered.

In an ideal world, specified limits would be close to the realistic worst-case environment, whereas, as we shall see in Section 1.3, this is not always true.

1.3 ELECTROMAGNETIC ENVIRONMENT

The information in this section is intended to provide a comparison of the various worst-case environments and to provide guidelines to equipment designers and those writing procurement specifications.

Sources of EMI can be divided into natural and manmade, with, in most cases, the natural sources of radiation present at a much lower level than the manmade. The majority of unintentional emissions occupy a wide range of frequencies, which we may call *broadband* in a nonstrict sense of the term. Intentional emissions, such as radio and television transmissions, are termed *narrowband* and in the strictest sense of the term are emissions that occur at a single frequency or are accompanied by a few frequencies at the sidebands. The strict definitions of narrowband and broadband, as used in EMI measurements, and addressed in Chapter 9, are dependent on both receiver bandwidth and the pulse repetition rate of the source.

Electric field strength is measured in volts/m, as described in Section 2.1. Another unit of measurement is the dBμV/m. The unit of broadband field strength as used in military standards is dBμV/m/MHz. Here the reference bandwidth of 1 MHz is included in the unit. Another unit is the dBμV/m/kHz, where the reference bandwidth is 1 kHz.

For the sake of comparison to other sources of broadband noise, we will arbitrarily use the military MIL-STD 461 RE02 limit for broadband emission from equipment measured at a distance of 1 meter from the source. Figure 1.4 is a reproduction of the RE02 limit for spacecraft. The RE02 limit is more stringent than commercial limits on broadband noise. For example, the West German Commercial Regulation contained in VDE 0875 for broadband limits, when scaled to a 1-meter measuring distance and converted to the 1-MHz reference bandwidth, imposes a limit of 78.5 dBμV/m/MHz from 30 to 300 MHz. This limit is 13.5 dB above RE02 at 200 MHz and 4 dB and 8.5 dB above at 30 MHz and 300 MHz, respectively. These limits are presented in greater detail in Section 9.4.

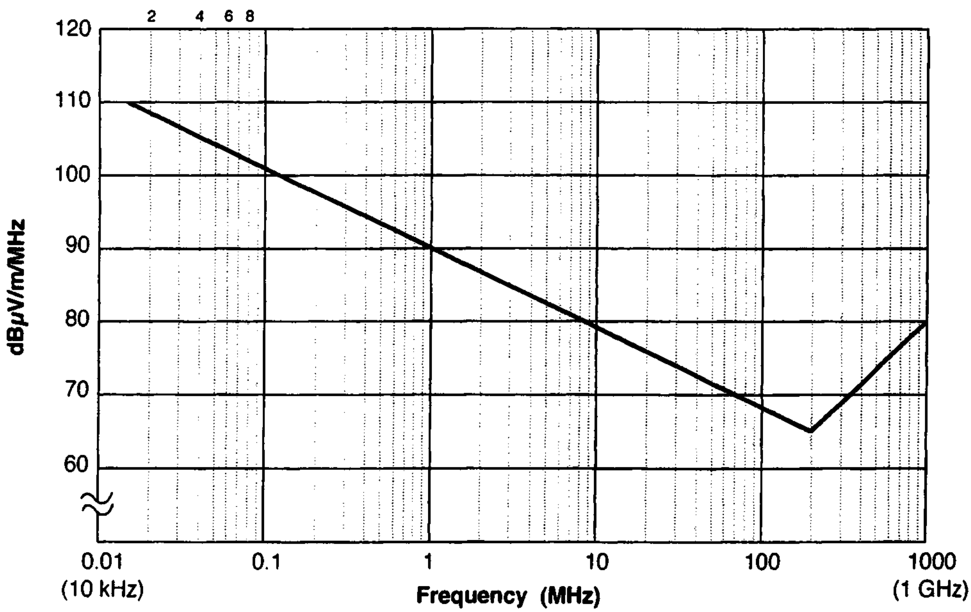

Figure 1.4 RE02 broadband emission limits for spacecraft.

The remainder of this chapter deals with radiated and conducted components of the electromagnetic environment. The radiated electromagnetic environment is treated in Sections 1.3.1–1.3.3 and the conducted electromagnetic environment in Section 1.3.4.

1.3.1 Natural Sources of Electromagnetic Noise

Natural sources of electromagnetic noise are

- Atmospheric noise produced by electrical discharges occurring during thunderstorms
- Cosmic noise from the Sun, Moon, stars, planets, and galaxy

Atmospheric noise is produced predominantly by local thunderstorms in the summer and by tropical-region thunderstorms in the winter. The electromagnetic emissions from thunderstorms are propagated over distances of several thousand kilometers by an ionospheric skywave, and thus potential EMI effects are not localized. In the time domain, atmospheric noise is complex, but it may be characterized by large spikes on a background of short random pulses or smaller pulses on a higher continuous background.

Upper and lower limits for atmospheric radio noise displayed in the frequency domain are shown in Figure 1.5(D), ranging in level from a maximum of 108 dBμV (0.25 V)/m/MHz

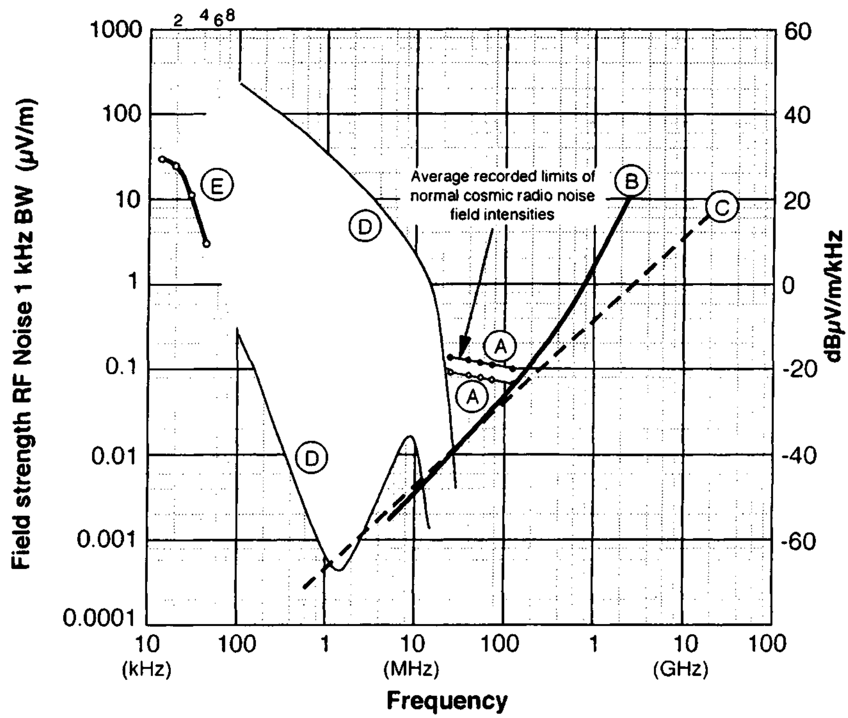

A Average daily upper and lower limits of normal cosmic radio noise field intensities
B Noise field intensities corresponding to internal noise of well-designed receiver
C Noise field intensities (in one plane of polarization) produced by "black-body" radiation at 300 K
D Upper and lower limits of atmosphere noise intensities (Nat. Bureau of Standards Circ. No. 462) Also radio propagation unit report RPU-5.
E Atmospheric radio noise intensities measured in the Arctic

Figure 1.5 Atmospheric, cosmic, and thermal noise levels. (From Ref. 2.)

to a minimum of −6 dBμV (0.5 μV)/m/MHz at 100 kHz. Figure 1.5(E) also plots the atmospheric noise measured in the Arctic, which describes a yearly variation of approximately 7 dB as well as a systematic daily and seasonal variation. From measurements in Canada, the daily and seasonal variation is from 91 dBμV/m/MHz to 106 dBμV/m/MHz. Compared to our arbitrarily chosen RE02 broadband reference limit, the upper-limit atmospheric noise may be close to the RE02 limit at 100 kHz and 20 dB below the limit at 10 MHz.

Cosmic noise is a composite of noise sources comprised of sky background radio noise, which is caused by ionization and synchrotron radiation (which undergoes daily variation), and solar radio noise, which increases dramatically with an increase in solar activity and the generation of solar flares. Secondary cosmic noise sources are the Moon, Jupiter, and Cassiopeia-A. At 30 MHz, the average cosmic noise is 34 dB below the RE02 limit.

A comparison of the relative intensities of atmospheric and cosmic sources and the frequency range of emissions are shown in Figure 1.6. The average daily upper and lower limits of the normal cosmic noise are shown in Figure 1.5(A). Additional sources of emissions exist at lower levels, including the thermal background. The theoretical thermal background from the Earth's surface is shown in Figure 1.5(C) with the internal thermal noise of a well-designed receiver for comparison purposes.

The EMI effect on radio communications is often described as "static" due to the impulsive nature of atmospheric noise. A second source of transient EMI, which may be incorrectly attributed to atmospheric noise, is precipitation static discharge in the proximity of the receiving antenna. Static discharge on the ground is caused by a buildup of charge on the surface, resulting in a corona discharge. Correct grounding and bonding of conductive elements, use of high-breakdown-voltage dielectrics, static discharge coating, and transient suppression devices are some of the methods used to avoid static charge buildup and protect the receiver input circuit.

Because of the wide frequency span over which natural emissions occur, they may cause EMI in HF/VHF/UHF/SHF transmissions.

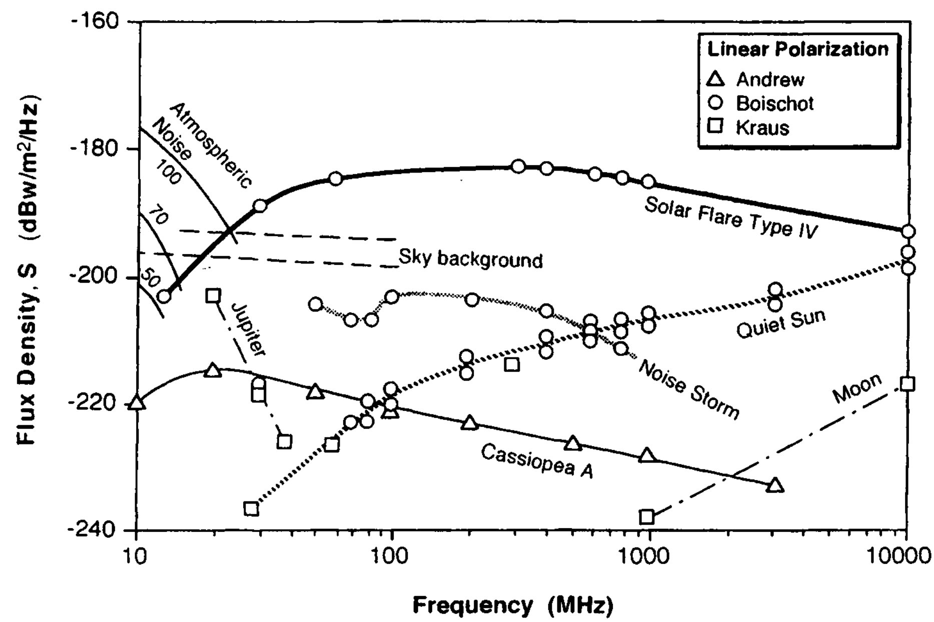

Figure 1.6 Comparative levels of cosmic noise sources. (From Ref. 1, © 1969 IEEE.)

1.3.2 Manmade Electromagnetic Noise

Some of the major sources of manmade electromagnetic noise are

- Arc welders
- RF heaters
- Industrial, scientific, and medical (ISM) equipment
- AC high-voltage transmission line
- Automotive ignition
- Fluorescent lamps
- Microwave ovens
- Hospital equipment
- Diathermy equipment
- Communication transmitter intentional and spurious radiation
- Electric motors

Each of these sources will be discussed with reference to the RE02 specification limit.

Heliarc welders use an RF arc at a typical fundamental frequency of 2.6 MHz. The spectrum occupancy of the heliarc welder emission covers the frequency range from 3 kHz to 120 MHz and thus contains frequencies lower than 2.6 MHz. The typical EMI effect on radio is a "frying" noise. Representative levels of radiation from a substantial population of RF-stabilized arc welders measured at a distance of 305 m are (1)

Frequency	Radiation level
0.7 MHz	75 dBμV/m/MHz
25 MHz	82 dBμV/m/MHz and
	80 dBμV/m/MHz (10 mV/m/MHz)
30 MHz	70 dBμV/m/MHz

The level is 4 dB above the RE02 limit at 30 MHz and is naturally much higher at distances closer than 305 m. For example, at a distance of 2 m from an arc welder, the E field level at 30 MHz is approximately 124 dBμV/m/MHz (1.5 V/m), which is 50 dB (316 times) above the RE02 limit. In extrapolating for distance at these frequencies, either a $1/d$ or $1/d^{1.5}$ law is used (d = distance), depending on frequency and other criteria. From measurements at 14 manufacturing plants, the peak level of emission from arc welders was found to be 0.1 V/m at a measuring distance of 1–3 m (5). Unfortunately, the bandwidth of the measuring instrument was not given, so it is not possible to convert the measured level to a broadband unit of measurement.

In measurements described in Ref. 3, a heliarc welder exhibited significant emissions from 14 kHz to 240 MHz. However, when measured at a distance of a few miles, only the fundamental frequency of 2.6–3 MHz remained at a significant level. In measurements at different locations on 152 welders, comprising 54 different models, the highest emission measured at 305 m was 64 dBμV/m. Of the 152 welders, 31 produced emissions above 40 dBμV/m and only 6 above 54 dBμV/m. Some welders generated levels as low as 0 dBμV (1 μV)/m. The low-level emitters were characterized by one or more of the following: short welding leads; low-impedance ground; shielded wiring, including supply; and enclosure in a shielded building. High-level emitters, in contrast, were characterized by one or more of the following: poor grounding; unshielded wires; and proximity to power lines, which picked up the emissions and reradiated them.

The Federal Communications Commission (FCC), in Document 47 CFR Part 18, place a limit of 10 μV/m at 1600 m on industrial heaters and RF-stabilized arc welders below 5.725 MHz. Converting this to the 305-m distance used in the preceding survey and applying a $1/d$ law results in a limit of 34.4 dBμV/m. From the survey it is clear that many existing arc welder installations do not comply with the FCC limit.

The fields generated by induction and dielectric-type RF heaters are principally narrowband, with peaks extending up to about the ninth harmonic. Induction heaters are used for forging, case hardening, soldering, annealing, float zone refining, etc., while dielectric-type heaters are typically used to seal plastic packages. The fundamental operating frequency for induction heaters is from 1 kHz to 1 MHz, and for dielectric heaters is from 13 MHz to 5.8 GHz. In measurements on 36 induction heaters, the minimum and maximum emissions at a distance of 30 m varied from 30 dBμV (31.6 μV)/m to 114 dBμV (0.75 V)/m (4). Since these emissions are narrowband (NB), the 1-MHz reference bandwidth is omitted in the measurement unit used.

We have so far used the relatively low-level military broadband radiated emission limit (RE02) as a reference when comparing natural and manmade emission levels. To continue to use this comparison for narrowband noise, the narrowband RE02 limit may be used.

The emissions from four different manufacturers and 10 different models of dielectric heater when measured at a distance of 30 m ranged from a maximum of 98.8 dBμV (87 mV)/m and a minimum of 75 dBμV/m (5.6 mV) at the fundamental (27 MHz) and reduced to a maximum of 84 dBμV (15.8 mV) and a minimum of 38 dBμV (79 μV) at the sixth harmonic (162 MHz).

No measurements of the conducted noise placed on the power line by these devices are available. However, the radiated emissions at 30 m were found to be above the typical ambient levels of 0.15–0.9 mV/m measured in offices, electronic laboratories, and computer facilities, but they do not pose a severe EMI threat. This is illustrated by a cursory survey of the 35,434 complaints of interference with radio communication lodged with the UK regulatory authority over a 12-month period. This survey reveals that 143 complaints were attributed to ISM sources, 11 to medical apparatus, and 66 to RF devices not tuned to designated frequencies, but not one complaint was attributed to induction or dielectric heating equipment.

The levels of noise measured at 14 manufacturing sites from a variety of ISM equipment is shown in Figure 1.7. The 14 manufacturing plants included discrete and continuous production plants, an automotive tool and die shop, a chemical plant, a heavy equipment manufacturer, an aerospace manufacturing plant, newspaper printers, paper and pulp plants, and metal smelting plants. The levels are given in volts per meter, with no information as to the bandwidth of the measuring instrument. Assuming the bandwidth used was narrow enough to capture only one of the spectral lines of emission, then the electromagnetic field levels contained in Figure 1.7 will have the same magnitude as a narrowband emitter of the same field strength, at the specified frequency of maximum emission.

When a broadband field is expressed in broadband units, the magnitude is invariably higher than the same field expressed in a narrowband unit. Here we use the term *broadband field* loosely to indicate a field comprised of a number of frequencies. A broadband unit of measurement uses a reference bandwidth, typically 1 MHz (e.g., dBμV/m/MHz), whereas a narrowband unit does not specify a bandwidth (e.g., dBμV/m). However, the bandwidth used in a narrowband measurement is always less than 1 MHz. In a broadband measurement of broadband noise, many of the random or harmonically related spectral lines are captured in the receiver bandwidth. In a narrowband measurement, only one of the spectral lines is captured in the receiver bandwidth.

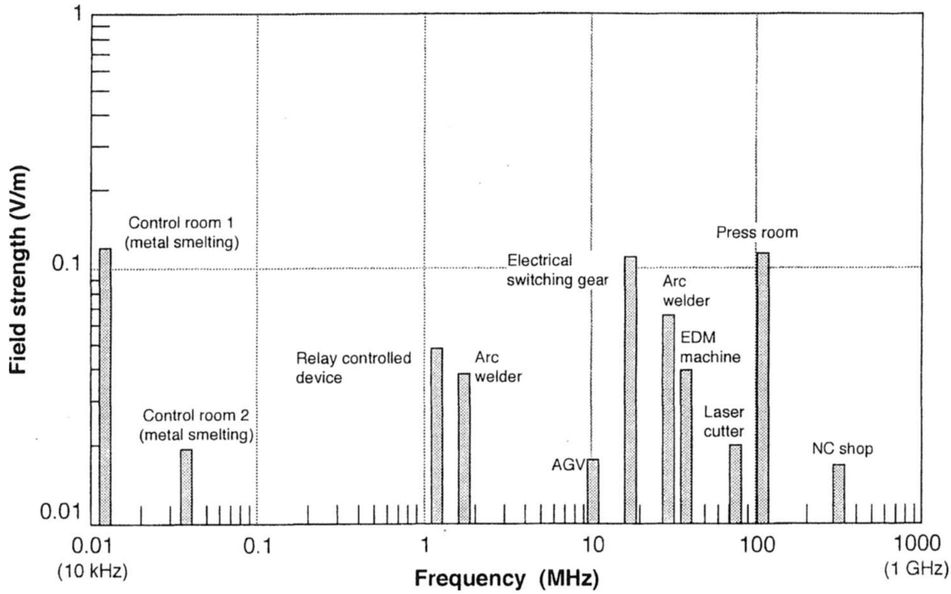

Figure 1.7 Peak field measurements from ISM sources. (From Ref. 4.)

For example, assume a broadband signal source generating harmonically related spectral lines at 1 kHz intervals apart with a constant amplitude over a 1-MHz span. Assume the field strength at some distance from the source, for the sake of our example, is 50 dBμV/m/MHz. If we were to make a narrowband measurement with a 1-kHz measuring bandwidth, then only one spectral line is measured and the field amplitude is reduced to −10 dBμV/m, expressed in narrowband terms. In this way, coherent broadband noise decreases as a function of 20 dB/decade of bandwidth. It is therefore incorrect to directly compare the magnitude of narrowband sources, for example, those "intentional emitters" contained in Section 1.3.3, to broadband sources. The subject of broadband and narrowband measurements are dealt with in Chapter 9 and sources of broadband noise in Chapter 3.

The susceptibility of equipment and cables to an impinging broadband or narrowband field is dependent, among other factors, on cable and enclosure resonance effects, the bandwidth of the equipment (including signal interfaces), and the transient response of the cable and structure. These factors are considered in subsequent chapters.

It is common to experience EMI to AM reception in cars that are driven in close proximity to, or under, high-voltage transmission lines. Figure 1.8 illustrates the spectrum occupancy of transmission line noise with, as expected, a maximum at the power line frequency of either 50 or 60 Hz. The curves in Figure 1.8 are from several sources, and the numbers in brackets indicate the distance (meters) from the line at which measurements were made.

Ignition noise level is dependent on traffic density and proximity. In the time domain, ignition noise is characterized by bursts of short- (ns) duration pulses with a burst duration of from a microsecond to milliseconds. The repetition rate of the bursts is dependent on the RPM, the number of cylinders of the motor, and the number of cars. When measured in close proximity to the road, these bursts vary in amplitude and direction with traffic flow. In cosmopolitan areas, ignition noise is a major contributor to the electromagnetic environment. The average of measurements taken in three cities at a roadside location for a traffic flow of 30 autos per minute are 60 dBμV/m/MHz at 100 MHz decreasing to 50 dBμV/m/MHz at 1 GHz. Ignition noise is

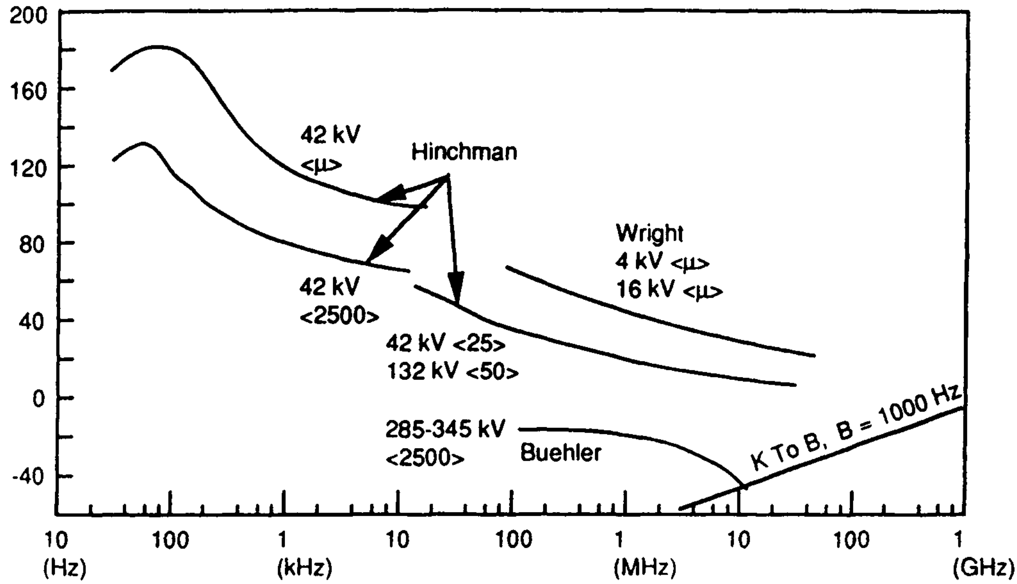

• Observation point location relative to the sources in feet <25>, <50>, etc. ; <μ> beneath conductor

Figure 1.8 Transmission line noise (numbers in brackets are measuring distances in meters). (From Ref. 1, © 1969 IEEE.)

also present from 10 kHz upwards, and levels as high as 80 dBμV/m/MHz have been measured at 10 kHz.

Fluorescent and gaseous discharge tubes produce impulsive radio noise similar to power line noise in its waveform characteristics. The level of noise from 10 kHz to 1 MHz was measured in a shielded room with the lights on and the ambient noise with the lights off. The highest fluorescent light emission was at 300 kHz, measured at 89 dBμV/m/MHz, and the RE02 BB limit at 300 kHz is 98 dBμV/m/MHz. Thus, although the ambient is just below the specification limit, all subsequent measurements were made with the fluorescent lights off. For MIL STD 461 measurements, the ambient should be at least 6 dB below the specification limit. The remaining incandescent lamps in the shielded room did not add to the electromagnetic ambient. The average level of radiation from fluorescent lamp fittings measured at a distance of 1 meter is shown in Figure 1.9.

Field-strength measurements of microwave ovens operating in the ISM band at 915 MHz were measured in the laboratory at distances of 3.05 m and 305 m. Measurements were also made outside a large condominium containing 385 ovens. The measurements were made on one make of oven and similar models. The maximum field strength measured in the laboratory was 1.5 V/m at 3.05 m and 11 mV/m at 305 m. The field strength measured outside the condominium building would have been altered by some shielding due to the building structure and reflections from the ground and nearby buildings. The maximum field strength measured was 8.9 mV/m at 920 MHz at a measuring distance of 152 m from the two buildings comprising the condominium (6).

The electromagnetic environment in hospitals has been of growing concern as the number of EMI problems experienced in hospitals has increased. Measurements have been made in ten American hospitals in a number of locations, including operating rooms, intensive care

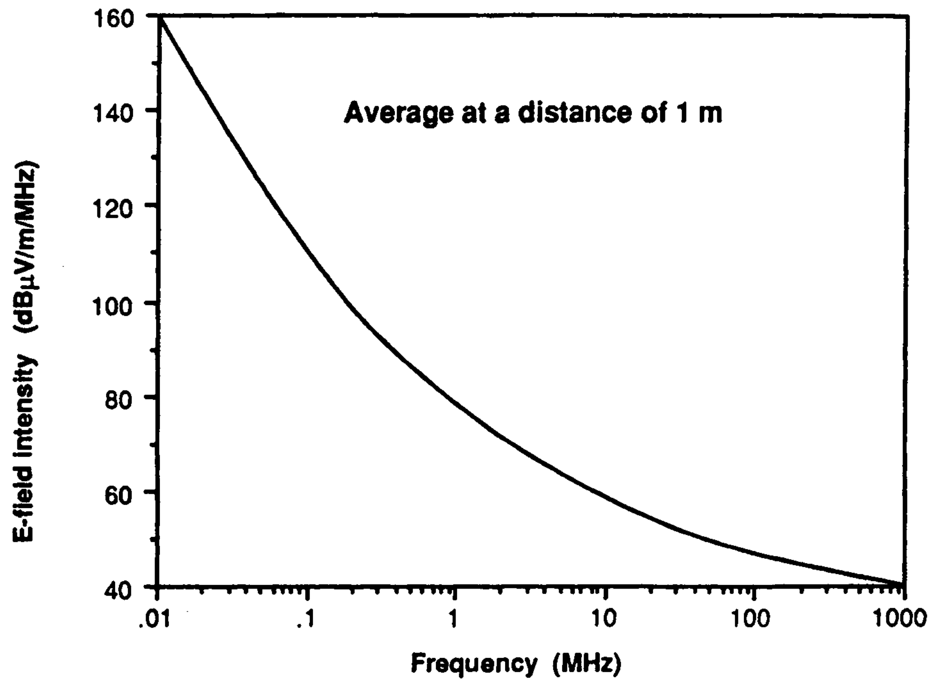

Figure 1.9 Average level of radiation from fluorescent lamps.

units, chemistry labs, special procedure rooms, and physical therapy facilities. In the majority of locations, E fields as high as 3 V/m/MHz were measured. It should be emphasized that the measurement results are displayed in broadband units. If the measurements had been made with a narrowband bandwidth and displayed in narrowband units, the majority of emissions would have reduced in amplitude but with peaks at 70 kHz and 1–5 MHz remaining at approximately 3 V/m. These peak emissions are from diathermy or electrosurgical units, which use high-frequency currents to achieve bloodless surgery and are generators of narrowband noise. Figure 1.10 is a composite of the worst-case field levels measured in all locations at the 10 hospitals surveyed (7).

When these unintentional manmade high-level sources of radiation are compared to our standard RE02 level, the sources may have intensities of 60 dB above (i.e., 1,000 times) the RE02 limit.

In addition to RF electromagnetic fields, magnetic fields at power line frequencies are ever-present. Due to the concern for the potential health hazard of magnetic fields, a number of measurements were made in a home and in an office building. The magnetic field strength in one room on the 1st floor in the office building was sufficient to result in distortion of computer monitor displays. The displays were susceptible to magnetic fields with magnitudes of 1.3–3 A/m. The magnetic fields in this 1st floor varied from a low 0.016 A/m to the maximum of 3 A/m at 60 Hz. On the 5th floor of the same building, the magnetic field varied from 0.00485 A/m to 0.0428 A/m. The highest magnetic fields measured in the basement of the same building was 1.63 A/m, close to a power transformer. A survey was also conducted at several locations in a home; the result of these measurements are shown in Table 1.1.

One technique for reducing 60-Hz magnetic fields from wiring is to keep line and neutral in any two-phase circuit or the A, B, C, and neutral conductors in close proximity or preferably

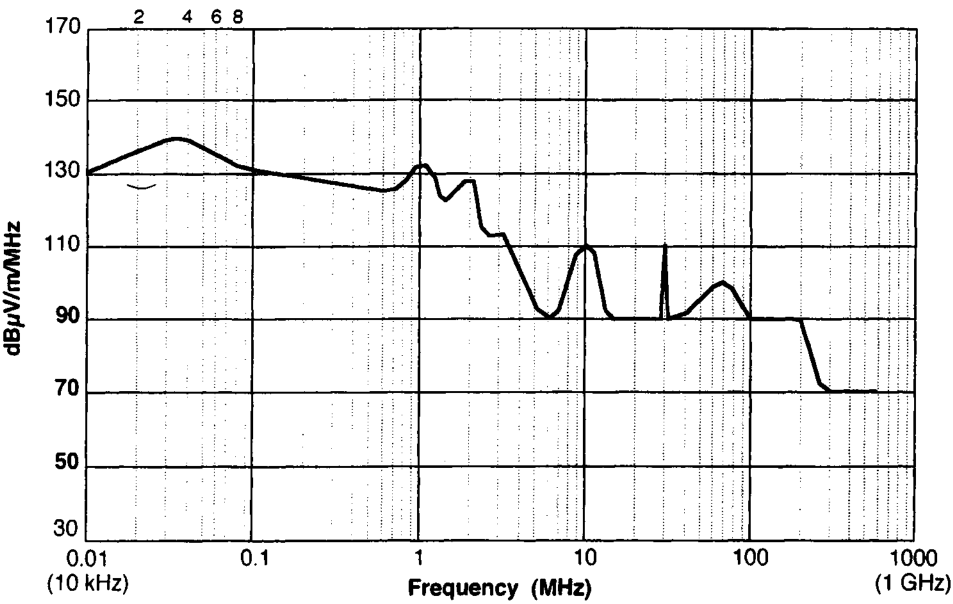

Figure 1.10 Composite worst-case field levels in hospitals. (From Ref. 2. © 1975 IEEE.)

twisted together. Section 2.1.3 discusses the reduction effect seen with twisted-pair cable in detail. An alternative is to run the cables in a high-permeability conduit. Measurements were made on a galvanized cold-rolled-steel seamless conduit with a wall thickness of approximately 1.2 mm (15/32″), and an attenuation of approximately 16 dB at 60 Hz was seen. Section 6.2 describes low-frequency magnetic field shielding in detail.

1.3.3 Intentional Emitters

The electromagnetic environment is also crowded with the intentional emissions from radio, television, and radar transmitters, all of which can interfere with equipment that is not intended for any form of reception as well as receivers tuned to a different frequency. One of the most frequent causes of EMI is electromagnetic fields produced by radio transmitters. The EMI effect may be confined to annoyance, for example, due to the spurious operation of a garage door

Table 1.1 Magnitude of Magnetic Fields Measured in a Home

Location of magnetic field measurements in a home	Magnetic field (A/m)
20 cm from top of stove	4.86
20 cm from oven door	0.4
20 cm from electric food mixer	4
20 cm from electrical panel	0.82
20 cm from 120–250-V autotransformer	46.2
2 m from hi-fi setup	0.1
Center of kitchen; all appliances off except for refrigerator	0.1
20 cm from toaster	0.81

caused by the use of a CB radio. There also exists documentation of far more serious effects, such as the destruction of a warship attributed indirectly to EMI (due to interference with communication) or the crash of an aircraft as the direct result of EMI (flying in close proximity to a high-power transmitter).

Radio transmissions are narrowband, with limited emissions at the harmonics of the fundamental continuous wave (CW). If these waves are modulated, then the resulting sidebands are also transmitted. In addition to frequencies related to the fundamental, a transmitter may radiate the local oscillator frequency and broadband noise generated within the stages of the transmitter. The composite of spurious, broadband, and harmonically related noise from a transmitter is typically at least 70 dB down from the fundamental. The radiated fields from transmitting antennas are dependent on proximity, transmitter output power, directivity of the antenna, relative height between antenna and measuring point, and proximity of reflecting or intervening absorbing material or structures, etc. Measurements have been made in two major urban centers in Canada (Montreal and Toronto, Ref. 7). From a large number of measurements made close to ground level, a typical field-strength value developed at usual transmitter–receiver distances was computed. The results are shown in Table 1.2. The maximum typical E field at a fixed distance of 100 m is shown in Figure 1.11.

An electromagnetic RF ambient survey is often made before erecting a receiving antenna or before the installation of potentially susceptible equipment. Examples of peak emitters encountered in such measurements are a radar signal measured at a site in Goosebay, Labrador, that exhibited a frequency of 1280 MHz and a level of -21 dB-W/m^2 (i.e., an E field of 1.73 V/m); an AM radio transmitter in Alice Springs, Australia, generated E fields of 4 V/m at 4.83 MHz incident on nearby receiving equipment; and, at a proposed site in Hong Kong, E fields of 3.75 V/m at 12 MHz were measured at the proposed location of receiving equipment. Many apartment and office buildings have antennas mounted on the roof. In one apartment building, Bell cellular antennas were mounted on the roof, and the E fields, at 880 MHz, measured in two apartments were 7.86 V/m and 6.48 V/m, respectively. On the balconies of these same apartments, the maximum E field was at 12 V/m and 12.9 V/m, respectively. The ambient inside a household that contains an amateur radio transmitter with the antenna mounted on the roof was measured at 30 V/m inside the home. Transceivers (walkie-talkies) can generate fields as high as 55 V/m at 823 MHz at a distance of 12 cm from a 5-W transceiver (8). The power generated by a cellular phone at a distance of 2.5 cm from the human head is absorbed by the head at the same rate as an incident field of 41 V/m (10). In Ref. 10, ambient measurements were made on apartment buildings in 15 different cities in the United States. The median exposure for

Table 1.2 Typical Ambient Field Strengths (Ref. 8)

Frequency (MHz)	Field strength[a] (V/m)
0.5–1.6	0.6
26.9–27.4	<0.1
54–88	0.07
88–108	0.15
108–174	0.05
174–216	0.07

[a] Typical field strength in major urban centers from broadcast transmitters.
Source: Ref. 8.

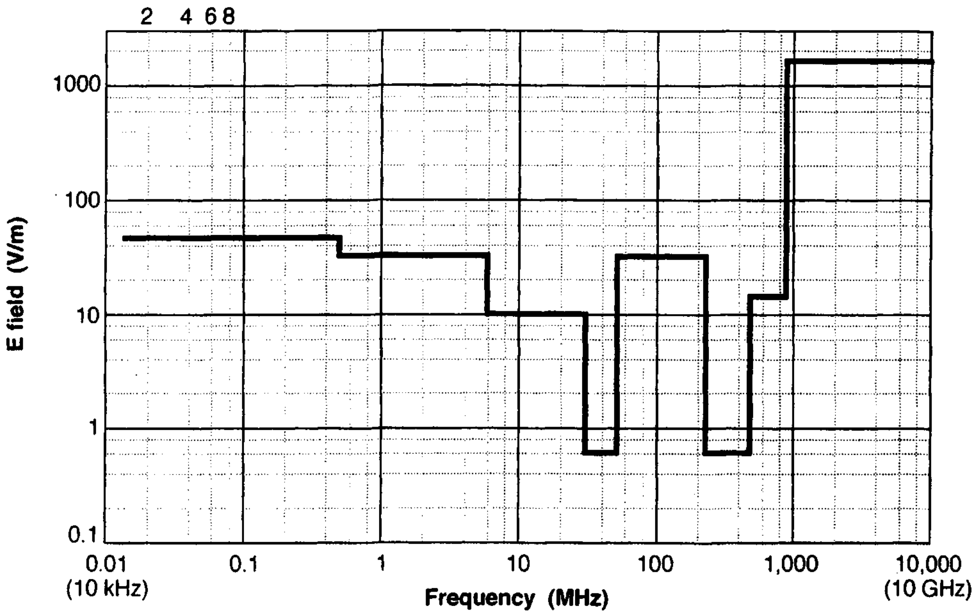

Figure 1.11 Average and peak fields from radio transmitters at a distance of 100 m.

the inhabitants of all cities was 0.137 V/m, and 99.9% of the inhabitants were exposed to fields of less than 1.94 V/m. Thus we can conclude that ambients with magnitudes of volts per meter are uncommon, but are increasingly the cause of EMI in apartment and office buildings. Electric fields having volts-per-meter magnitudes are potential sources of interference to equipment even when the passband of the equipment is far from the interfering frequency. Case studies for this type of EMI are contained in Chapter 12.

The preceding summary of measured spectrum occupancy and radiated emission levels from unintentional and intentional sources is intended to provide guidelines to manufacturers whose equipment must achieve EMC in these harsh environments. One important piece of information presented with the data is the measuring distance from the source. In measurements it has been observed that the low-frequency component falls more rapidly with increasing distance than those at VHF and UHF. The mechanism for E field reduction with distance and frequency is discussed in Chapter 2. When predicting the electromagnetic ambient level at a given location, not only is the distance from potential sources of EMI an important consideration but also the presence of conductive structures close to the emission source, such as walls, buildings, and ground topology. When structures are behind or to the side of the source, they act as reflectors; they act as shields when the structures are intervening. Chapter 6 discusses the shielding effectiveness of structures and soil.

1.3.4 Conducted Noise on Power Lines

The electromagnetic environment is confined not only to electromagnetic fields but also to signals/noise existing in a transmission medium. Thus the noise conducted on equipment power lines must be accounted for when characterizing an electromagnetic ambient. For example, a computer on a machine shop floor, located at some distance from numerical control machines, may be immune to the radiated field levels but susceptible to conducted noise. Therefore, in addition to immunity to electromagnetic fields, achieving EMC entails immunity to conducted noise, present predominantly on power lines but also on signal interfaces and grounds. To predict susceptibility for equipment on which no EMC requirements are placed, data on expected maximum amplitude, frequency content, and waveform type (e.g., CW or spike) that may exist on the power supply in a given electromagnetic environment is required.

The conducted noise currents flowing out of medical equipment into a known load connected to the power line was measured in the survey made in 10 hospitals. The impedance of the load is not given in Ref. 11; however, a typical value is 50 Ω. A 400-Hz highpass filter was included in the measurement setup to reduce the magnitude of load current measured at 60 Hz and its harmonics by the current probe. Figure 1.12 is a composite of the maximum conducted noise currents measured in all locations at the 10 hospitals (7). In other measurements in a hospital environment, voltage spikes as high as 3,000 V have been measured on the AC power line.

Unfortunately, the amount of data available from measurements of conducted noise current or voltage is limited. An alternative approach is to use the specified susceptibility test levels described in Chapter 9 for the relevant type of equipment (i.e., military, ISM, or vehicle-mounted equipment). Where susceptibility test levels have not been developed for the equipment type, then the regulations concerning conducted emission limits for equipment such as digital, household appliance, portable tools, etc. may be used to predict the conducted power line noise level. When using emission limits in a prediction, some correction must be made for the specific or worst-case power line impedance and the number of devices sharing the same power line. For example, in a laboratory environment, several computers, hand tools, RF sources, and a refrigerator may share a common power line. A worst case AC, 120-V, 60-Hz power line source impedance plotted against frequency is shown in Figure 5.28a. Taking a composite of the noise currents from all sources, a composite noise voltage developed across the worst-case source impedance may be calculated, to arrive at susceptibility test/design levels.

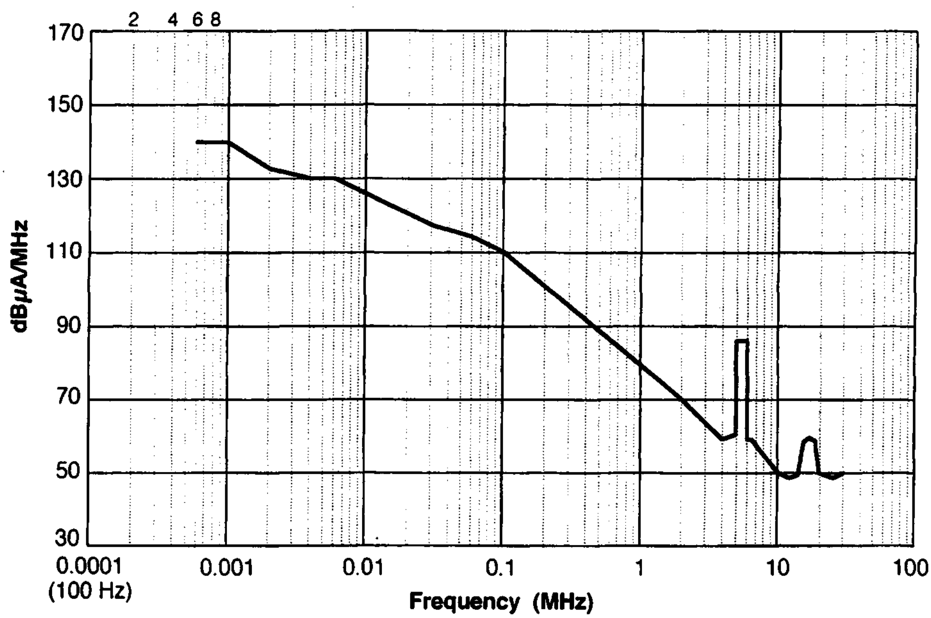

Figure 1.12 Composite of conducted AC power line noise currents measured at 10 hospitals. (From Ref. 2. © 1975 IEEE.)

REFERENCES

1. E.N. Skomal. The dimension of radio noise. 1969 IEEE Symposium on EMC, Vol. 69, C3-EMC, June 17–19.
2. H.V. Cottony. Radio noise of ionospheric origin. Science, Vol. 111, No. 2872, p. 41; January, 1950.
3. H.V. Cottony, J. R. Johler. Cosmic radio noise intensities in the VHF band. Proceeding of the IRE, September 1952, pp. 1050–1060.
4. R. Nielson. Ethernet performance in harsh industrial environments. Control Engineering 1988, Vol. 35, No. 10.
5. A.S. McLachlan. Radio frequency heating apparatus as a valuable tool of industry and a potential source of radio interference. 7th International Zurich Symposium and Technical Exhibition on Electromagnetic Compatibility, Zurich, 1987.
6. A. Tell. Field strength measurements of microwave oven leakage at 915 MHz. IEEE Transactions on Electromagnetic Compatibility, May 1978, Vol. EMC-20, No. 2.
7. Government of Canada Department of Communications. EMCAB 1, Issue 2.
8. John Adams. Electric field strength measured near personal transceivers. National Institute of Standards and Technology. IEEE EMC Symposium record 1993.
9. Paolo Bernardi, Marta Cavagnaro, Stefano Pisa. Evaluation of the SAR distribution in the human head for cellular phones used in a partially closed environment. IEEE transactions on Electromagnetic Compatibility, August 1996, Volume 38, Number 3.
10. Daniel D. Holihan. A technical analysis of the United States environmental protection agency's proposed alternatives for controlling public exposure to radiofrequency radiation. IEEE EMC Symposium record 1987.
11. R.J. Hoff. EMC measurements in hospitals. 1975 IEEE International Symposium on Electromagnetic Compatibility.

2

Introduction to E and H, Near and Far Fields, Radiators, Receptors, and Antennas

Judging by the response from attendees of seminars, this chapter may be the least popular with design and system engineers.

The concept of radiation from, and coupling to, interface cables, PCB tracks, wiring, etc. is generally foreign to engineers, despite involvement with equipment containing digital, analog, RF, and control circuits. The reason may be that it is difficult to envisage interconnections as antennas, or circuit elements, or to see the potential for crosstalk between conductors. This is particularly true when equipment exhibits EMI or fails an EMC requirement and the engineer is under the pressure of schedule to find the quick fix usually demanded by management. In order to make simple EMC predictions or solve an EMI problem efficiently, an understanding of the principles of radiation and coupling, including frequency dependency and resonance effects, is essential.

Even the choice of an effective diagnostic test or the evaluation of a problem for either a radiated or a conducted source are difficult without this understanding. The title of this chapter may appear to imply that radiators and receptors are somehow different from antennas. Of course this is not true. One antenna engineer, when asked to define an *antenna*, replied, "What is not an antenna?" It used to be said by TV repair technicians, not totally in jest, of a high-field-strength location that a piece of wet string would serve as an antenna.

One investigator has examined the resonant frequency and receiving properties of leaves and fir cones, modeled as log periodic antennas, and questioned the effects of RF currents flowing, as a result of electromagnetic fields, on their surfaces. The differentiation made in this chapter between radiators, receptors, and antennas is merely to distinguish between structures intentionally designed to radiate and receive and those not. It will be seen that much of the antenna theory is applicable to nonintentional antennas, for example, in investigating the magnitude of current flow caused by an incident field on a structure and the radiation from a current-carrying conductor. Many good books exist on the subject of wave theory and antennas. Then why the need for this chapter? The magnitude of an electromagnetic field at some distance from an AC source varies with time. In the measurement and prediction of field magnitude for EMI analysis or in meeting a limit, it is the peak magnitude that is required. Therefore it has been possible to simplify the field equations presented in this book by eliminating the time-dependent terms. In EMC we are interested both in highly efficient resonant antennas and in the nonintentional radiation and coupling, to nonresonant structures, with impedances not matched to the termination impedance. Most antenna books are confined to the analysis of antennas that are highly efficient and relatively narrowband. However, many of the equations developed for antennas are quite applicable to any conductive structures.

The formulas contained in this chapter are used in the predictions contained in subsequent chapters and are presented as *magnitudes* (i.e., they may be used directly). Derivations for the equations are omitted and may be found in the reference material. In order to make life as simple as possible, the equations for coupling to and radiation from wires and cables as well as crosstalk between cables have been incorporated into computer programs written in BASIC and provided at the end of this and other chapters. However, an understanding of the correct model to use and the limits on its applicability is still required.

In addition, this chapter will enable the reader to make, calibrate, and correctly use simple magnetic field probes and E field antennas, and it introduces the meaning of terms, such as *gain* and *antenna factor*, used with EMI measuring antennas.

2.1 STATIC AND QUASI-STATIC FIELDS

In order to understand electromagnetic waves in proximity to current-carrying conductors as well as in free space, it is helpful to examine static electric and magnetic fields. In addition, at low frequency and at close distances to the source, it is often the reactive near field or quasi-static field that couples strongly, and these fields can be computed using the following DC analyses.

2.1.1 DC Electric Field

An electric field exists between the plates of a capacitor to which a potential V_0 is applied (Figure 2.1). The electric field intensity is

$$E = \frac{V_0}{h} \quad \text{[V/m]} \tag{2.1}$$

where h is the distance between the plates, measured in meters. Thus E is a magnitude per unit length. For example, if 10 V were applied to plates 10 cm apart, the field strength between the plates would be 100 V/m. The electric field has electric lines of force associated with it that are tangent to the electric field and are proportional in strength to the electric field strength. The electric field intensity can be measured by inserting a small dipole into the field (Figure 2.1). The component of the electric force tangential to the two conductive arms of the probe moves electrons in the conductors, and a voltage appears across the arms.

The voltage induced into a thin probe is substantially independent of the radius and proportional to the length of the probe. In practice, the conductive wires connected to the probe would disturb the electric field and Eq. (2.1) would not be strictly correct. The field between two infinite parallel plates is uniform, and in the field between the plates we find

$$V_1 = Eh_d \tag{2.2}$$

where

E = electric field strength [V/m]

h_d = effective dipole length

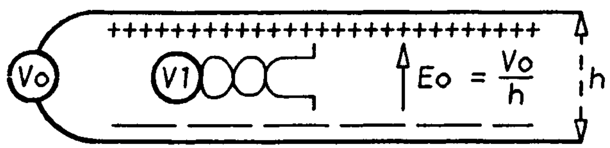

Figure 2.1 A cross section between parallel plates.

In a nonuniform field, the electric probe measures the average intensity of the field occupied by the probe; hence h_d should be as small as possible. The electric field probe described is the simplest example of a receiving antenna. Electric field lines may start on a positive charge and end on a negative charge, as shown in Figure 2.1, or they may start on a positive charge and end at infinity or start at infinity and end on a negative charge or with time-varying fields form closed loops that neither start nor end on a charge.

2.1.2 DC Magnetic Field

An electric current is surrounded by a magnetic field of force. The magnetic field around a very long wire carrying a constant current is given by

$$H = \frac{I}{2\pi r} \quad [\mathrm{A/m}] \tag{2.3}$$

and illustrated in Figure 2.2.

Magnetic field lines always form closed loops around current-carrying conductors because magnetic charges do not exist. The magnetic field is, like an electric field, a magnitude per unit length. For example, the magnetic field 10 cm from a wire carrying 10 A is 16 A/m and reduces to 1.6 A/m at a distance of 1 m. Expressed in another way, if the circumference of the field line at 10-cm distance is 0.628 m, the magnetic field strength is then 10 A/0.628 m = 16 A/m. Equation (2.3) may be found by dividing up the conductor into infinitesimal lengths (current elements) through which the current flows. The total field is then the sum of the contributions from all of the current elements stretching out to infinity on both sides of the measuring point. When the length of the wire is not infinite but much longer than the measuring distance r, Eq. (2.3) may still be used with a normally acceptable small error in the computed field strength. If the wire changes direction, then the equation for computing the field from a current loop may be applicable.

In practice it is uncommon to find short lengths of isolated current-carrying conductors. One exception may be where a conductor enters a space through a shield and then exits the space after a short distance via a second shield. The approximate magnetic field from this specific example is then

$$H = \frac{I}{4\pi r^2} \quad [\mathrm{A/m}] \tag{2.4}$$

It is very common to find a second return conductor in close proximity to the supply conductor, with the return conductor carrying exactly equal and opposite current to the supply.

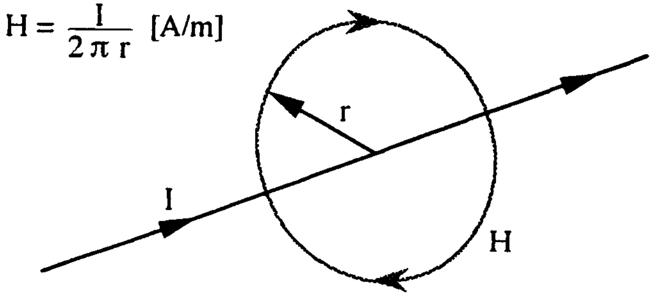

Figure 2.2 Magnetic field around a long conductor.

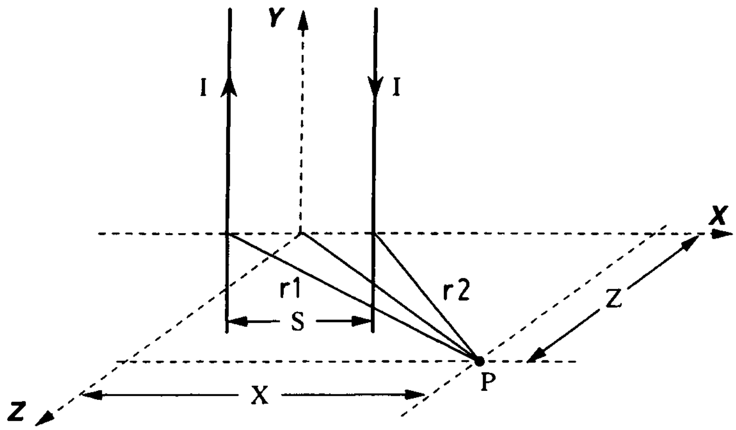

Figure 2.3a Configuration of a two-wire line.

This configuration is shown in Figure 2.3a. Because the field magnitude for the two conductors is not the same in the plane of the loop, the x-axis, as it is tangential to the plane of the loop, the z-axis, two field magnitudes H_z and H_x must be computed.

The derivation of the following equations for H_z and H_x may be found in Ref. 1 as well as in other textbooks on electromagnetic theory:

$$H_z = \frac{I}{2\pi}\left(\frac{x + S/2}{r_1^2} - \frac{x - S/2}{r_2^2}\right) \tag{2.5}$$

$$H_x = \frac{I}{2\pi}\left(\frac{z}{r_1^2} - \frac{z}{r_2^2}\right) \tag{2.6}$$

All distances, such as x, z, r_1, and r_2, are in meters.

From Eqs. (2.5) and (2.6) we see that the field on the x-axis at the center of the two conductors is zero and on the z-axis it is twice the magnitude computed for the z-component either side of the center. This may be seen graphically in Figure 2.3b, where the fields from the two conductors are in antiphase on the x-axis and in phase on the z-axis at the center of the conductors.

When probing around the two conductors with a magnetic field measuring probe, the change in measured field may be seen with change in probe location and orientation in the x- and z-axes around the conductors.

Twin conductor cables carrying 50–20-kHz AC power are potential sources of high magnetic fields at close proximity to the conductor. The closer together the conductors are, the lower the resultant H field. Where the conductors are separated and, for example, routed around the inside of an enclosure, the magnetic field is at a maximum, and the correct prediction method for magnetic field from a current loop is Eq. (2.7).

2.1.3 Twisted-Pair Wires

In order to minimize the generation of magnetic fields from conductors, twisted-pair wire is used. The magnetic fields from each loop of the twisted wires are in antiphase and therefore tend to cancel. At the exact center of the loop and equidistant from all loops, assuming all loops

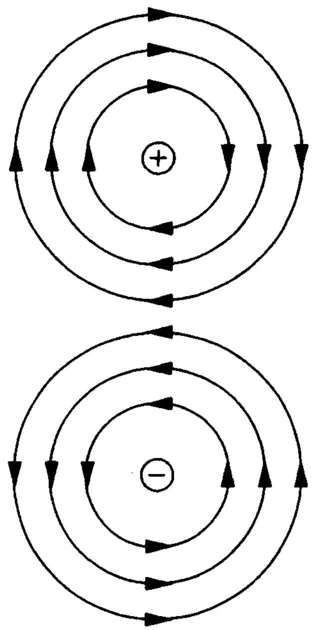

Figure 2.3b Field distribution around a two-wire line.

are of equal size, the total magnetic field is zero. The realistic situation is that not all loops are equidistant from the measuring point and that the sizes of the loops are not exactly equal. Figure 2.4 illustrates the resultant fields and their directions, which may be computed for any location by computing the individual fields from each loop. Then the total field may be graphically estimated from the vector product or vector analysis may be used.

The magnetic field from a twisted pair contains a radial component, x, a component down the axis of the pair, z, and a circumferential component, ϕ, due to the helical nature of the twist. The field at some distance from the wire, p, is dependent not only on p but on the pitch distance, h (distance for one cycle of twist), as well as the distance between the center of the twisted pair and the center of one conductor of the pair.

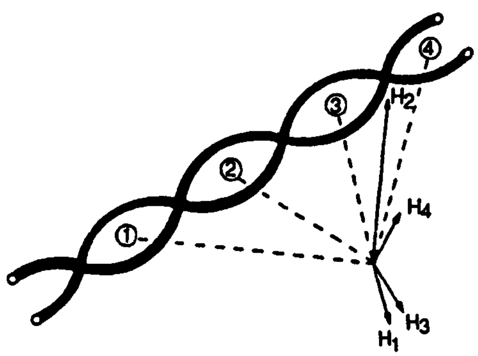

Figure 2.4 Resultant fields and their directions for an individual loop of a twisted pair.

At distances very close to the twisted pair, the field may be higher than for the two-wire line. However, the field very quickly reduces in magnitude with increasing distance p. From measurements in Ref. 2 it was found that the magnetic field strength from a twisted pair reduces more rapidly, as a function of $1/r^3$, than the field from an untwisted pair or a coaxial cable in which the center conductor is not concentric or on which an unbalanced current flows, which reduce as a function of $1/r^2$.

We use the term $1/r^n$ throughout this chapter. In order to illustrate the meaning, imagine that the magnetic field has been measured at a distance of 1 cm from a twisted wire pair and that the field at 10 cm is required. The change in distance between measuring point and predicted point is 10 cm/1 cm = 10, the reduction in field strength is therefore $1/10^3 = 1/1000$.

From measurements and predictions on twisted-pair cable with a large pitch distance of 3 inches (i.e., only 0.33 twists per inch) from Ref. 3, the reduction in field for the twisted-pair cable is approximately $1/r^{10}$, or 60 dB, for a doubling in distance p. From the same reference, the reduction in field for an untwisted cable is 12 dB (i.e., $1/r^2$) for a doubling of distance. A comparison between the reduction in field versus distance for both a twisted pair and an untwisted pair is shown in Figure 2.5. In Ref. 4, generalized curves using the ratios of a/h and p/h have been constructed for B_r, B_ϕ, and B_z. These generalized curves are reproduced in Figure 2.6. The y-axis of Figure 2.6 is magnetic field strength, in decibels/gauss for 1 ampere of current flow. To calculate the field components from the figure:

1. Find the number of decibels for the ratio a/h.
2. Add the decibels for the ratio of p/h.
3. For the B_r and B_z fields, add $20 \log(1/2.54xh)$ [cm] or $1/h$ [inches]) to the number of decibels obtained in step 2. For the B_ϕ field, add $20 \log(1/2.54p)$ [cm] or l/p [inches] to the number of decibels obtained in step 2.
4. To correct for the actual current flow I, add $20 \log I/l$ to the number obtained in step 3.

The field magnitude at some point or points in close proximity to a twisted pair is of interest when the voltage induced into either a loop or a wire, which crosses the pair at some angle, is required. Where the concern is not the electromagnetic field incident on a point but

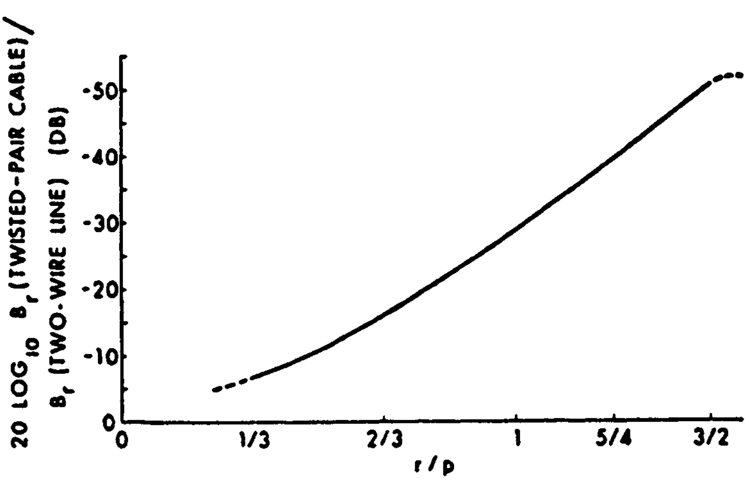

Figure 2.5 Comparison of the reduction in field vs. distance curves for both a twisted pair and an untwisted pair. (© 1968 IEEE.)

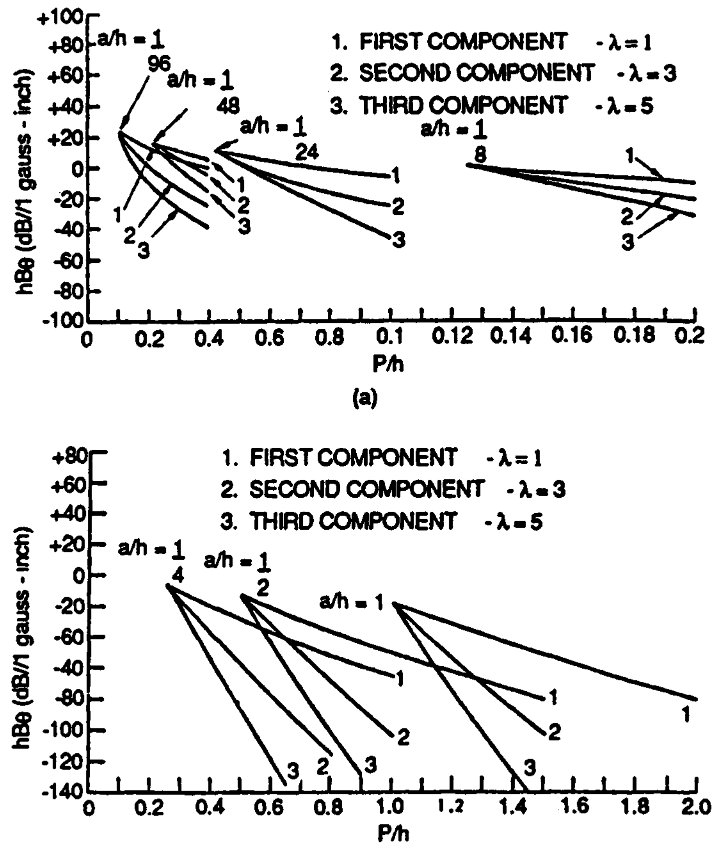

Figure 2.6 Field reductions as a function of a/h and p/h.

on a cable or wire running the length of the twisted wire pair, then a current is induced into the receptor wire. Again these currents tend to cancel, but not exactly due to varying distance and orientation between the twisted wire source and the receptor wire, unequal loop areas, and an odd number of loops. End effects where large loops may exist due to the termination of the twisted pair must also be considered. For the evaluation of crosstalk, the worst-case magnetic field generated down the length of the twisted pair may be estimated for a given distance from the twisted pair and used with the cable crosstalk equations and computer program found in Chapter 4. This program allows the prediction of coupling to either a single wire above a ground plane, a two-wire line, or a shielded cable.

The susceptibility and radiation from twisted pairs from 20 kHz to GHz (i.e., above the frequency where the quasi-static equations are valid for long distances from the source) is considered in Section 2.2.6.

2.1.4 DC and Quasi-Static Fields from a Loop

The radial magnetic field from a loop (i.e., in the x-axis) at a point coaxial to the loop at DC and low frequency in close proximity is given by

$$H_x = \frac{Ir^2}{2(r^2 + d^2)^{1.5}} \quad [\text{A/m}] \tag{2.7}$$

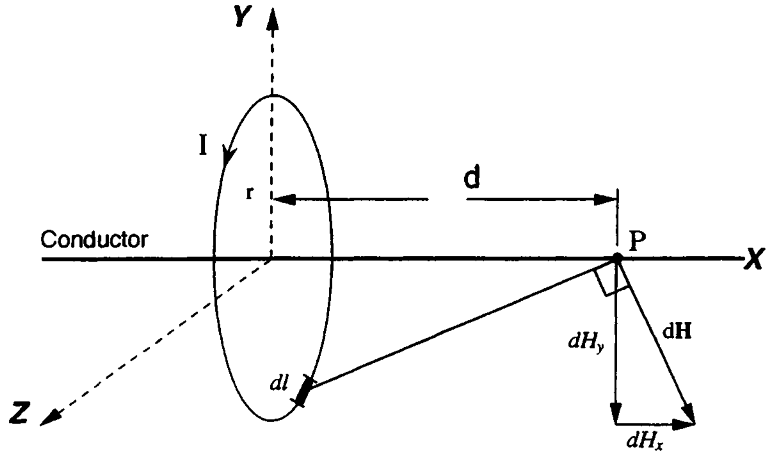

Figure 2.7 Configuration for the magnetic field from a loop.

where

d = distance from the loop [m]
r = radius of the loop [m]
I = current carried by the loop [A]

The loop and measuring point are shown in Figure 2.7. The components of the magnetic field in the y-axis at point p cancel, and thus H_y is zero.

2.2 ELECTRIC WAVES ON WIRES AND IN FREE SPACE

Connecting a sinewave generator to parallel conductors of length greater than the wavelength, λ, results in the generation of a wave along the length of the conductors. Parallel conductors can be considered chains of small inductors in series and small capacitors in parallel. We thus expect a delay in the transmission of voltage down the length of the conductors. The wave profile is shown in Figure 2.8.

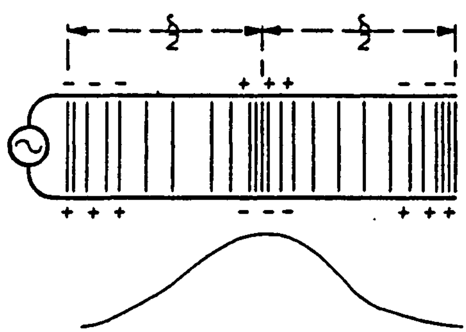

Figure 2.8 Distribution of charge and waves on parallel plates.

The distance between the crests of the sinewave is called the *wavelength*, λ. If the wave moves down a conductor so that the time between successive crests is t, then the velocity of the wave is

$$v = \frac{\lambda}{t}$$

The frequency is given by

$$f = \frac{1}{t}$$

Hence,

$$v = \lambda f$$

The velocity of a wave in free space or air is a constant 3.0×10^8 m/s, and the relationship between frequency and wavelength is

$$f\,[\text{MHz}] = \frac{300}{\lambda\,[\text{m}]}$$

$$\lambda\,[\text{m}] = \frac{300}{f\,[\text{MHz}]}$$

The velocity for a medium is given by

$$\frac{1}{\sqrt{\mu\mu_r\epsilon\epsilon_r}}$$

where

μ = permeability of free space = $4\pi \times 10^{-7}$ [H/m] = 1.25 [μH/m]

μ_r = relative permeability

ϵ = dielectric constant of free space = $1/36\pi \times 10^9$ = 8.84 [pF/m]

ϵ_r = relative permittivity

The wave velocity of a transmission line is given by

$$\frac{1}{\sqrt{LC}}$$

where

L = inductance of the line per unit length

C = capacitance per unit length

Figure 2.8 shows the distribution of charge in the form of electric lines of force. Lines of force are considered to be tangential to the electric field E. Clusters of dense lines of force exist where the charge density is high, and in the next cluster the lines of force are oppositely directed. Loops of current are also present, formed partly on the conductors and partly in the space between the plates.

Thus a magnetic field is present around the parallel plates. The current flow in the space between the conductors is named the *displacement current*, and, as we shall see in Section 7.6.3.1, it is important when considering the common mode current on a line. The open circuit

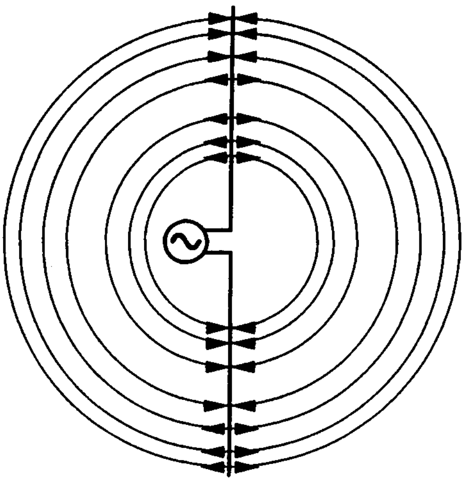

Figure 2.9 Lines of force around divergent conductors.

transmission line of Figure 2.8 results in standing waves along the length of the line, due to reflection of the wave arriving at the end of the line. If the conductors are not parallel but rather divergent, then the lines of force are as shown in Figure 2.9.

2.2.1 Radiation

The dipole antenna depicted in Figure 2.10 is said to be short, because charge reaches the ends of the antenna in much less than a period; expressed differently, the length of the antenna is much less than a wavelength. The current flow in conductors of the two-wire transmission line driving the antenna are of the same magnitude but 180° out of phase, and standing waves are created on the transmission line. When the length of the antenna is less than the wavelength, the standing wave current along the length of each arm of the antenna is in phase and the fields radiated from both arms will reinforce. As the discharge begins, the lines of force diminish and after a half period are at zero. During this period, the lines of force reaching out to P are

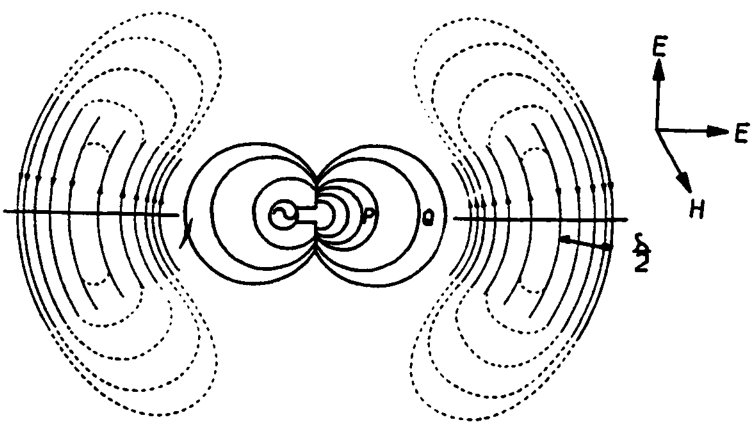

Figure 2.10 Detached lines of force around a short dipole antenna.

cancelled; however, a fraction of the lines of force spread out to Q, and this cluster of lines becomes detached at the end of the first half-period. The cluster of lines of force move on, and new lines of force take their place. The width of the configuration of lines remains $\lambda/2$, with the area over which the lines of force spread increasing with increasing distance r from the antenna. The area can be proven to equal $\pi\lambda r$.

In accordance with our conception of lines of force, the density of the lines of force is proportional to the electric intensity. The number of lines of force issuing from the antenna is proportional to the charge and, therefore, to the current in the generator. The fraction of the lines of force detached from the antenna is proportional to the length $2l$ of the antenna. Magnetic and electric fields exist in the equatorial plane of the antenna (Figure 2.10). In the equatorial plane, the magnetic field, in amps per meter, is proportional to

$$\frac{2\mathrm{Il}}{\pi\lambda r}$$

The radial electric field is the field that has the same direction as the static or quasi-static field, and it is given, in volts per meter, by

$$\frac{2\mathrm{Il}}{4\pi r^2}$$

and therefore diminishes as a function of $1/r^2$ with distance r. The electric field in the meridian (i.e., in the plane of the antenna arms) is given by

$$\frac{2\mathrm{Il}Z_W}{\pi\lambda r}\cos\theta$$

where θ is the angle between the direction of the antenna arm and the measuring point.

The ratio of E/H has the dimension of an impedance and is often referred to as the wave impedance, Z_W, used in the preceding expression. The electric intensity E and the magnetic intensity H in free space take the place of the voltage and current at the terminals of a circuit. Therefore, $E = Z_W H$ and $H = E/Z_W$.

The physical dimensions of E and H are those of voltage and current per unit length. The ratio of E/H is dependent on the proximity of the wave to the source of emission. Very close to the source, where the field contains radial components, it is called the *induction field*. Further away, where some field components decrease as $1/r^3$, it is called the *fresnel region*. Still further from the source, where the fields fall off as $1/r$, it is called the *far-field* or *fraunhoffer region*. The fields in the fresnel and fraunhoffer regions both radiate. At low frequency and in close proximity to the dipole antenna, the reactive or quasi-static field exists and does not radiate.

The distances at which far-field conditions occur are dependent, among other factors, on the size of the antenna. Where the size D of an antenna is less than $\lambda/2$, then the near-field/far-field interface distance is defined as

$$r = \frac{\lambda}{2\pi} \tag{2.8}$$

where $D > \lambda/2\pi$, the interface distance is $r = D/2\pi$.

This definition is useful in EMC because it describes the distance at which the magnetic and electric fields from an electric current element or current loop begin to reduce as a function of $1/r$. When D is much less than $\lambda/2\pi$, the antenna approximates a point source, and the phase is a function of the distance r from the source. When the dimension D approaches $\lambda/2\pi$, a correction for phase error may be made, as described in Section 2.2.2. The phase error expressed, in degrees, can be defined as the difference in the following path lengths: between the closest point of the antenna to the measuring point and the furthest point of the antenna to the measuring point.

For a high-gain antenna, the interface distance is often considered to be

$$r > \frac{4D^2}{\lambda}$$

at which distance the phase error is less than 22.5°. For the equation to be useful, the aperture dimension of the antenna, D, should be large compared to the wavelength. In the far-field region, Z_W is equal to the intrinsic impedance of free space, which is commonly expressed as either ($R_c Z_c$, n or p).

The intrinsic impedance of free space is equal to

$$\sqrt{\frac{\mu_o}{\epsilon_o}}$$

which is 376.7 Ω, or very nearly 120π or 377 Ω. As we have seen, μ_o is the permeability of free space ($4\pi \times 10^{-7}$ [H/m]) and ϵ_0 is the dielectric constant of free space ($1/36\pi \times 10^9$ [F/m]).

At large distances from a short antenna, phase differences can be ignored and the resultant field can be termed a *plane wave* with an electric field intensity proportional to

$$\frac{2(377)Il}{\pi\lambda r}$$

For a plane wave, the electric and magnetic field intensities in free space are always in phase and perpendicular to each other and to the direction of propagation. Often the electric wave from an antenna is more complex with regard to phase and doubly so in the near or induction field of an antenna.

In problems of EMC, unintentional sources of electromagnetic emissions are primarily from current loops or current elements, whether from PCB tracks, intraunit, interunit, or system wiring and cables. Thus we shall concentrate on fields from current loops and current elements and in the current induced into loops and short lengths of conductor by electromagnetic fields.

2.2.2 Current Elements as Radiators

A *current element* is defined, for the purpose of EMC, as an electrically short length (i.e., $l < \lambda$) of current-carrying conductor connected to the current source at one end and disconnected, or at least connected via a high impedance, from ground at the other end. Strictly, the current source should be disconnected from ground at both ends. The practical use of an isolated wire to which no generator or return current path is connected as a model in EMC predictions may appear extremely limited. However, a practical example is in the modeling of a shielded cable on the center conductor of which a current flows and returns on the inside of the shield. In our example, the shielded cable is connected to a well-shielded enclosure at each end. If the shield of the cable is not perfect, then some small fraction of the current flowing on the inside of the shield will diffuse through the shield to the outside. If the length of the cable is less than the wavelength, λ, then the current flow on the outside of the shield will reduce to zero at the termination with the enclosures at both ends and remain relatively constant over the length of the cable.

For certain cable and measuring distance configurations, discussed later, the electric current element model may be used with either one or both ends connected to a return path. In addition, the electric current element model is strictly valid when the distance from a plane conductor or ground plane is much greater than the wavelength. When the proximity is closer, the current element equations may be used and corrected for the effect of reflections in the plane conductor, as discussed in Section 9.3.2. When the proximity of the ground plane is much less than the wavelength, λ, and the length of the current element is equal to or greater than λ, then the equation for radiation from a transmission line contained in Section 7.6 is applicable.

The current on a current element is assumed to be constant over its length. When applying the formulae for the current element to an electrically short length of wire or cable (i.e., $l < 0.1\lambda$) disconnected from ground at both ends, then the current distribution is as shown in Figure 2.11a, and the electromagnetic radiation from the short wire is approximately half of the value of the current element. The current distribution for a length of wire which is resonant (i.e., $l = 0.5\lambda$) is sinusoidal, as shown in Figure 2.11b, and the radiation is approximately 0.64 that of the current element. A more accurate approach that is particularly useful when the length of the wire is greater than the wavelength, as shown in Figure 2.11c, is to break up the wire into a number of current elements and compute the composite field from all sources. If the distance from the wire, at which the magnitude of the field is required, is much closer than the wavelength, then the current element equations may be used with no correction, because the contribution to the total field from the current elements at some distance from the point of calculation is negligibly small. Even where the wire is terminated at one or both ends, the current element equation

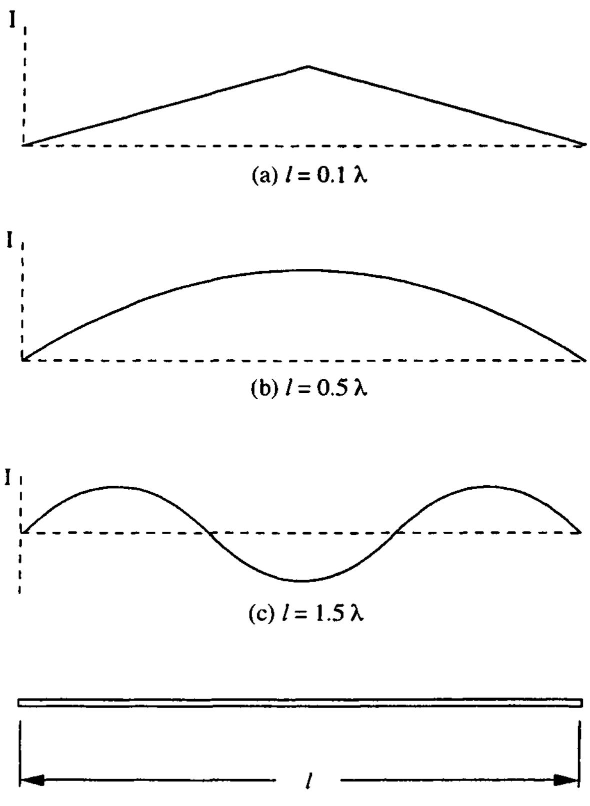

Figure 2.11 Current distribution on a wire of length l.

may still be used at close proximity, as long as the return current path is at a large electrical distance from the wire. If, as often happens, the return path is in close proximity, then the formulae for fields from either a transmission line or a current loop, whichever is applicable, should be used. In calculating the field strength, the magnitude of the current flow on the wire must be known. The current may be calculated; however, a simpler approach is to measure by means of a current probe.

Thus we see from the foregoing discussion that the current element, as a model, has more practical applications than may at first be realized.

2.2.3 Current Loops

The current loop is a valuable model for use in predicting radiation and coupling. The cable connecting two units in a rack or two units mounted one upon the other often forms a loop. Likewise, where a cable is routed along the ground or in a cable tray and then is connected to equipment, a loop is often formed. The wiring inside an enclosure (or the tracks on a printed circuit board, PCB) often takes the shape of a loop. Another use of the current loop model is in the design of a simple antenna, which may be constructed and used as either a source of, or to measure, magnetic fields.

2.2.4 Spherical Waves

To understand spherical waves (i.e., those present close to an antenna or an electric current element or loop), we shall use the spherical coordinate system. Figure 2.12 shows the field vector around an electric current element, sometimes referred to as an *infinitesimal dipole*. The simplified field equations for a nondissipative medium such as air are

$$E_\theta = \left(jRc\frac{I_S}{2\lambda r}\right)\left(1 - \frac{\lambda^2}{4\pi^2 r^2} - j\frac{\lambda}{2\pi r}\right)\sin\theta \tag{2.9}$$

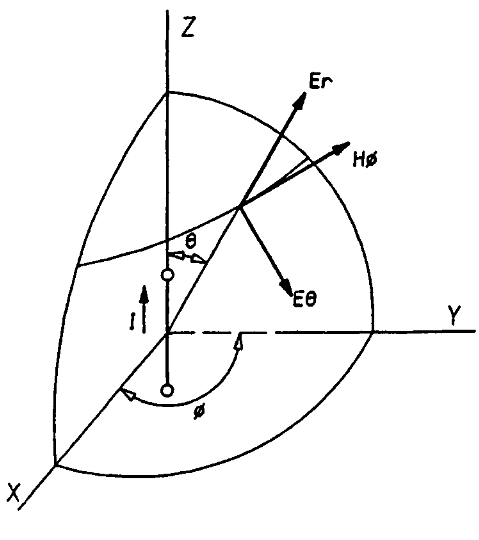

Figure 2.12 Field vector around electric current element.

$$H_\phi = \left(j\frac{I_S}{2\lambda r}\right)\left(1 - j\frac{\lambda}{2\pi r}\right)\sin\theta \tag{2.10}$$

$$E_r = \left(\frac{Z_W I_S}{2\pi r^2}\right)\left(1 - j\frac{\lambda}{2\pi r}\right)\cos\theta \tag{2.11}$$

Expressed as magnitudes, these become

$$|E_\theta| = 377\frac{I_S}{2\lambda r}\sqrt{1 - \left(\frac{\lambda^2}{4\pi^2 r^2}\right)^2\left(\frac{\lambda}{2\pi r}\right)^2}\sin\theta \tag{2.12}$$

$$|H_\phi| = \frac{I_S}{2\lambda r}\sqrt{1 - \left(\frac{\lambda}{2\pi r}\right)^2}\sin\theta \tag{2.13}$$

$$|E_r| = 377\frac{I_S}{(2\pi r)^2}\sqrt{1 - \left(\frac{\lambda}{2\pi r}\right)^2}\cos\theta \tag{2.14}$$

In the far field of the electric current element, where we assume $r/\lambda \gg \pi/2$, and using the intrinsic impedance of free space (377) for Z_W, the field equations simplify to

$$E_\theta = j\left(\frac{60\pi I_S}{\lambda r}\right)\sin\theta \tag{2.15}$$

$$H_\phi = j\left(\frac{I_S}{2\lambda r}\right)\sin\theta \tag{2.16}$$

$$E_r = 60\frac{I_S}{r^2}\cos\theta \tag{2.17}$$

In the far field it can be seen that E_θ and H_ϕ are the predominant radiation components, with E_r as the induction (or reactive) component that soon decays at large distances from the current element.

The open-circuit voltage induced in the loop is

$$V_{ab} = -j2\pi f\,\mu_o H_\phi S \tag{2.18}$$

where

μ_o = permeability or inductivity of air or vacuum, $4\pi \times 10^{-7}$ [H/m]
S = area of the loop
$\mu_o H_\phi = B$ = flux density

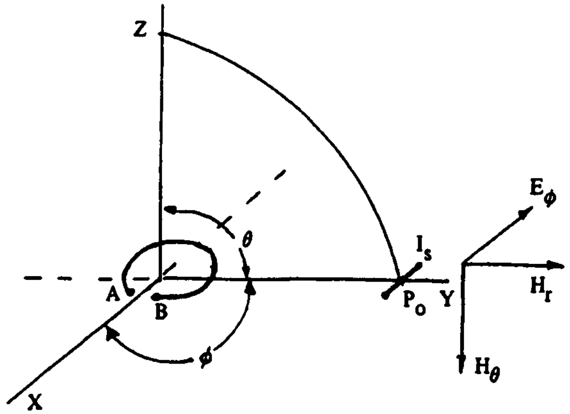

Figure 2.13 Field vector around a current loop depicts a small loop with a current element at position P_o.

The value of H_ϕ can be found from the current I flowing in the current element at position P_o in Figure 2.13 and from Eqs. (2.10) and (2.18) as follows:

$$V_{ab} = -j\omega\mu\left(\frac{j\beta I_S}{4\pi r}\right)\left(1 + \frac{1}{j\beta r}\right)S \tag{2.19}$$

where $\beta = 2\pi/\lambda$. As a magnitude, this is

$$|V_{ab}| = 2\pi f\mu\left(\frac{\beta I_S}{4\pi r}\right)\sqrt{1 + \left(\frac{1}{\beta r}\right)^2}\, S \tag{2.20}$$

2.2.5 Receiving Properties of a Loop

From Eq. (2.18), the receiving properties of the loop can be expressed as

$$V = 2\pi f\mu_o H_\theta S \cos\theta = \frac{2\pi Z_W H_\theta S \cos\theta}{\lambda} = \frac{2\pi E_\phi S \cos\theta}{\lambda} \tag{2.21}$$

where θ is the angle between the normal, or perpendicular, to the plane of the loop and the magnetic intensity H_θ, as shown in Figure 2.13.

Equation (2.21) gives the open-circuit receiving properties of a loop. The impedance of the loop and the impedance across which the voltage is developed must be accounted for when predicting either the voltage developed across the load or the current flowing in the loop. In Chapter 7, on cable coupling, the EMI voltage induced in a loop formed by a wire or cable by a field is examined further.

The inductance of a loop of wire or a wire above a ground plane, which forms a loop with its electromagnetic image in the ground plane, is given by

$$L = \frac{\mu_0}{\pi}\left[l \ln\frac{2hl}{a(l + d)} + h \ln\frac{2hl}{a(h + d)} + 2d - \frac{7}{4}(l + h)\right] \tag{2.22}$$

where a is the radius of the wire, in meters, l is the length of the wire, in meters, h is either the distance between the wires or twice the distance between the wire above a ground plane to account for the electromagnetic image of the wire in the ground plane, and

$$d = \sqrt{(h^2 + l^2)}$$

The impedance of the loop and load as a magnitude is

$$Z = \sqrt{(Z_L^2 + 2\pi f L^2)}$$

With current applied to the loop and assuming even current distribution around the loop (i.e., $S \ll \lambda$), the field components at any point around the loop can be found from

$$E_\phi = \frac{R_c \beta^2 IS}{4\pi r}\left(1 + \frac{1}{j\beta r}\right) e^{-j\beta r} \sin\theta \tag{2.23}$$

$$H_\theta = \frac{\beta^2 IS}{4\pi r}\left(1 + \frac{1}{j\beta r} - \frac{1}{\beta^2 r^2}\right) e^{-j\beta r} \sin\theta \tag{2.24}$$

$$H_r = \frac{j\beta IS}{2\pi r^2}\left(1 + \frac{1}{j\beta r}\right) e^{-j\beta r} \cos\theta \tag{2.25}$$

Expressed as magnitudes, these become

$$|E_\phi| = 377\frac{\beta^2 IS}{4\pi r}\sqrt{1 + \frac{1}{\beta^2 r^2}} \sin\theta \tag{2.26}$$

$$|H_\theta| = \frac{\beta^2 IS}{4\pi r}\sqrt{\left(1 + \frac{1}{\beta^2 r^2}\right)^2 + \frac{1}{\beta^2 r^2}} \sin\theta \tag{2.27}$$

$$|H_r| = \frac{\beta IS}{2\pi r^2}\sqrt{\left(1 + \frac{1}{\beta^2 r^2}\right)} \cos\theta \tag{2.28}$$

These equations are useful in computing the fields generated by a current loop in the induction field, in the near field, and in the far field. For example, Eq. (2.28) may be used to obtain the approximate value of the radial induction/near field when the radius of the loop is less than the measuring distance. Equation (2.28) should always be used when the measuring distance is greater than six times the radius of the loop. At low frequencies and for distances closer than the radius of the loop, Eq. (2.7) or (11.1), which provides the DC or quasi-static radial field, should be used.

In order to examine the ratio between E and H fields generated by a loop, as shown in Figure 2.13, the values of E and H fields from a 0.01-m circular loop with a generator current

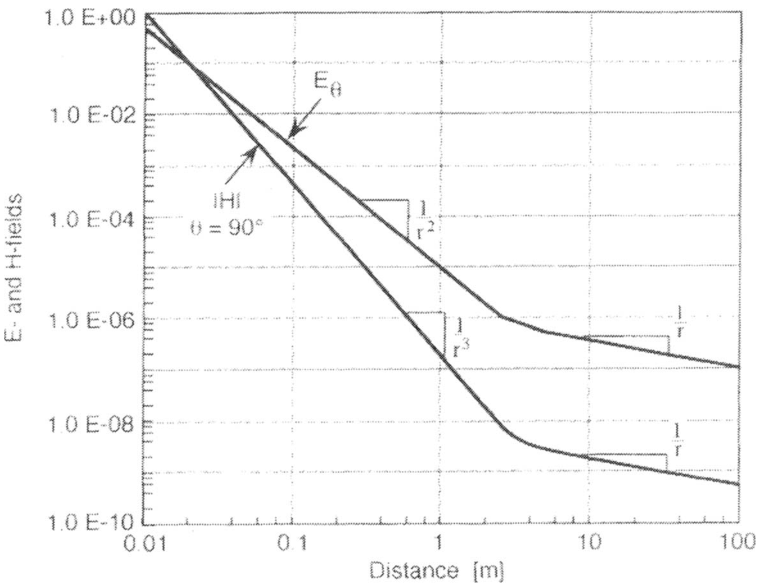

Figure 2.14 *E* and *H* fields vs. distance.

of 1 mA at 10 MHz is plotted against distance from the loop in Figure 2.14. In Figure 2.16 the ratio E/H (i.e., the wave impedance) has been plotted. It can be seen that the near-field/far-field interface for the small current loop is at approximately 4 m, which corresponds well with the definition of $\lambda/2\pi = 30$ m/6.28 = 4.7 m. The wave impedance for the small current loop is given by

$$Z_W = \frac{Z_c 2\pi r}{\lambda} \leq 377\ \Omega \tag{2.29}$$

(e.g., at 0.1 m, $Z_W = 7.9$, and this is called a *magnetic* or *low-impedance field*).

Also, from Figures 2.14 and 2.15 it can be seen that in the near field, H_θ reduces as a function of $1/r^3$, as does H_r, whereas E_ϕ reduces as a function of $1/r^2$ (where r = distance). Had we been examining a small dipole or current element (i.e., $1 \ll \lambda$), then E_θ would have followed a $1/r^3$ law with distance and H_ϕ a $1/r^2$. The wave impedance would then equal

$$Z_W = \frac{Z_c \lambda}{2\pi r} \geq 377\ \Omega \tag{2.30}$$

and the field is then called an *electric* or *high-impedance field.* It appears from Figure 2.16 that the wave impedance increases above 377 close to the $\lambda/2\pi$ transition zone, which is not true. Instead a transition zone exists, and the $(1/r^2)$-to-$(1/r)$- and the $(1/r^3)$-to-$(1/r)$ transitions are not abrupt. Numerous measurements on a single current-carrying cable and on multiple cables located on a nonconductive table 1 m above the floor in a shielded room have confirmed that the current element is the correct model for the cable configuration. The measurements have also shown that the transition zone exists. It has been seen from a number of the measurements that the circumferential magnetic field H_θ from a cable reduces approximately as a function of $1/r^2$ up to a certain distance, thereafter reducing by $1/r^{1.5}$ up to a certain distance, and thereafter reducing by $1/r$.

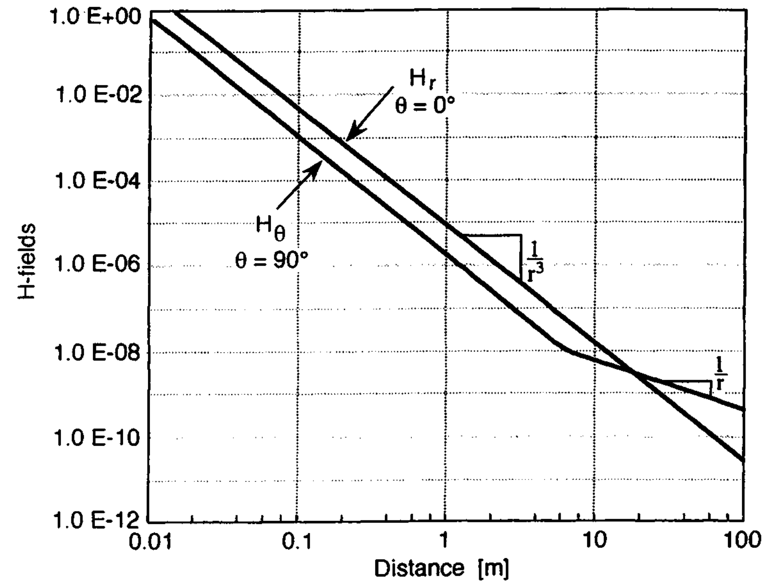

Figure 2.15 H_θ and H_r vs. distance.

Chapter 9 and Section 9.3.2 discuss measurement techniques and compare predictions, based on cable current magnitude, to measured levels and reduction with distance. Equations 2.26, 2.27, and 2.28 are valid when the loop is electrically small (i.e., the perimeter is much less than the wavelength).

For a large loop, where the perimeter approaches one-half the wavelength, standing waves

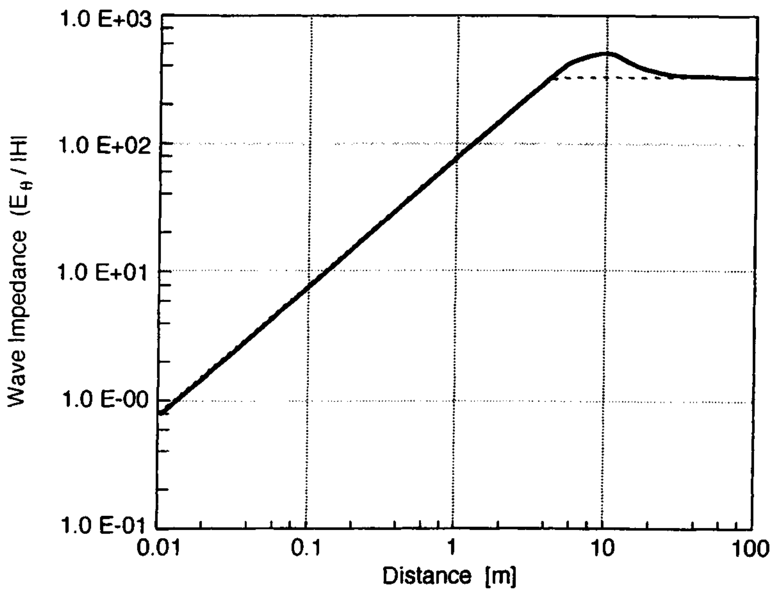

Figure 2.16 Wave impedance vs. distance.

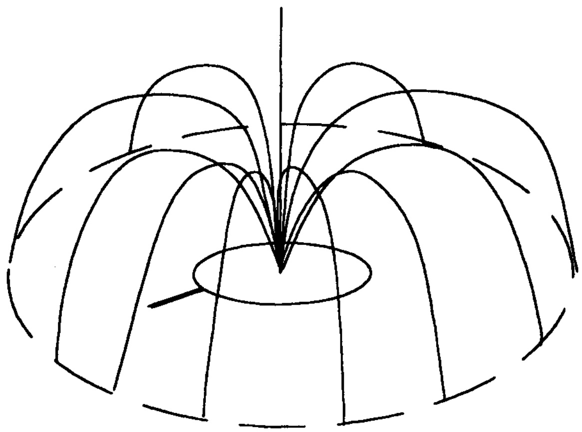

Figure 2.17a Radiation pattern for a small loop, E_ϕ, $P < 0.1\lambda$.

are generated on the loop and the current is no longer constant around the loop. At frequencies where the ratio P/λ, where P is the perimeter of the loop, in meters is 0.5, 1.5, 2.5, . . . , the loop exhibits the characteristics of a parallel resonant circuit (termed an *antiresonance*), and the input current and radiation from the loop are greatly reduced.

At frequencies where the ratio P/λ is 1, 2, 3, . . . , the loop behaves as a series resonant circuit, and the current is limited only by the DC and radiation resistance.

The input impedance of the loop is a minimum at resonance and a maximum at an antiresonance. For example, when the circumference of the loop P is equal to λ, the input impedance is approximately 100 Ω, and when $P = 2\lambda$, the input impedance is approximately 180 Ω. At the first antiresonance, when $P = 0.5\lambda$, the input impedance is approximately 10 kΩ; and when $P = 1.5\lambda$, the input impedance is from 500 Ω to 4000 Ω, depending on the ratio of the radius of the loop to the radius of the conductor.

In addition, the radiation pattern changes, with reduced radiation from the plane of the large loop and maximum radiation from the plane of the small loop; these are the E_ϕ field of Figure 2.13. Figures 2.17a and 2.17b illustrate the E_ϕ radiation pattern for the small loop and

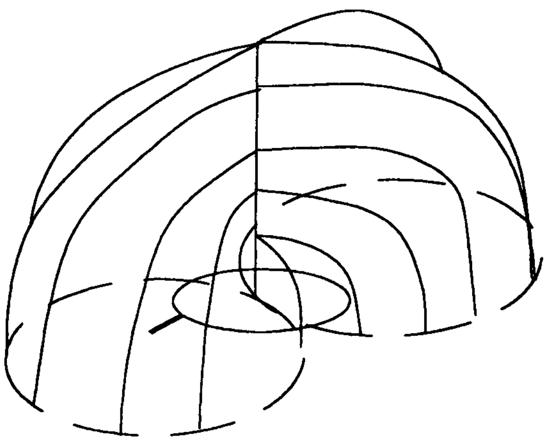

Figure 2.17b Radiation pattern for a large loop, E_ϕ, $P = \lambda$.

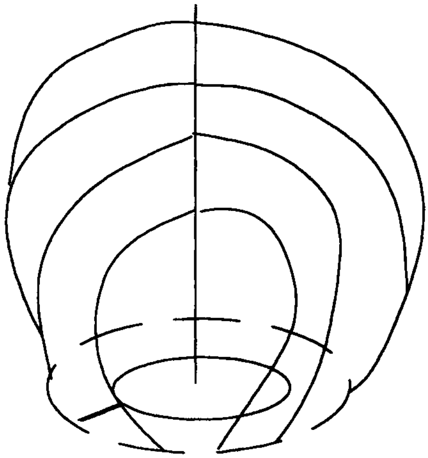

Figure 2.17c Radiation pattern for a large loop, E_θ, $P = \lambda$.

the large loop, where $P = 0.1\lambda$ and λ, respectively. With the large loop in addition to the E_ϕ field, which is small in the vertical plane, a second component E_ϕ, which has a maximum value in the vertical plane and is zero in the horizontal plane, is generated. Figure 2.17c shows the radiation pattern for the E_θ field. The directivity in the vertical plane (at 90° to the plane of the loop, where $\theta = 0$) with sinusoidal current distribution around it is provided in Table 2.1. The power gain of the loop, when the ratio of the radius of the loop to the radius of the conductor is 30, is 1.14 when $P = 0.6\lambda$ and 3.53 when $P = 1.2\lambda$.

The radiation resistance of the large loop, compared to 31,200 $(\pi a^2/\lambda^2)^2$ for a small circular or rectangular loop, is shown in Figure 2.18 from Ref. 5.

2.2.6 Far-Field Radiation from a Twisted Wire Pair

The EMC literature contains a model for the prediction of radiation from a twisted pair based on the model of a helix described in Ref. 5. For a helix whose dimensions are much less than the wavelength, the radiation is primarily from the sides of the helix, and the axial-mode radiation is at a minimum.

Table 2.1 Directivity of the E_θ Field for a Large Loop

P/λ	Directivity
0.2	0.7
0.4	0.9
0.6	1.12
0.8	1.3
1.0	1.5
1.2	1.58
1.4	1.67
1.6	1.58
1.8	1.25
2.0	0.75

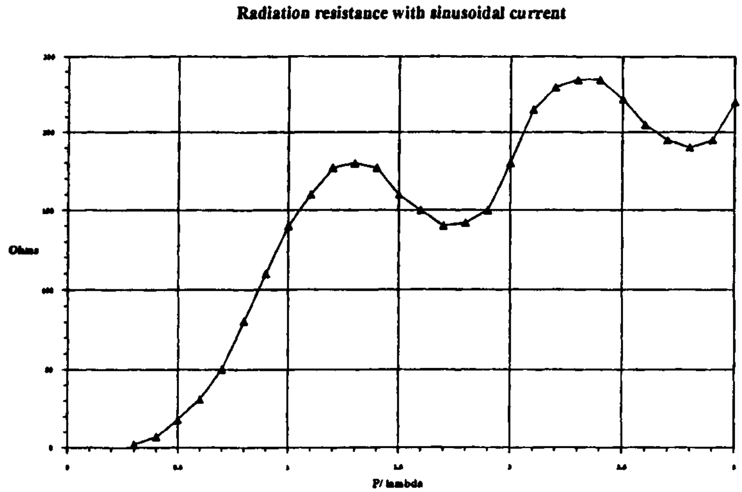

Figure 2.18 Radiation resistance of large loop.

The helix may be modeled as a series of small current loops and current elements, as shown in Figure 2.19a, and this model may be of use in an EMC prediction where a single wire takes the form of a helix. In this case, the far-field radiation is found from the sum of the loop and element sources. The physical layout of a twisted pair is shown in Figure 2.19b, from which it is seen that the twisted pair forms a bifilar helix in which both helices are identical but displaced in position axially down the length of the pair. The axial displacement is determined by the distance between the two wires. An important parameter in controlling the radiation from the pair is the distance between the wires and the pitch of the twist. Decreasing both the distance and the pitch will decrease the radiation. For commercially available twisted-pair wire made up as a cable, the distance between the two wires is approximately 0.3 cm, and the pitch is from 3.8 to 4.4 cm. The current elements in the equivalent circuit are therefore longer than the diameter of the loops in this practical example.

Because the two helices are axially in the same plane and the current flow is in opposite directions, the equivalent circuit is as shown in Figure 2.19c. Assuming an even number of twists with the total length of the pair less than 0.5λ, we may see from the equivalent circuit

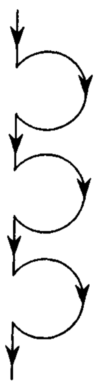

Figure 2.19a Equivalent circuit of a helix comprised of current elements and current loops.

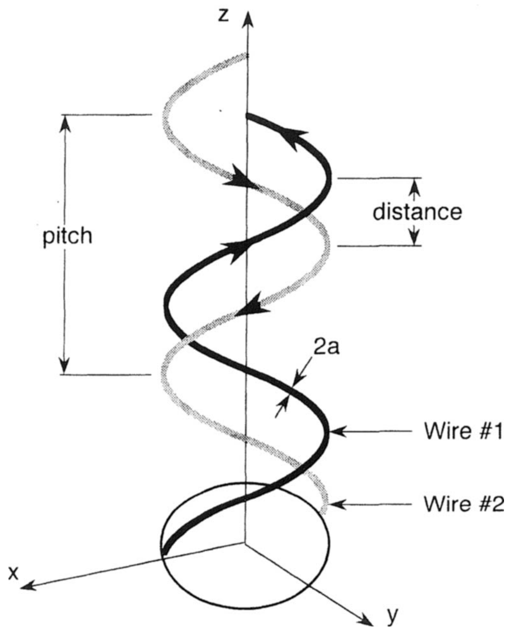

Figure 2.19b Physical layout of a twisted wire pair illustrating the bifilar helix form of the cable.

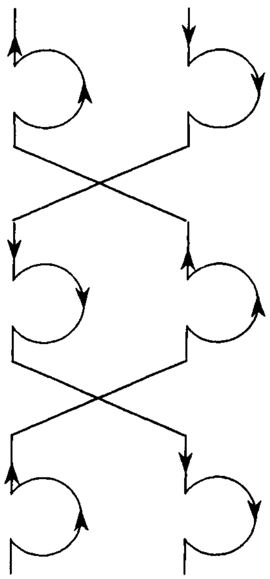

Figure 2.19c Equivalent circuit of a twisted pair.

that the fields from the current elements and current loops tend to cancel at a considerable distance from the source. This is not surprising, based on the physical layout of the pair. Measurements from a twisted pair have confirmed that the far-field radiation is lower than for an untwisted pair.

Where the total length of the twisted-pair line is greater than 0.5λ, the current flow in the two wires changes direction at some point down the length of the pair, and the cancellation of fields from the loops and elements is not as complete. In the limiting case where the pitch is equal to the wavelength, the axial radiation from two adjacent loops and current elements tends to add, and the level of radiation is higher than for an untwisted-pair cable. This occurs for the majority of twisted pairs in the gigahertz frequency range, which is typically, but not exclusively, above the frequency of emissions from unintentional sources, such as logic and converters.

The major source of radiation from the twisted pair is not from loops and elements but from the common-mode current, which inevitably flows on both conductors of the cable. One source of common-mode current is displacement current, which flows in the space between the two conductors; this source, along with others, is discussed in Section 7.6.

Likewise, when a field cuts a twisted-pair cable, the induced differential-mode currents are at a relatively low magnitude, whereas the common-mode current is identical to that of an untwisted pair. Calculations for differential-mode voltage and common-mode current flow resulting from an incident field and the effect of unbalanced input impedance on the noise voltage developed are discussed in subsequent chapters.

2.3 RADIATED POWER

In addition to E and H fields, we may consider antenna transmitted and received power. *Radiated power* is defined as the average power flow per unit area and is expressed in watts per square meter. In a perfect, lossless, isotropic antenna, the power is radiated equally in all directions and must pass through every sphere of space. The relationship between the power and the E and H fields is given by the Poynting vector cross-product

$$\vec{P} = \vec{E} \times \vec{H}$$

The Poynting vector is merely a convenient method of expressing the movement of electromagnetic energy from one location in space to another, and it is not rigorous in every instance when applied to antennas. It has been shown that in the far field, the ratio E/H is a constant and is termed the *wave impedance*. In the far field, the E and H fields are mutually perpendicular and perpendicular to the direction of propagation. Therefore,

$$P = EH = \frac{E^2}{Z_W}$$

Because the E and H fields each decay by the factor $1/r$ in the far field, the power decays by the factor $1/r^2$ and the radiated power is then

$$W = \frac{P_{\text{in}}}{4\pi r^2} \quad [\text{W/m}^2] \tag{2.33}$$

The $1/4\pi r^2$ term may be visualized by considering the power flow as spreading out from the source in the form of a sphere. If the radiation pattern were truly in the shape of a sphere, then the source would be an isotropic radiator. No practical antenna is an isotropic radiator; the least directive radiator is a current element and a current loop, both of which have the same radiation pattern.

The antenna gain is a measure of the "directivity" of the antenna. In antenna terminology, the term *directivity* is reserved to describe the ratio of power at beam peak, assuming no losses, to the power level realized with the same input power radiated isotropically. Where ohmic losses in the antenna are low and cable/antenna impedances are matched, the directivity D and the gain G are virtually the same. The gain is defined as the ratio

$$\frac{4\pi W_{\text{max}}}{P_{\text{in}}}$$

where P_{in} is the antenna input power. The gain of the perfect isotropic antenna is thus 1. Neither the equation for radiated power nor that for antenna gain is valid in the near field of the antenna. The received power of a receiving antenna is likewise not constant in the near field nor equal to the gain in the far field, because near-field contributions radiating from the antenna, which would be in phase in the far field, can cancel in the near field. The radiated power at a distance r from an antenna with gain G is given by

$$W = \frac{GP_{\text{in}}}{4\pi r^2} \tag{2.34}$$

The input voltage to the antenna for a given input power is

$$V_{\text{in}} = \sqrt{P_{\text{in}} R_{\text{in}}}$$

where R_{in} is the antenna input or radiation resistance.

The E field generated by the antenna, using V_{in} and assuming the antenna input impedance is 50 Ω and equals the radiation resistance, is given by

$$E = \frac{V_{\text{in}}}{r\sqrt{628/Z_W G}} \tag{2.35}$$

where r is the distance from the antenna, in meters.

The *radiation resistance* is defined as that part of the antenna impedance that contributes to the power radiated by an antenna. In the case of a resonant antenna, such as a dipole, the antenna input impedance equals the radiation resistance. For the tuned dipole, the input impedance equals 70–73 Ω, and for a tuned monopole it equals 30–36 Ω, depending on the radius of the conductors used and assuming the conductor radius is small compared to the antenna length. We use the term *tuned* to denote that the antenna length has been adjusted so that the antenna is resonant at the frequency of interest.

For an electrically small dipole or monopole antenna, where l, which is the length of one arm, is much less than $\lambda/4$, the input impedance is predominantly capacitive and is higher than the resonant value. The radiation resistance is then only a small fraction of the input impedance.

The *effective area* of an antenna (A_e) is defined as the ratio of the power received at the antenna load resistance (P_r) to the power per unit area of incident wave (W). If the antenna impedance is matched to the load impedance, then $P_r = WA_e$.

The effective capture area, or *aperture*, of a receiving antenna (A_e) is dependent on the actual area and efficiency of the antenna. The physical area of a rectangular-aperture antenna, such as the horn antenna, is the length times the width. For a circular antenna, such as a dish, the area is πr^2. The effective aperture is the physical aperture times the aperture efficiency, η_a. For example, η_a is approximately 0.5 for a dish antenna. The effective area can be expressed in terms of gain, thus

$$A_e = \frac{G\lambda^2}{4\pi} \tag{2.36a}$$

So

$$G = \frac{4\pi A_e}{\lambda^2} \quad \text{and} \quad P_r = \frac{WG\lambda^2}{4\pi}$$

The $\lambda^2/4\pi$ term does not imply that with increasing frequency, waves decrease in magnitude. It means that at higher frequency, the area over which a given power flow occurs is smaller.

The equation for gain must also include a correction for losses. In the specified aperture efficiency for an antenna, losses due to reflections caused by a mismatch between the transmission line driving the input terminals of the antenna and the antenna input impedance should be included. Where aperture efficiency or realized gain is not specified and Eq. (2.36) is used to determine the gain of an antenna, any loss due to transmission-line-to-antenna impedance mismatch must be calculated to arrive at the realized gain (G_{re}). G_{re} equals $G \times L$, where L is the loss. The loss may be found from the transmission line/antenna reflection coefficient, K, using $L = 1 - K^2$:

$$K = \frac{1 - Z_{ant}/Z_L}{1 + Z_{ant}/Z_L} \tag{2.36b}$$

where

Z_{ant} = antenna input impedance
Z_L = impedance of the transmission line connected to the antenna

For two antennas in free space in the far-field region, both polarization matched and ignoring losses in cables baluns and due to impedance mismatch, the received power is given by combining Eq. (2.34) for transmitted power, using the antenna input power, with the equation for received power (Eq. 2.36a), which gives

$$P_r = \left(\frac{G_t P_{in}}{4\pi r^2}\right)\left(\frac{G_r \lambda^2}{4\pi}\right) \tag{2.37}$$

which may be simplified to Eq. (2.38):

$$P_r = P_{in} G_t G_r \left(\frac{\lambda}{4\pi r}\right)^2 \tag{2.38}$$

where

P_r = received power at the input of the receiving device
P_{in} = input power to transmitting antenna
G_t = gain of transmitting antenna
G_r = gain of receiving antenna

If we express the received power in dbW and the antenna gains in decibels, then Eq. (2.38) is

$$P_r = P_t + G_t + G_r - 20 \log \left(\frac{4\pi r}{\lambda}\right) \tag{2.39}$$

The received power is readily converted to voltage at the input of the receiver when the receiver input impedance is known (assuming the cable impedance matches the terminating impedance) by $V = \sqrt{P_r Z_{in}}$. The power equation is useful in calculating free-space propagation loss in the basic antenna-to-antenna EMC prediction. For this prediction, additional factors due to the unintentional nature of the coupling have to be accounted for. Some of these additional factors, which are discussed in Chapter 10, are:

Non line-of-sight coupling
Antenna polarization and alignment losses
Intervening atmospheric effects
Frequency misalignment losses

2.4 UNITS OF MEASUREMENT

The unit dBW was used to describe power; the following are some definitions of commonly used units.

dB: The decibel (dB) is a dimensionless number that expresses the ratio of two power levels. It is defined as

$$\text{dB} = 10 \log \frac{P_2}{P_1}$$

The two power levels are relative to each other. If power level P_2 is higher than P_1, then dB is positive; vice versa, dB is negative. Since

$$P = \frac{V^2}{R}$$

when voltages are measured across the same or equal resistors, the number of decibels is given by

$$\text{dB} = 20 \log \frac{V_2}{V_1}$$

A rigid voltage definition of dB has no meaning unless the two voltages under consideration appear across equal impedances. Thus above some frequency where the impedance of waveguides varies with frequency, the decibel calibration is limited to power levels only.

dBW: The decibel above 1 W (dBW) is a measure for expressing power level with respect to a reference power level P_1 of 1 W. Similarly, if the power level P_2 is lower than 1 W, the dBW is negative.

dBm: The decibel above 1 mW in 50 Ω. dBm = 1 mW = 225 mV (i.e., 225 mV^2/50 = 1 mW). Since the power level in receivers is usually low, dBm is a useful measure of low power.

dB μV: The decibel above 1 μV is a dimensionless voltage ratio in decibels referred to a reference voltage of 1 μV and is a commonly used measure of EMI voltage.

μV/m: Microvolts per meter are units used in expressing the electric field intensity.

dB μV/m: The decibel above 1 μV/m (dB μV/m) is also used for field intensity measurement.

μV/m/MHz: The microvolt per meter per megahertz is a broadband field intensity measurement.

dB μV/m/MHz: The decibel above 1 μV/m/MHz.

μV/MHz: Microvolts per megahertz are units of broadband voltage distribution in the frequency domain. The use of this unit is based on the assumption that the voltage is evenly distributed over the bandwidth of interest.

The following log relationships, which have been used in this chapter to convert magnitude to decibels, are useful to remember:

$$\log(AB) = \log A + \log B$$

$$\log\left(\frac{A}{B}\right) = \log A - \log B$$

$$\log(A^n) = n \log A$$

Appendices 2 and 3 show the conversion between electric fields, magnetic fields, and power densities.

2.5 RECEIVING PROPERTIES OF AN ANTENNA

In accordance with the reciprocity theorem, certain characteristics of a receiving antenna, such as pattern shape and return loss, remain the same when the antenna is used for transmitting. Likewise, the power transfer between two antennas, not necessarily identical, is the same regardless of which is transmitting and which receiving. One important consideration when applying the reciprocity theorem is that it applies to the terminals to which the voltage is applied in the case of the source, and to the terminals to which the voltage is measured in the case of the receptor. The pattern of power reradiated by a receiving antenna is different from its radiation when used as a transmitting antenna. In problems of EMI it is often the current flow on a structure, cable, or wire that is required, and it should be remembered that the current distribution on a radiating structure is often different from that on the receptor structure, even when both structures are identical, and the power level most certainly is. An explanation for the coupling of an E field to a wire receiving antenna follows.

A field incident on the receiving antenna is assumed to have an angle of incidence that results in a voltage developed across the terminals of the antenna. This open circuit voltage V is proportional to the effective height, sometimes referred to as the effective length, of the antenna, which is seldom equal to the physical height of the antenna; thus, $V = h_{\text{eff}}E$. For aperture antennas, the ratio between the power developed in the antenna load and the incident power is known as the *effective aperture* of the antenna.

When the antenna input impedance equals the load impedance, a division of 2 occurs in the antenna received voltage. When the antenna impedance is greater than the load impedance, the voltage division is greater than 2. The loss due to antenna/load impedance mismatch is accounted for in the equation for the gain of the antenna, which is a term in the equation for h_{eff}.

A second potential source of loss is due to a mismatch between the wave impedance and the radiation resistance of the antenna, and this is accounted for in determining the effective height of the antenna. The physical length of the wire antenna and the wavelength of the incident field both determine the radiation resistance and, therefore, the voltage developed.

2.5.1 Conversion of Power Density to Electric Field Intensity

For EMI measurements, the value of E and H field intensity is normally required, and it is possible to find these intensities from the power density at some distance from the source. To convert from power density P_d in the far field to electric field intensity at the measuring point:

$$P_d = \frac{E^2}{Z_W} \quad [\text{W/m}^2] \tag{2.40}$$

and

$$E = \sqrt{Z_W P_d} = \sqrt{377 P_d} \tag{2.41}$$

2.5.2 Conversion of Power Density to Electric Field Intensity in Terms of Antenna Gain

A receiving antenna is often used in EMI as a measuring device to find either the power density or the incident E field. The power density may be found from the received power developed in the antenna load resistance using Eq. (2.23):

$$P_d = \frac{4\pi P_r}{\lambda^2 G_r} \tag{2.42}$$

where

P_d = power density at the receiving antenna
P_r = power into the receiver
G_r = gain of the receiving antenna

The value of the E field may be found from the power density using $P_d = E^2/Z_W$; the E-field-to-power relationship is then $E = \sqrt{P_d Z_W}$. Using Eq. (2.42) for P_d and assuming $Z_W = 377\ \Omega$, the electric field intensity E in the far field is given by Eq. (2.24):

$$E = \frac{68.77}{\lambda}\sqrt{\frac{P_r}{G_r}} \quad [\text{V/m}] \tag{2.43}$$

Assuming the field intensity measuring instrument has an input impedance of 50 Ω and V is the voltage measured by the instrument, P_r can be found from

$$P_r = \frac{V^2}{50}$$

Then E can be expressed as

$$E = \frac{9.7V}{\lambda}\sqrt{\frac{1}{G_a}} \quad [\text{V/m}] \tag{2.44}$$

2.5.3 Antenna Factor

Antenna factor AF or K is an important calibration term; it is defined as the ratio of the electric field to the voltage developed across the load impedance of the measuring antenna, as follows:

$$\text{AF} = \frac{E}{V} \tag{2.45}$$

where

AF = antenna factor numeric
E = field strength, in volts/meter
V = voltage developed across the load

The voltage developed is given by

$$V = \frac{Eh_{\text{eff}}}{(Z_{\text{ant}} + Z_L)/Z_L} \tag{2.46}$$

Thus for an antenna where $Z_{\text{ant}} = 50\ \Omega$, $V = Eh_{\text{eff}}/2$. For a resonant dipole where $Z_{\text{ant}} = 72\ \Omega$, $V = Eh_{\text{eff}}/2.46$; and for a resonant monopole, $Z_{\text{ant}} = 42\ \Omega$, $V = Eh_{\text{eff}}/1.84$. The equation for h_{eff} is

$$h_{\text{eff}} = \frac{Z_{\text{ant}} + Z_L}{Z_L}\sqrt{\frac{A_{\max}R_r}{Z_w}} \tag{2.47}$$

where

$$\begin{aligned} A_{\max} &= \text{maximum effective aperture} = \frac{G\lambda^2}{4\pi} \\ &= 0.135\lambda^2 \text{ for a resonant dipole} \\ &= 0.119\lambda^2 \text{ for a small dipole} \\ Z_w &= \text{wave impedance} \\ R_r &= \text{radiation resistance} \end{aligned} \tag{2.48}$$

At resonance, the radiation resistance equals the antenna impedance. For a short dipole, from Ref. 5,

$$R_r = 197\left(\frac{2H}{\lambda}\right)^2$$

And for a monopole,

$$R_r = \frac{197\ (2H/\lambda)^2}{2}$$

H is the physical height of one arm of the dipole or of the rod of the monopole. The gain in Eq. (2.48) must include the loss correction for any Z_{ant}-to-Z_L impedance mismatch. This is true when Z_{ant} is higher than Z_L. However, when the load impedance is higher than the antenna impedance, the voltage developed across the load is either the same magnitude or higher than when Z_{ant} and Z_L are matched, even though reflections occur. In determining the AF, it is the ratio E/V that is of interest and not reflected power. Therefore when the load impedance is higher than the antenna impedance, K (given by Eq. 2.36b) is set to zero, the loss is zero, and the gain is unchanged.

The $Z_{\text{ant}} + Z_L$ term is included in both Eq. (2.46) for V and Eq. (2.47) for h_{eff}, and thus Eq. (2.47) may be expressed as

$$V = E\sqrt{\frac{A_{\max}R_r}{Z_W}} \tag{2.49}$$

Assuming the antenna is matched to the terminating impedance,

$$V = \frac{h_{\text{eff}}E}{2} \tag{2.50}$$

In some textbooks, either the antenna-to-load mismatch is ignored or an unterminated antenna is examined, in which case $V = h_{\text{eff}}E$. Assuming $R_r = Z_{\text{ant}} = Z_{\text{term}}$ (i.e., impedance of the antenna termination), for a dipole,

$$h_{\text{eff}} = 2\sqrt{\frac{A_{\max}Z_{\text{term}}}{Z_W}} \tag{2.51}$$

Thus for $Z_{\text{term}} = 50\ \Omega$ and $Z_W = 377\ \Omega$,

$$h_{\text{eff}} = \frac{\lambda\sqrt{G}}{4.87} \tag{2.52}$$

For a monopole, the effective height is half the value given by Eqs. (2.51) and (2.52). Using Eqs. (2.44), (2.46), and (2.52) for antenna factor and antenna height gives us

$$\text{AF} = \frac{9.73}{\lambda\sqrt{G}} \tag{2.53}$$

Expressed in decibels this is

$$\text{AF}_{\text{dB}} = 20\log\left(\frac{9.73}{\lambda}\right) - G \qquad [\text{dB}]$$

and, from Eq. (2.53),

$$G = \left(\frac{9.73}{\text{AF}\lambda}\right)^2$$

or

$$G = 20\log\left(\frac{9.73}{\lambda}\right) - \text{AF}_{\text{dB}} \qquad [\text{dB}]$$

The relationship between AF and frequency is plotted in Figure 2.20a for a number of constant-gain antennas. One example of a constant-gain antenna is the half-wave tuned resonant dipole in which the physical length of the arms are adjusted to ensure that the total length of both arms is nearly $\lambda/2$.

For example, the effective height of a half-wave dipole is given by

$$h_{\text{eff}} = \frac{\lambda}{\pi}$$

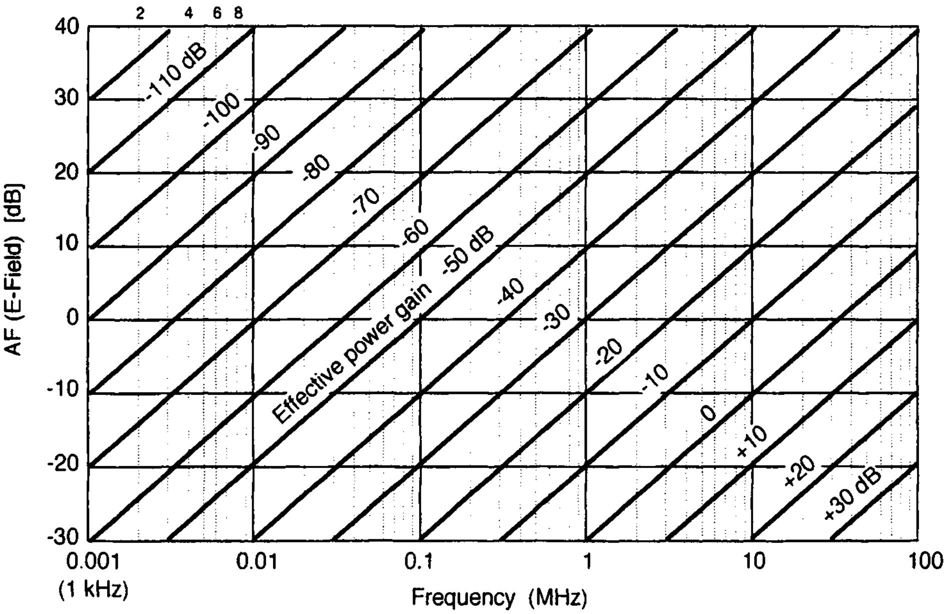

Figure 2.20a AF versus f for constant-gain antennas.

For a monopole, it is

$$h_{\text{eff}} = \frac{\lambda}{2\pi}$$

where h is the physical height of both arms of the antenna $= \lambda/2$ in free space (assuming sinusoidal current distribution and an unterminated antenna).

When the physical height of an antenna is much smaller than $\lambda/2$, the current distribution is not sinusoidal but rather of a triangular shape, with maximum current at the center and zero current at either end, and the effective height is one-half of the physical length of both arms of the dipole. For a monopole, h_{eff} is one-half of the physical length of the monopole rod.

For a true electric current element or infinitesimal dipole, $h_{\text{eff}} = h$. An equation that may be used when the physical length of the antenna is not $\lambda/2$ but is approaching this length is

$$h_{\text{eff}} = \frac{\lambda}{\pi} \tan\left(\frac{H}{2}\right) \tag{2.54}$$

where

$H = \beta h = 2\pi h/\lambda$

h = physical length of the dipole antenna or the length of the rod of the monopole antenna

H_{eff} for the monopole is one-half the value given by Eq. (2.54). The foregoing values of h_{eff} for nonterminated antennas do not include losses due to impedance mismatch, so Eq. (2.47), using gain and maximum effective area, has a more general application, especially in EMC prediction.

Consider the following example: At 100 MHz, the effective height of a half-wave dipole is 3 m/3.142 = 0.955. From Eqs. (2.45) and (2.46), and assuming far-field conditions and $Z_{term} = 50\ \Omega$ and $R_r = Z_{ant} = 70\ \Omega$,

$$\mathrm{AF} = \frac{2.4}{h_{eff}} = 2.5$$

which, expressed in decibels, is 8 dB. Figure 2.20b shows AF versus frequency for a $\lambda/2$ dipole; here the loss from the mismatch between the antenna impedance (70 Ω) and the terminating impedance (50 Ω) has been included. Manufacturers of antennas designed for EMI measurements usually publish gain and AF figures, whereas antennas designed for communications are typically supplied with gain calibration figures only. The antenna factor graphs published by manufacturers of broadband antennas are measured either on an open field site or in a semi-anechoic chamber. In either case, the results have been corrected for the effects caused by the reflection from the ground or the floor of the chamber. However, should the antenna then be used in a shielded room, as recommended in MIL STD 462 EMC test methods, where the antenna is positioned 1 m away from the equipment under test (EUT) and the ground plane, then the actual antenna factor can be greatly different from the published figures. This error is caused primarily by reflections from ceiling, walls, and floor, standing waves in the shielded room, and capacitive loading on the antenna due to ground plane proximity. Section 9.5.1 includes a description of techniques available to reduce these errors.

Where large standing waves exist, the ratio of E to H fields may vary from nearly zero to very high values (theoretically from zero to infinity), depending on the region (enclosure or cavity). In practice, the value of magnetic field measured in a shielded room is more constant than the E field.

One method of measuring the antenna factor is to use two identical antennas in the test setup shown in Figure 2.21. Two paths for the received voltage are obtained, one directly via the matching network into 50 Ω (V_{50dir}) and the second the radiated path (V_{50rad}). For two identical antennas, where $G_t = G_r$, and using Eq. (2.37), the product of the two gains is given by

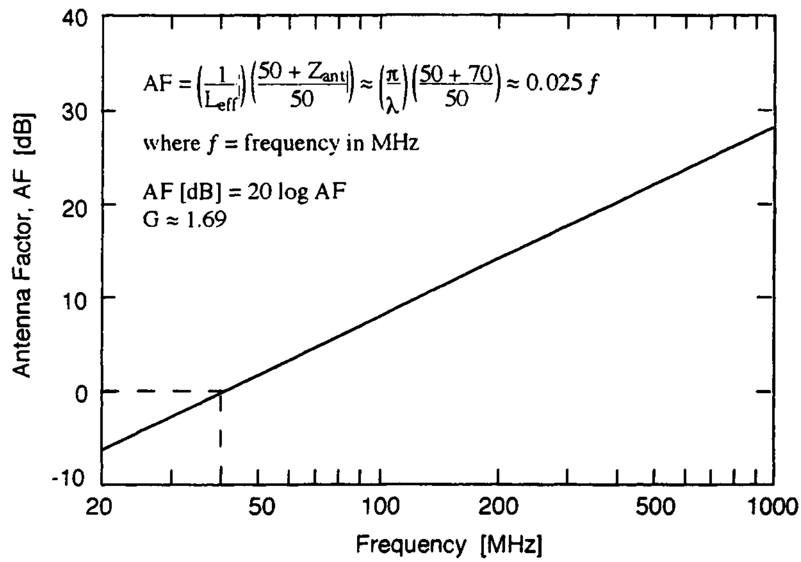

Figure 2.20b AF versus f for a $\lambda/2$ dipole and a 50-Ω receiver.

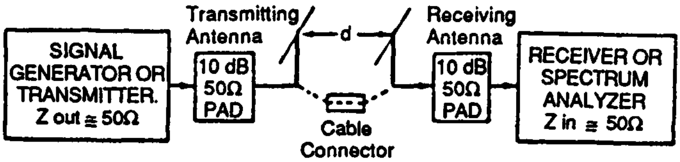

Figure 2.21 Test setup for the two-antenna method of determining AF. (From Ref. 20.)

$$G_t G_r = \frac{P_{\text{rad}}}{P_{\text{dir}}}\left(\frac{4\pi r}{\lambda}\right)^2$$

where

P_{rad} = radiated power measured by the receiver

P_{dir} = power measured by direct connection

Because $G_t = G_r$, the antenna realized gain, G_{re}, is

$$G_{\text{re}} = \sqrt{\frac{P_{\text{rad}}(50)}{P_{\text{dir}}(50)}\left(\frac{4\pi r}{\lambda}\right)^2}$$

Now

$$\frac{P_{\text{rad}}}{P_{\text{dir}}} = \frac{V_{\text{rad}}(50)^2}{V_{\text{dir}}(50)^2}$$

where $P(50)$ is the power into 50 Ω and $V(50)$ is the voltage developed across 50 Ω. Therefore,

$$G_{\text{re}} = \frac{V_{\text{rad}}(50)}{V_{\text{dir}}(50)}\frac{4\pi r}{\lambda}$$

and from Eq. (2.29),

$$\text{AF} = \frac{9.73}{\lambda\sqrt{G_{\text{re}}}}$$

If this calibration is conducted in a shielded room where subsequent EMI measurements are to be made and the receiving antenna is located at a fixed and marked location, which is then used for subsequent measurements, then the measured AF will have compensated, to a large extent, for the errors caused by reflections inherent in the test location.

Because the realized gain has been determined using this method, no further compensation due to wave-impedance-to-load-impedance mismatch is required and the near-field AF for the antenna may be obtained. It is therefore important that the distance between the two antennas, used in obtaining the AF, be duplicated when using the calibrated antenna for EMI measurements, for at different distances the AF calibration is not valid. Any loss due to the mismatch between the antenna impedance and load is also included in the measured G_{re}. It is important to ensure that the generator is able to produce the same voltage across the antenna impedance as across the 50-Ω load. When this is not the case, and the reason is a high-input-impedance antenna, then a 50-Ω load at the generator end of the cable feeding the transmitting antenna may be included during the radiated path measurement and removed during the direct measurement. This ensures that the generator load is approximately the same for the radiated and direct path measurements. When the antenna impedance is high, the receiving and transmitting antenna connecting cables should be kept short and of equal length. For maximum accuracy, the same cable should be used in measurements with the antenna. Any attenuation due to the cables is not included in the two-antenna measurement technique, and the cables should be calibrated separately.

The antenna factor for a tuned dipole using the two-antenna calibration method in a shielded room, with the manufacturer's AF curve, is plotted in Figure 2.22. By plotting the AF curve over a narrower frequency range, Figure 2.23, the effect of resonances, antiresonances, and reflections may be clearly seen, and the AF curve may be used to calculate the field magnitude with higher accuracy than when the manufacturer's curve is used. The accuracy of the AF curve is sensitive to exact antenna location and to the presence of equipment or personnel in the shielded room. Techniques that are helpful in achieving good repeatability include the installation of a plumb bob directly above the receiving antenna location used in the two-antenna test setup. This location should be chosen for its usefulness. For example, MIL-STD-462 test requirements specify a distance for the measuring antenna of 1 m from the EUT (equipment under test), which is placed 0.05 m from the edge of a table covered with a ground plane that is bonded to the shielded room wall. Thus where MIL-STD measurements are made, one or more calibration points down the length of the table at a distance of 0.95 m from the edge of the ground plane would be useful.

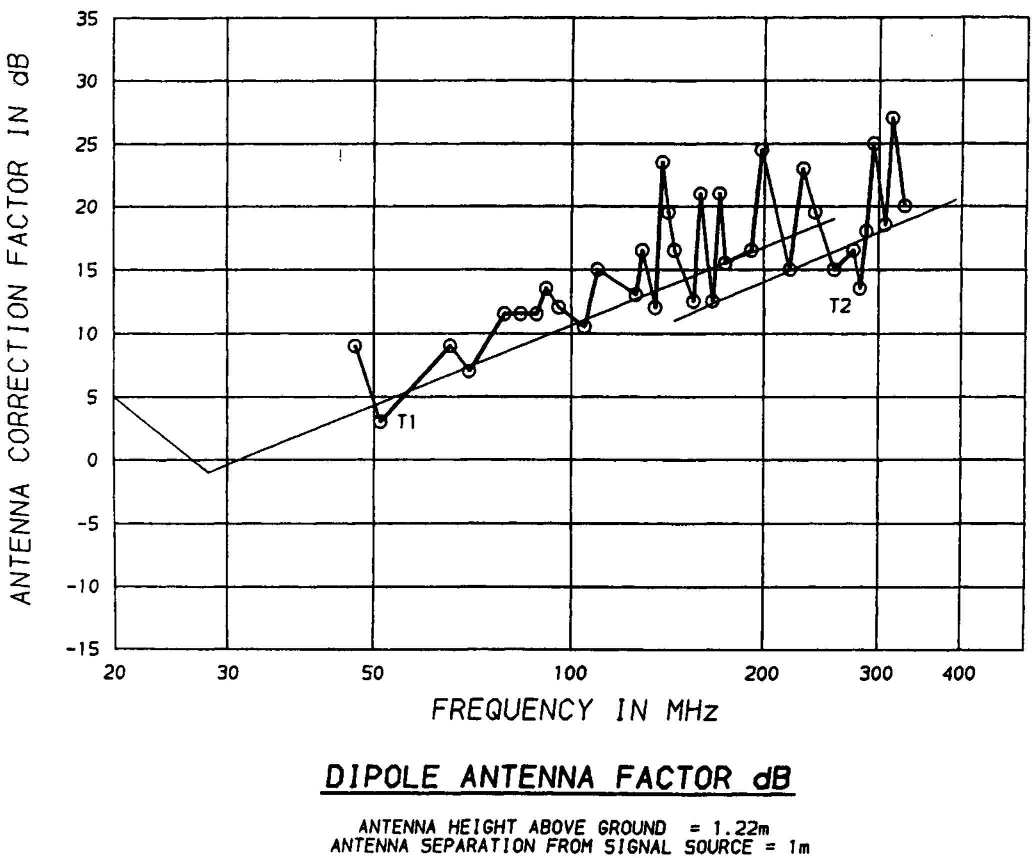

Figure 2.22 AF, in decibels, of a tuned dipole measured in a shielded room.

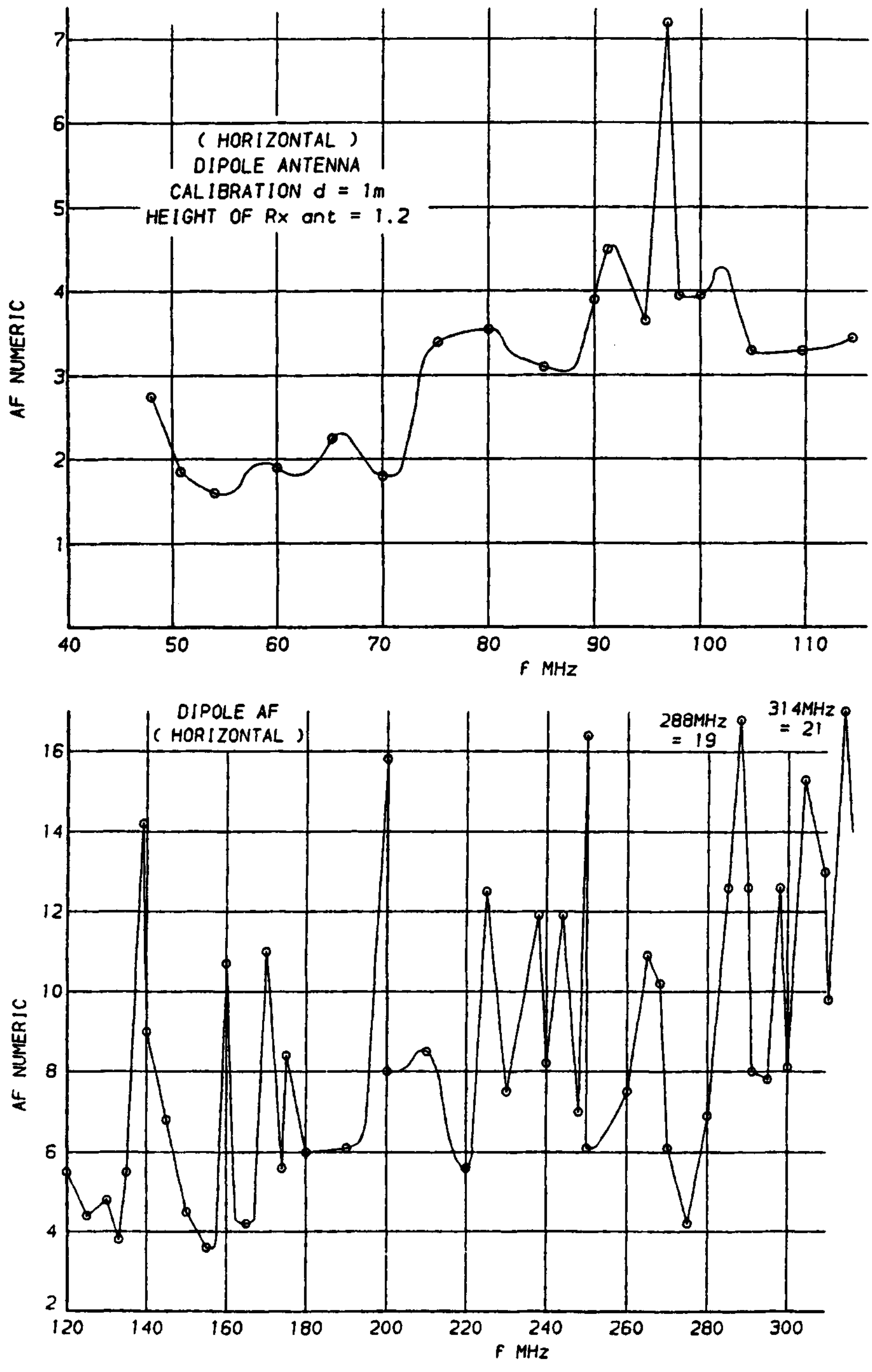

Figure 2.23 AF, numeric, for the same tuned dipole.

The antenna calibration and subsequent measurements using the antenna should be made in a room clear of equipment and personnel, or at least the same room configuration should be maintained for both.

If the two-identical-antenna test method is used for calibrating antennas to be used on an open area test site or in an anechoic chamber, then the calibration should be conducted on an open area test site. The site should preferably be without a ground plane and with the area between the two antennas covered in a combination ferrite tile and foam absorber material to absorb the reflected ground wave. Horizontal polarization of the antenna should be used to reduce the impact of the antenna feed cables, which are oriented vertically. The 6–12-dB 50-Ω attenuators should be included, as shown in Figure 2.21. Both antennas should be placed at least 4 m above the ground to reduce antenna-to-ground coupling. The distance between the antennas should be 10m to eliminate antenna-to-antenna coupling.

Alternative antenna calibration techniques are the reference Open Area Test Site (OATS) and the reference dipole calibration contained in ANSI C63.5 and described in Section 9.4.1. If correctly constructed, the four reference diopoles, designed to cover the 25–1000-MHz frequency range, will have antenna factors within 0.3 dB of theoretical. An alternative test method uses the GTEM cell, as described in Section 9.5.2.2. The antenna factor can also be calculated using either the "induced-emf method," numerical electromagnetics codes (NEC), MININEC, GEMACS, or the site attenuation. In the induced-emf method, mutual coupling between antennas is calculated by formulas given by S. A. Schelkunoff and H. E. King. These formulas usually replace the presence of the ground plane by images of the transmit and receive antenna. NEC, MININEC, and GEMACS use the moment method (MOM) to calculate the coupling between antennas, and with GEMACS using the MOM and GTD hybrid, the presence of a ground plane can be included. Reference 16 compares the accuracy of these analysis techniques to OATS, anechoic chamber, and GTEM measurements for symmetrical dipoles and horn and waveguide antennas. With symmetrical dipoles in horizontal polarization, the maximum deviation between the site-attenuation model and measurements was 3 dB. The maximum deviation between measurements and the induced emf, MOM, MININEC, and other calculations was 2.7 dB.

2.5.4 Receiving Properties of an Isolated Conductor/Cable

An *isolated cable* is defined as one disconnected from ground at both ends and at some distance from a ground plane. Although this configuration used as a model has limited practical use, one practical, albeit unusual, example of this cable configuration was, in a case of EMI, caused by coupling to a shielded cable. The cable was connected to a helicopter at one end and to equipment contained in an enclosure towed beneath the helicopter at the other end. With the helicopter airborne, the cable was isolated from ground at both ends. The more common cable configurations are discussed in detail in Chapter 7, on cable coupling; however, for the sake of completeness, here we examine coupling to an isolated cable. When a cable is disconnected from ground at both ends, the E field component of a wave that cuts the cable at an angle of 90° to its axis does not induce a current flow. In the case where a wave is incident on the cable such that the magnetic field component cuts it at an angle of 90° and the E field is in the plane of the cable, a current is induced. The magnitude of the current is determined by the length and impedance of the cable and the wavelength of the field. If the length of the cable is less than 0.1λ (i.e., nonresonant), then the average flow per second in the conductor of the cable is given approximately by

$$\frac{4\pi fBl}{Z_c}\left(\frac{\pi}{\lambda}\right)^2 \frac{(l/2)^2 - \frac{1}{2}l^2}{2}$$

where

f = frequency, in hertz
B = magnetic flux density
l = physical length of the conductor
$Z_c = \sqrt{R^2 + 2\pi fL^2}$

and where

R = total resistance of the conductor
L = total inductance of the conductor

Values of resistance and inductance for single conductors and for the shields of shielded cables are provided in Tables 5.1 and 4.2, respectively.

When the length of the cable equals $\lambda/2$, it is resonant and the characteristics of a resonant short-circuit dipole, sometimes referred to as *a parasitic element*, may be used. In a resonant dipole terminated in its radiation resistance and ignoring losses, half of the received power is delivered to the load and half the power is reradiated from the antenna. In a shorted resonant dipole, four times the power is reradiated, compared to the antenna matched dipole. The radiation resistance of the resonant dipole is approximately 70 Ω, and this is true regardless of the load. The reradiated power from the dipole is therefore $I^2 70$. Because the reradiated power for the short-circuit dipole is four times that for the matched dipole, the current flow is twice the value of that for a matched dipole.

The receiving characteristics of the dipole, described in the preceding section, may be used to find the current I in the load of a dipole. The average current in the same length of isolated cable (i.e., the short-circuit dipole) at the same frequency then has the value $2I \times 0.64$.

2.5.5 Monopole Antenna as a Measuring Device and in Prediction of Electromagnetic Compatibility

Few practical cable, wire, or structure configurations look like a dipole antenna, and thus it is not particularly useful as a model in EMC predictions. The monopole antenna is in principle a vertical wire above a ground plane, with the ground plane sometimes referred to as a *counterpoise*. The monopole receiving properties and to a lesser extent its transmitting properties are useful in EMC prediction. A cable connected to a metal enclosure, with the cable routed over a nonconductive table, may be represented by a monopole antenna as long as the far end of the cable does not connect to ground. That the cable is horizontal to the floor of the room does not change the validity of the antenna model. The far end of the cable may terminate in a small metal enclosure, in which case the model is similar to a top-loaded monopole antenna. If the far end of the cable loops down to a conductive floor, such as is found in shielded rooms, or terminates in equipment connected to ground, then the monopole model is not appropriate. Instead the model described in Section 7.4 for coupling to loops should be used. The cable, which we model as the rod of the monopole antenna, may be a shielded cable, with the shield terminating on the enclosure or a twin or multiconductor cable that terminates inside the enclosure. Whichever it is, we require the termination impedance in order to apply the monopole model. One additional good reason to examine the receiving properties of a monopole antenna is its usefulness as an EMC measurement antenna and its ease of construction. A 41-inch (1-m) monopole or rod antenna over a square-meter counterpoise is a common measurement antenna. Its useful frequency range is 14–30 MHz when it is not used as a resonant antenna. When the rod is adjustable from 1 m to approximately 0.2 m, the antenna may be used as a resonant monopole over the range 75–375 MHz. To cover the 300–1500 MHz, it is more convenient to manufacture a monopole with a smaller counterpoise, typically 30 cm by 30 cm, and a rod adjustable from 30 cm to 5 cm. For use in EMC predictions and in EMC measurements, the resonant and nonresonant characteristics of the monopole are required. When the length of the cable or rod is equal to $\lambda/4$, where λ is the wavelength of the incident field, then the antenna is resonant, the input impedance is 35–42 Ω, and the gain is 1.68 numeric. When the length of the rod is much less than λ, the gain is the same as the current element, which is 1.5, and the antenna input impedance is high.

For an electrically short monopole, the input impedance is approximately

$$Z_o = 10H^2 - j\frac{30}{H}\left(\frac{\omega - 2}{1 + \dfrac{2\ln 2}{\omega - 2}}\right)$$

or, as a magnitude,

$$|Z_o| = \sqrt{(10H^2)^2 + \left[\frac{30}{H}\left(\frac{\omega - 2}{1 + \dfrac{2\ln 2}{\omega - 2}}\right)\right]^2}$$

where

$$\omega = 2\ln\left(\frac{2h}{a}\right)$$

and h is the physical height of the rod and a is its radius. βh is defined as $2\pi h/\lambda$. As βh approaches 1, the antenna impedance tends to become resonant and at values of $\beta h = 1.5, 2.5, 3, 3.5, 4, 4.5, \ldots$ the monopole is resonant. Curves for the reactance and resistance of the dipole, for $\beta h = 0.5$–7, are provided in Fig. 2.24 and 2.25 from Ref. 6. The reactance and resistance of a monopole are one-half of the values for a dipole. The magnitude of the impedance of the monopole is

$$Z_o = \sqrt{Z_{oim}^2 + Z_{ore}^2}$$

where

Z_{oim} = reactance of the antenna

Z_{ore} = resistance of the antenna

The maximum open-circuit gain of the resonant monopole is 1.68; for the short monopole it is 1.5. By using Eq. (2.36b) to obtain the reflection coefficient due to the antenna-to-load mismatch, the realized gain G_{re} may be obtained. From Eq. (2.48) and using G_{re}, the value of A_{max} may be determined. Using A_{max} with the wave and radiation resistance in Eq. (2.49) gives us the voltage developed across the load, from which the load current may be calculated. The average current flow in the rod of the monopole is then equal to one-half the load current for the short monopole and 0.64 times the load current for the resonant monopole.

Consider an example of the calculations of antenna factor for a small tunable rod antenna at a frequency of 550 MHz. The AF of the antenna is

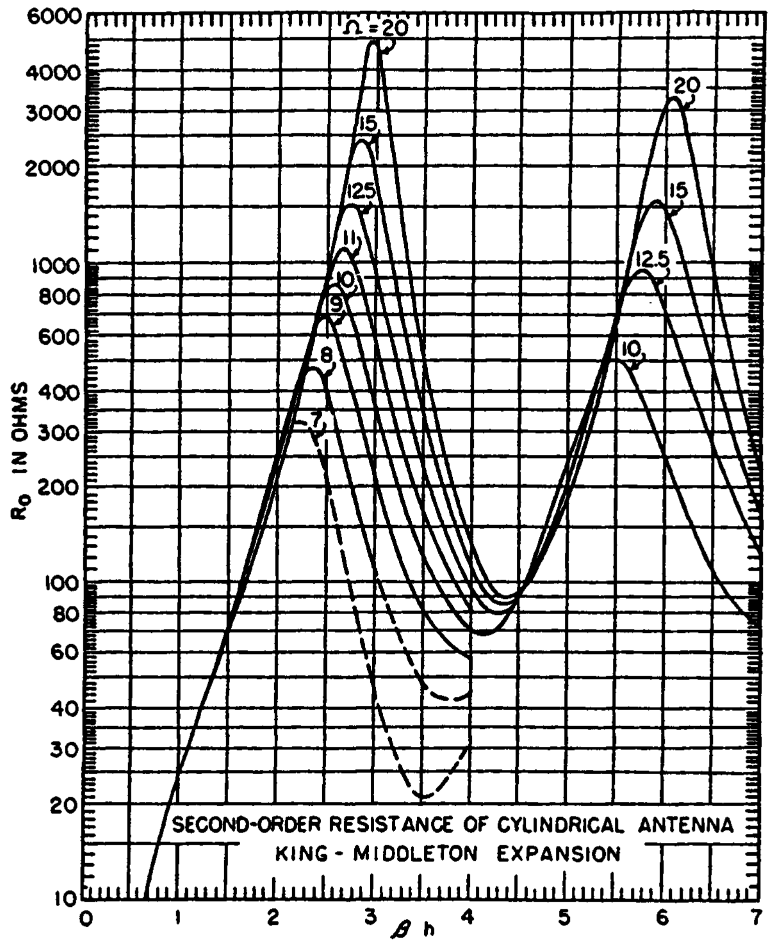

Figure 2.24 Input reactance of a dipole (monopole is half the dipole value). (From Ref. 6.)

$$\frac{E}{V} = \frac{1}{h_{\text{eff}}} = \frac{1}{\lambda/2\pi}$$

Therefore the AF at 550 MHz is 1/(0.545/12.56) = 23 = 27 dB.

The antenna factor of a tunable monopole over the 300–800-MHz frequency range is plotted in Figure 2.26. The calibration was made in a shielded room using the two-antenna test method. At 550 MHz, the measured AF = 26.2 dB, whereas the predicted AF is 27 dB. At other frequencies, a difference of ± 3 dB between predicted and measured AF is apparent. The measured antenna factor and gain for a 1-m rod antenna, calibrated at 1-m distance from a second identical antenna, over a 10 kHz to 30 MHz frequency range are shown in Figures 2.27 and 2.28. Consider the antenna factor at 20 MHz, where the antenna impedance is approximately 500 Ω and the wave impedance at a distance of 1 m is approximately 900 Ω. The reflection coefficient, from Eq. (2.36b) is

$$K = \frac{1 - 500/50}{1 + 500/50} = \frac{-9}{11} = -0.818$$

The loss is $1 - (-0.818)^2 = 0.33$, so the gain is $1.5 \times 0.33 = 0.496$.

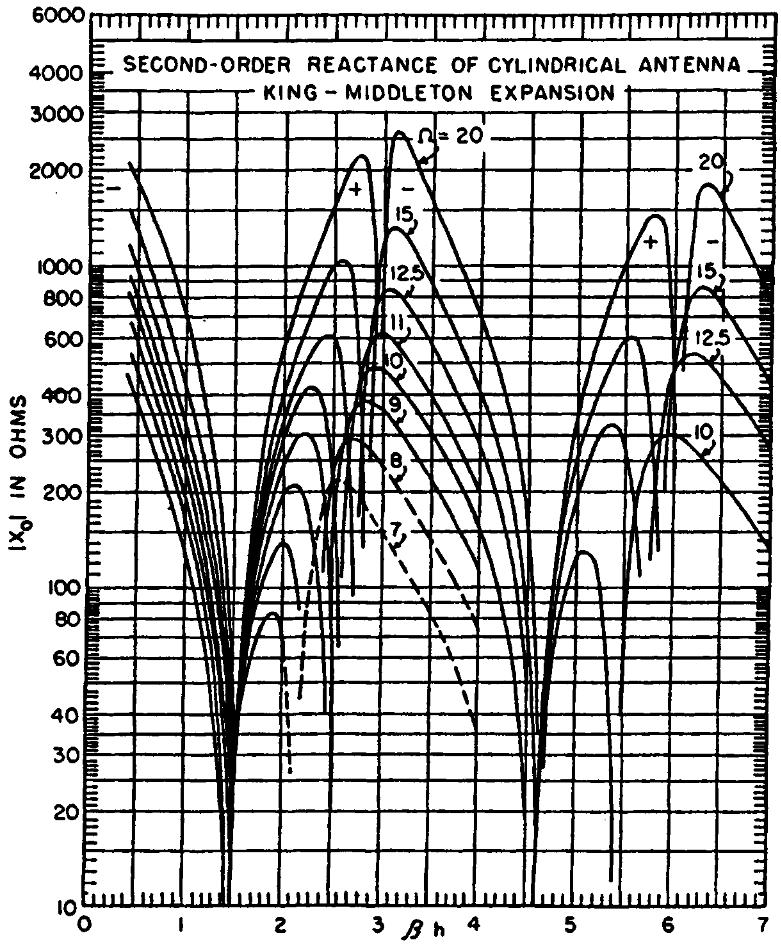

Figure 2.25 Input resistance of a dipole (monopole is half the dipole value). (From Ref. 6.)

The radiation resistance of the 1-m monopole at 20 MHz is

$$\text{radiation resistance} = \frac{197(2/15)^2}{2} = 1.75\ \Omega$$

The effective height, from Eq. (2.47), is

$$\text{effective height} = \frac{\sqrt{8.88 \times 1.75/99}}{2} = 0.065$$

The first term in Eq. (2.47) appears in the equation for the AF and is, in our example, omitted from both equations. Therefore, from Eqs. (2.45) and (2.49) the AF (E/V) is $1/0.065 = 15.4$. From the plot of the measured antenna factor for a monopole, Figure 2.27, the AF at 20 MHz is 6.2 and the difference between measured and predicted AF is 8 dB. The measurements were made in a shielded room, and thus some difference between measured and predicted AF is to be expected due to the proximity of the rod of the antenna to the conductive ceiling and due to reflections. An additional potential source of error is that the measurements

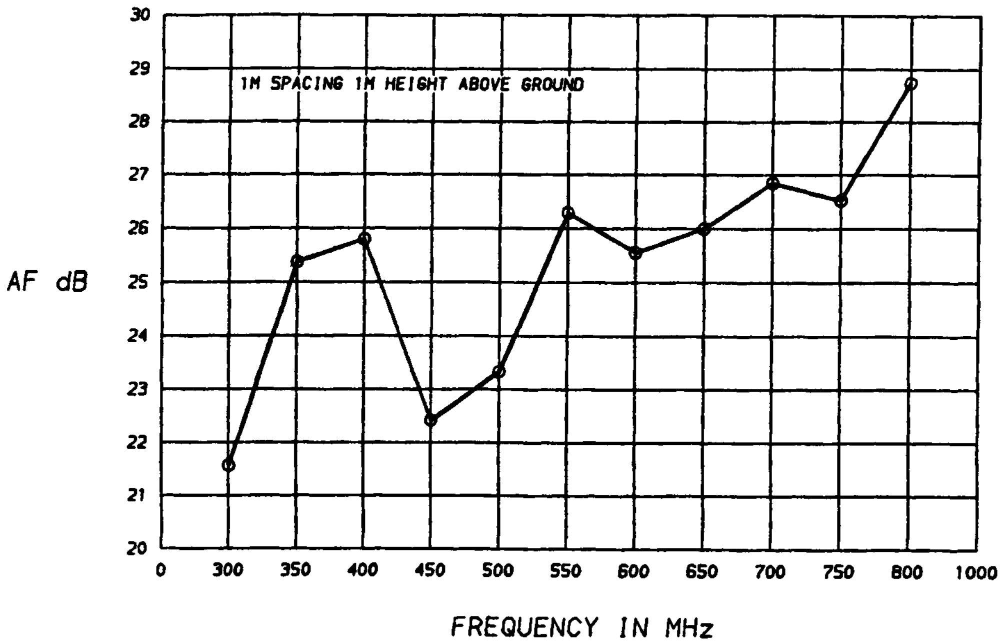

Figure 2.26 Measured AF, in decibels, of a resonant monopole.

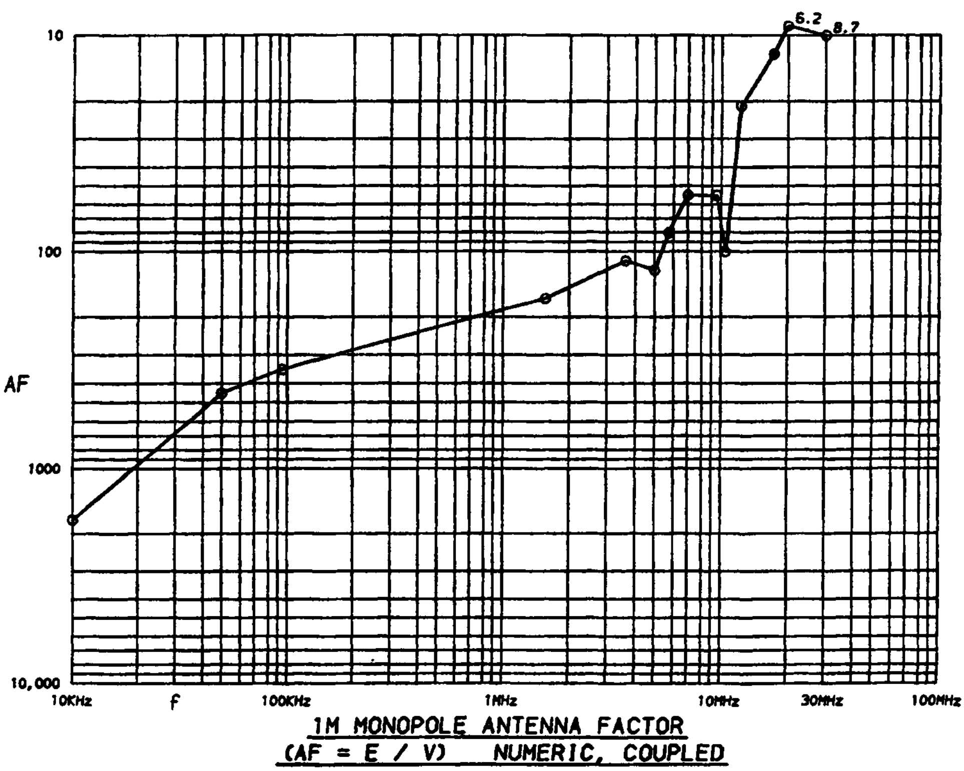

Figure 2.27 Measured AF, numeric, for a 1-m monopole.

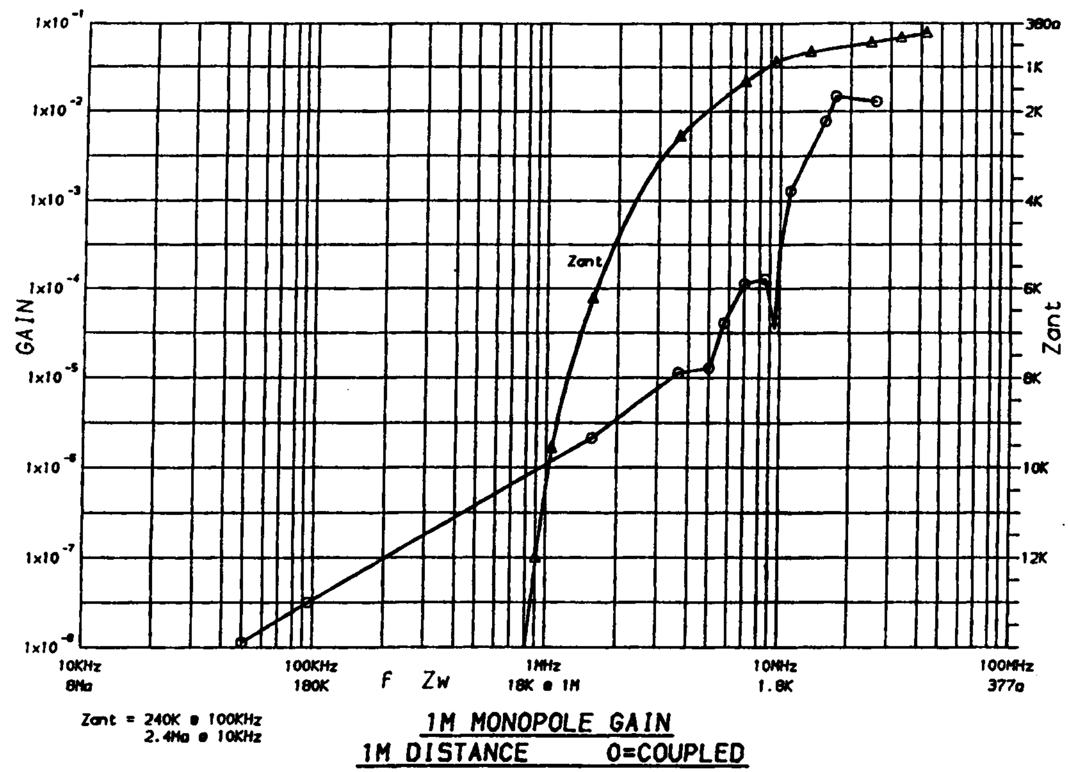

Figure 2.28 Measured gain of a 1-m monopole.

were made in the near field, where curvature of the radiated E field will reduce the coupling to the receiving antenna.

The monopole in our example is neither an effective E field measurement nor a communication antenna, due to the large mismatch between the antenna input impedance and the 50-Ω load impedance. The inclusion of a high-input impedance, e.g., FET, buffer, or amplifier positioned under the counterpoise and connected directly at the base of the antenna, will greatly increase the sensitivity of the antenna at low frequency. The two monopoles, located 1 m apart during measurements, are in the near field, and thus the quasi-static radial field terminates on the counterpoises of both antennas as well as on the rod of the receiving antenna.

The quasi-static coupling is via the very low (≅0.5 pF) mutual capacitance of the antennas. The mutual reactance of the antennas is therefore very high at the frequencies of interest, and minimal voltage is developed across the 50-Ω receiving antenna load impedance, due to the radial E field. When the antenna termination impedance is high, the quasi-static field will develop an appreciable voltage across the load and change the AF calibration of the antenna.

When the monopole model is used to predict the current flow on a shielded cable connected to a shielded enclosure, the load impedance is equal to the termination impedance of the shielded cable, typically the sum of the shield-to-backshell, male-to-female connector, and connector-to-bulkhead interface impedances. This termination impedance may then be used in the equations for the short nonresonant antenna to find the load voltage, from which the load current may be found. The current flowing on the shield of the cable is then one-half of the load current.

Where the shielded cable length is resonant, the characteristics of a resonant short-circuit monopole may be used to find the shield current. First the receiving properties of the resonant antenna into a matched load is used to find the load current. The average matched antenna current is then 0.64 times the load current, and the current flow on the short-circuit resonant antenna (cable shield) is twice that for the matched antenna.

A simple circuit comprising a MOSFET input stage followed by a single transistor gain stage, with an input impedance of 100 kΩ, was built and powered by a 9-V battery. The increase in gain at 10 kHz and 100 kHz was measured at 83 dB and 78 dB, respectively. The noise floor increased by 55 dB at 10 kHz and 42 dB at 100 kHz, with a resultant increase in signal-to-noise ratio of 28–36 dB.

2.6 SIMPLE, EASILY CONSTRUCTED E AND H FIELD ANTENNAS

This section presents the design of a number of easily constructed antennas for the measurement of either E or H fields. When considering time-varying waves, E and H fields are always present and either may be measured. One important aspect of the design of a measurement antenna is that the antenna differentiates between E and H fields. Thus an antenna designed to measure H fields should reject the influence of the E field component of the electromagnetic wave.

The advantage of physically small antennas is that the localized E and H fields in close proximity to sources such as enclosures, apertures, and cables may be readily measured. The larger dipole and commercial broadband antennas also have a place in measuring the composite field from all sources. Measurement techniques using both types of antenna are discussed in Chapter 9.

2.6.1 Shielded Loop Antenna

The simple loop antenna connected to a shielded cable is unbalanced with respect to the shield of the cable and therefore responds to both E and H fields. One technique used to reduce the influence of the E field is to shield the loop.

The schematic of a shielded loop antenna is shown in Figure 2.29a, with a photograph

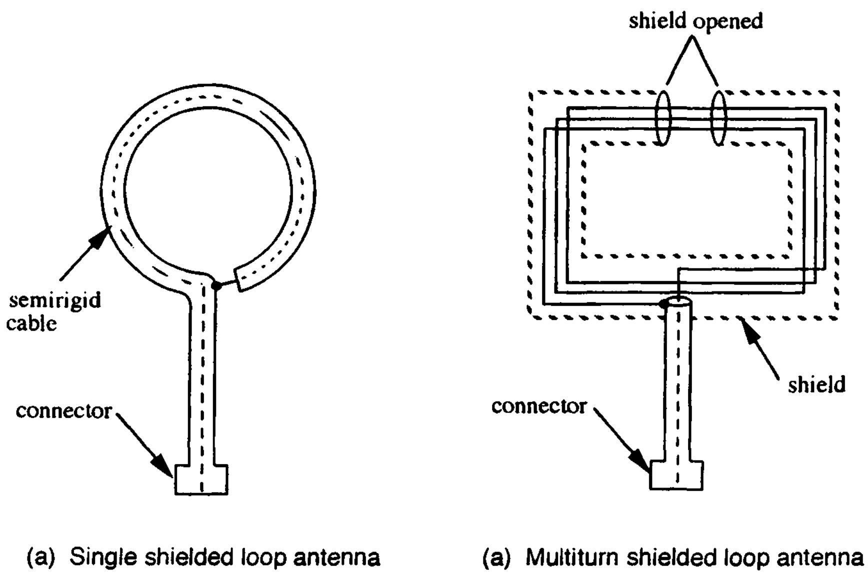

Figure 2.29 Shielded loop antennas.

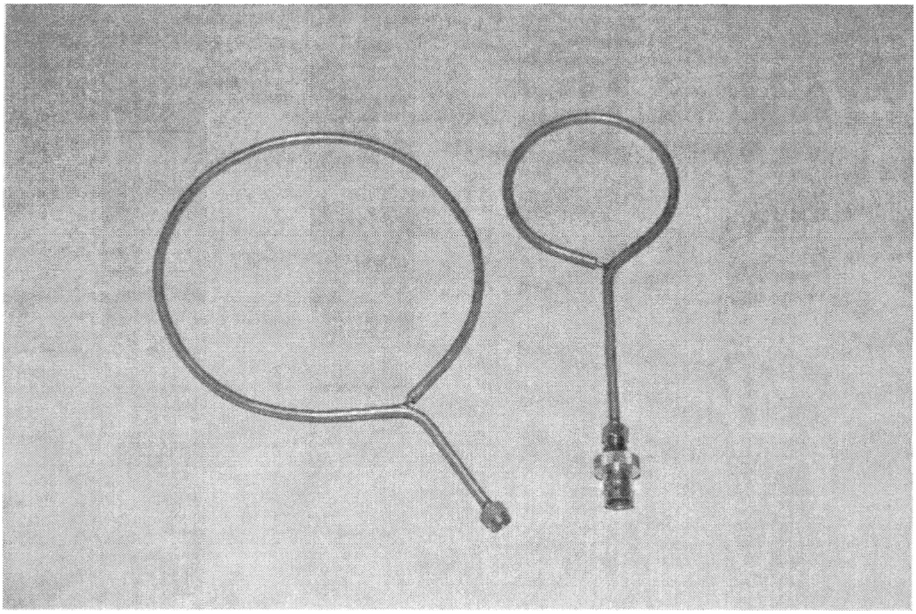

Figure 2.30 Photo of shielded loop antennas.

of an 11-cm and a 6-cm antenna given in Figure 2.30. The antenna is constructed from semirigid cable that is available in a number of different diameters. The shielded loop antenna becomes resonant above a frequency determined by the inductance of the loop and the capacitance between the center conductor and the outer sheath. The lower the capacitance of the semirigid cable used in the manufacture of the loop, the higher the useful frequency response. Calibration curves for the 6-cm loop, which has a useful upper frequency of greater than 15 MHz, and the 11-cm loop, which has a useful upper frequency of 10 MHz, are shown in Figures 2.31 and 2.32. The receiving properties of the 6-cm and 11-cm loops are close to the predicted properties when terminated in a 50-Ω load, and so calibration is necessary only to determine the upper frequency limit or where maximum accuracy is required. A word of warning: The measurement technique, unless it is carefully controlled, may result in less accuracy than the use of the predicted characteristics alone. Where the sensitivity of the single loop at low frequency is not sufficient, a multiturn shielded loop may be constructed. The multiturn antenna may be shielded by wrapping the turns with a conductive tape. The tape is connected to the outer surface of the coaxial connector as shown in Figure 2.29b. The shield must contain a gap around the circumference of the loop in order to avoid the shielding of the loop against magnetic fields.

The multiturn loop exhibits a lower resonance frequency than a single turn, due to its higher inductance and intrawinding capacitance.

2.6.2 Balanced Loop Antenna

A second extremely useful H field antenna is a 6-cm balanced loop antenna, the schematic of which is shown in Figure 2.33. The balanced loop antenna contains a balun constructed from a two-hole ferrite bead. Baluns are used in a number of balanced antennas, both E and H field types, to match the antenna to the unbalanced coaxial cable. The cable and associated equipment are unbalanced because the shield of the cable and the outer shell of the coaxial cable are

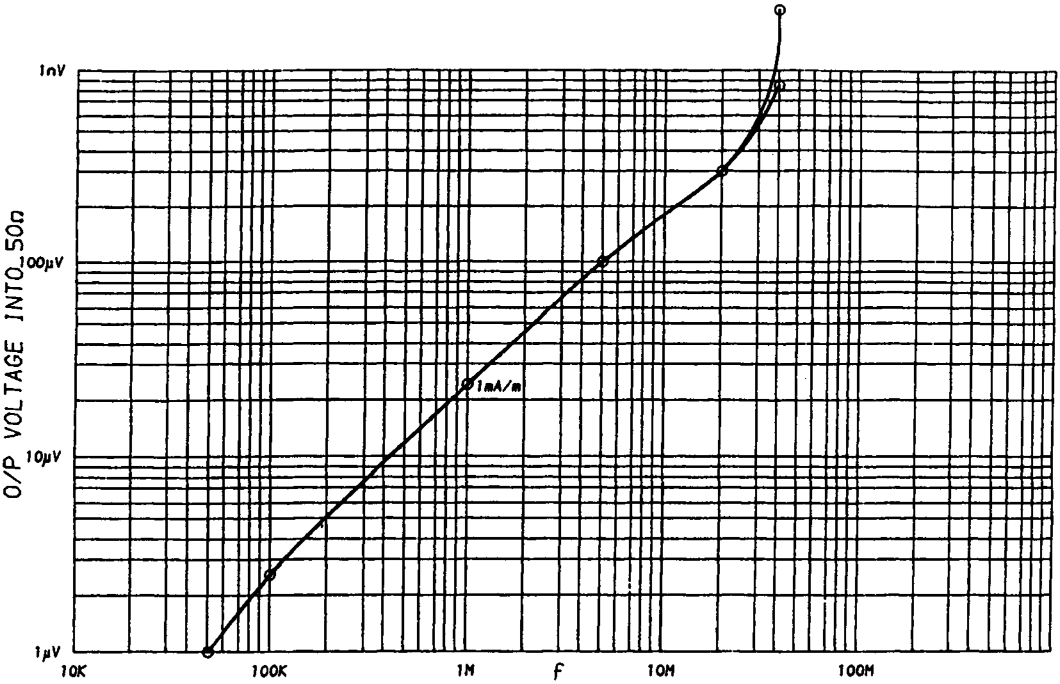

Figure 2.31 Calibration curves for a 6-cm shielded loop antenna, upper limit 15 MHz.

connected to ground, via the enclosure that is connected to safety ground on the majority of equipment. In the balanced loop antenna, the E field induces equal and opposite voltages into the primary (loop side) of the balun, and thus, ideally, zero E-field-induced voltage appears across the secondary of the balun.

In practice, some capacitive imbalance exists both in the intrawinding capacitance of the balun and between the loop and the metal enclosure housing the balun. Any imbalance results in an incomplete cancellation of the E-field-induced voltage. In addition, the capacitance, with the inductance of the loop, determines the resonant frequencies of the loop. In a carefully designed antenna, the connections from the loop to the primary of the balun should have a characteristic impedance of 200 Ω. The secondary connection to the coaxial connector mounted on the enclosure should have an impedance of 50 Ω. The center tap of the primary of the balun is connected to ground via the enclosure. Ideally this connection should be made via a low impedance, such as a short length of wide PCB material. The calibration curve of a balanced loop antenna is shown in Figure 2.34. This antenna was not constructed with maximum care in the layout, and some of the kinks in the calibration curve may be the result. Nevertheless, the measured characteristics are within 4 dB of the predicted. The sensitivity of this simple antenna is approximately 46 dB above that of the Hewlett-Packard HP 11940A near-field magnetic field probe, which costs almost 100 times as much. It should be added that the HP probe, due to its very narrow tip, is invaluable for locating emissions from printed circuit board tracks and integrated circuits. In addition, the HP probe covers the wider, 30–1000-MHz frequency range, compared to the 20–200 MHz for the simple loop. One potential source of measurement error in the small loop antennas is produced by E-field-induced current flow on the shield of the coaxial interconnection cable. The shield current induces a voltage in the center conductor of the cable, which adds to the signal from the antenna.

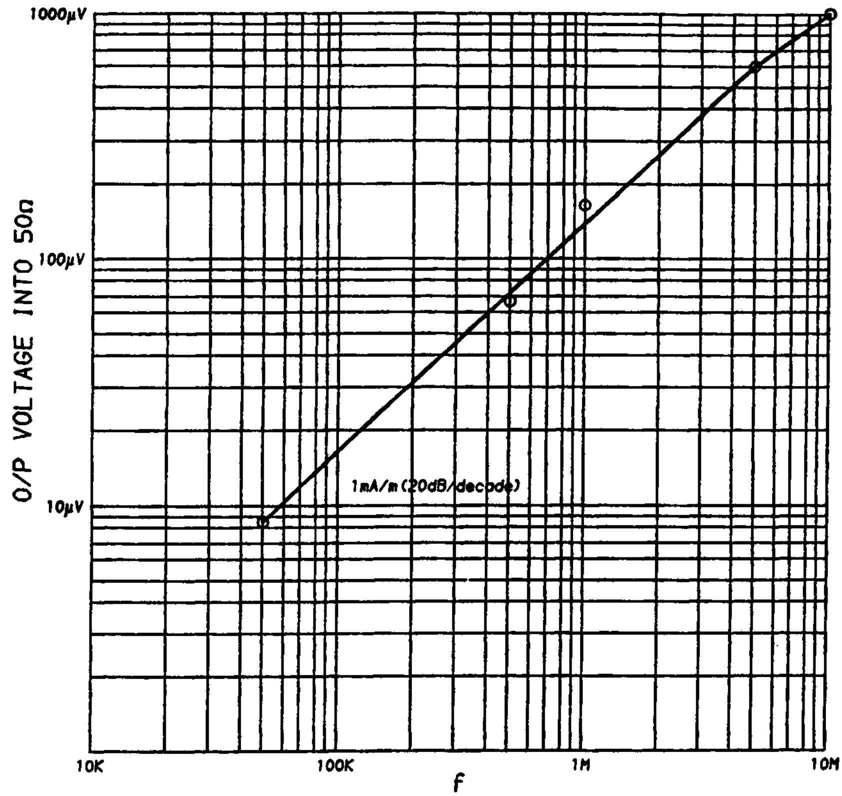

Figure 2.32 Calibration curve for an 11-cm shielded loop antenna, upper limit 10 MHz.

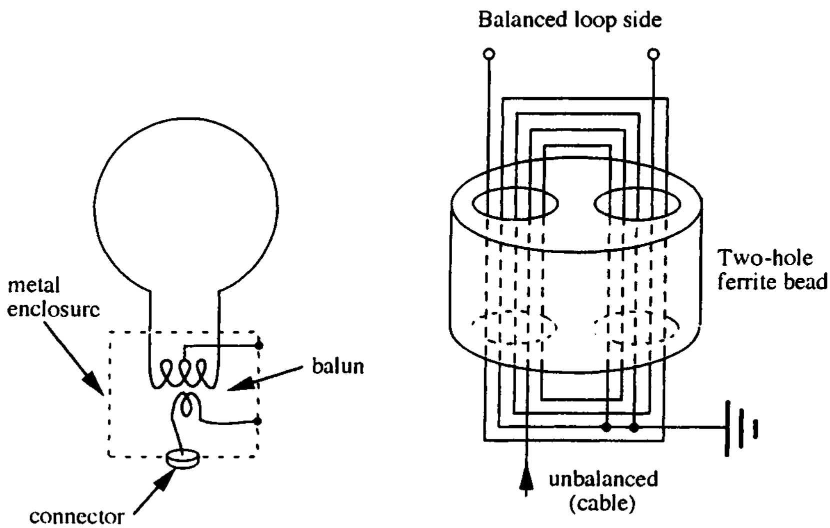

Figure 2.33 Schematic of a balanced loop antenna and construction details of the balun.

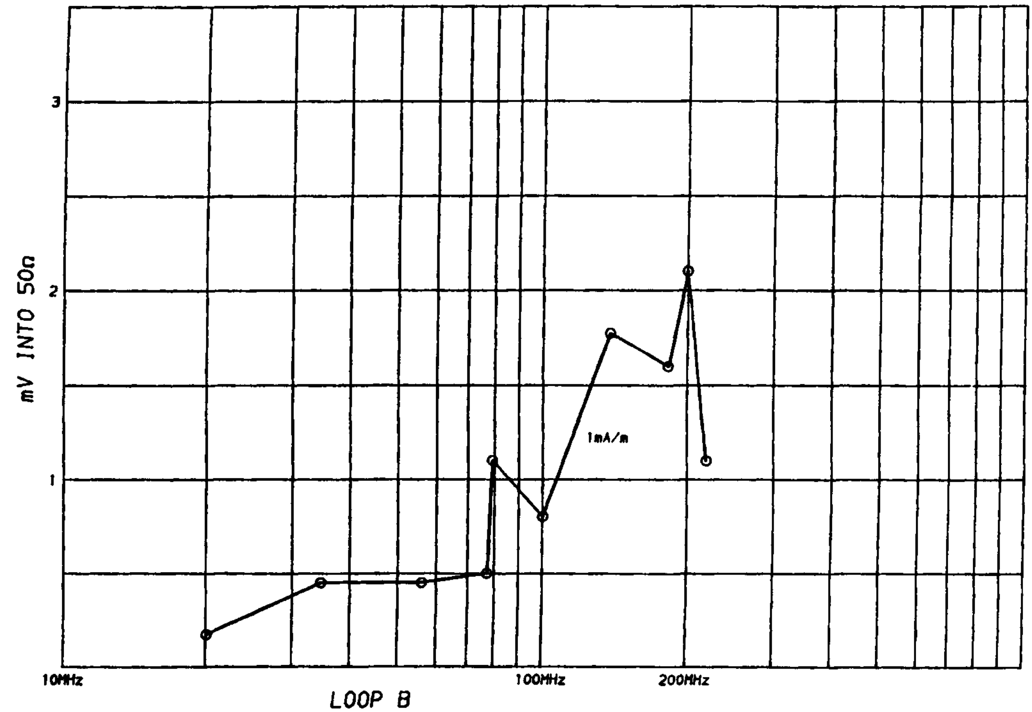

Figure 2.34 Calibration curve of a balanced loop antenna.

In other chapters we will see that H field measurements are typically more reliable in locations where reflections cause measurement errors. We shall see that measurement errors may be reduced by computing the magnitude of the E field, at some distance from the measuring point, from the magnitude of the H field at the point. The calibration of the example H field antennas are in mV/mA/m. However, an alternative is to use the H field antenna factor, defined as H(A/m)/V.

2.6.3 E Field Bow Tie Antenna

The balun incorporated into the balanced loop antenna may also be used to match a broadband E field "bow tie" antenna to the coaxial cable. The schematic diagrams of a bow tie antenna for the 20–250-MHz and 200–600-MHz frequency ranges are shown in Figure 2.35. The impedances of the 20–250-MHz and 200–600-MHz antennas with 2/1 voltage- and 4/1 impedance-ratio baluns are shown in Figure 2.36 and are derived from Ref. 7.

The bow tie is useful in measuring both the radiation from an EUT in close proximity as well as the level of the E field in a radiated susceptibility (immunity) test. The small bow tie, with 10-cm-long elements, although designed for 200–600 MHz, has been calibrated from 25 MHz to 1000 MHz. At low frequency, the antenna factor is high, in common with all physically small antennas, and great care has to be exercised, in both calibration and use, to ensure that the coupling to the feed cable is not higher than that to the antenna. To reduce the coupling, use a double-braid shielded cable with many ferrite baluns mounted on the cable; and when monitoring susceptibility test levels, orient the cable vertically for horizontally polarized fields and antenna, and orient it horizontally for vertically polarized fields and antenna. Figure 2.37

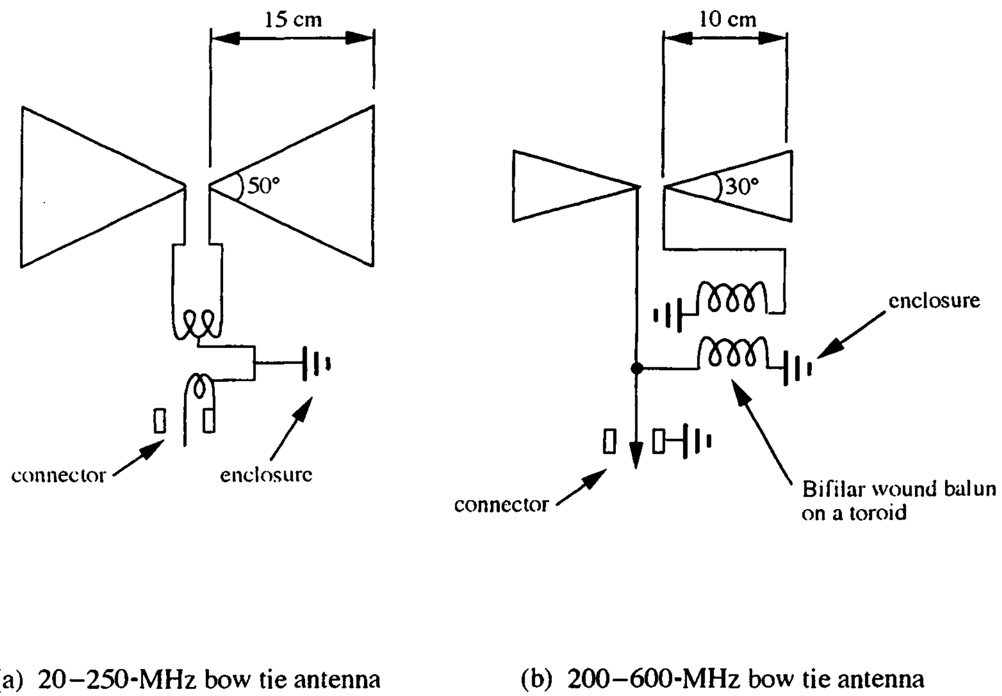

Figure 2.35 Bow tie antennas.

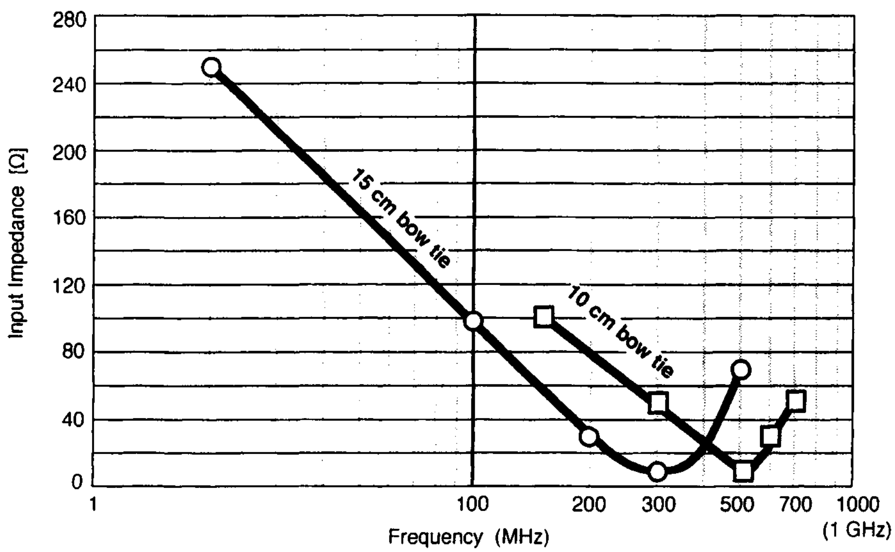

Figure 2.36 Input impedance calibration curves for the 15-cm and 10-cm bow tie antennas. (From Ref. 7.)

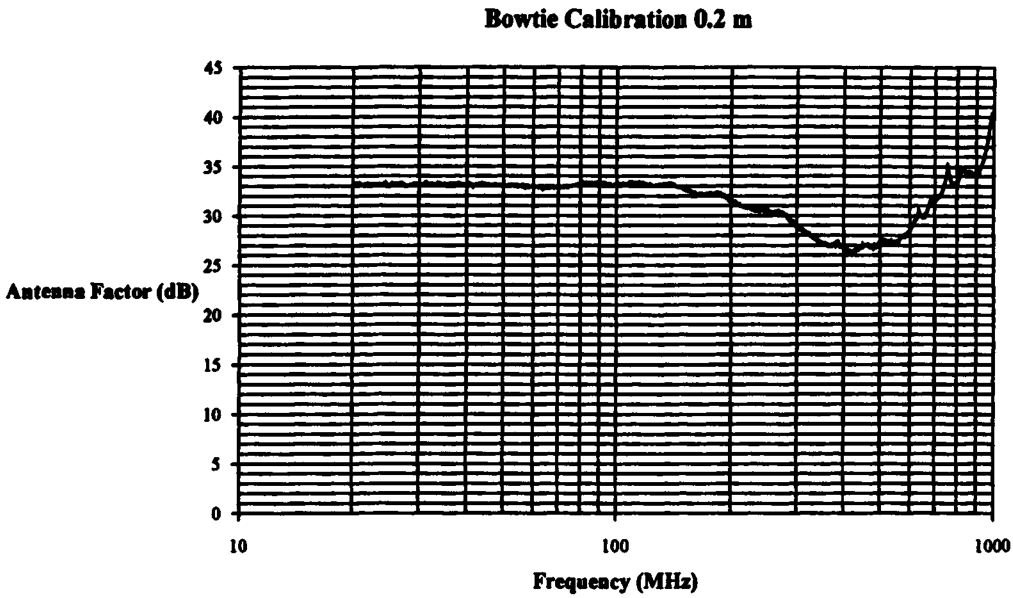

Figure 2.37 Bow tie antenna factor at 0.2 m.

shows the 10-cm bow tie calibration at a distance of 0.2 m; Figure 2.38 shows it at a distance of 1 m, with the antenna horizontally polarized, and 1 m above a ground plane. The antenna was constructed on a rectangular-shaped PCB with the two bow tie elements etched out of the PCB material, with a BNC connector mounted in the center of the antenna and with the balun located close to the connector as shown in Figure 2.38.

2.6.4 Monopole Antennas

The 1-m and the tunable resonant monopole antennas described in Sections 2.5.5 and 2.5.6 cover the 14-kHz–30-MHz and 300–800-MHz frequency ranges, respectively, and the simple construction of these antennas is illustrated in Figure 2.39. The monopoles with ground plane do not require a balun to match the antenna to the cable, which is one reason for their widespread use.

2.6.5 Tuned Resonant Dipole Antennas

The schematic of the dipole with a typical balun used over the 40–300-MHz frequency range is shown in Figure 2.40. The calibration curve for this antenna in a shielded room and the theoretical open field test site calibration is shown in Figure 2.22. The construction details of a similar balun, showing how the coaxial cable is wound on formers and attached to the connector, are presented in Figure 2.41. The construction details are reproduced by courtesy of the Electrometrics Corporation.

2.6.6 Helical Spiral Antennas

Helical spiral antennas, which cover the 800-MHz–18-GHz frequency range, as shown in Figure 2.42, are relatively simple to construct. The larger antenna is 26.5 cm long and 12 cm in diameter

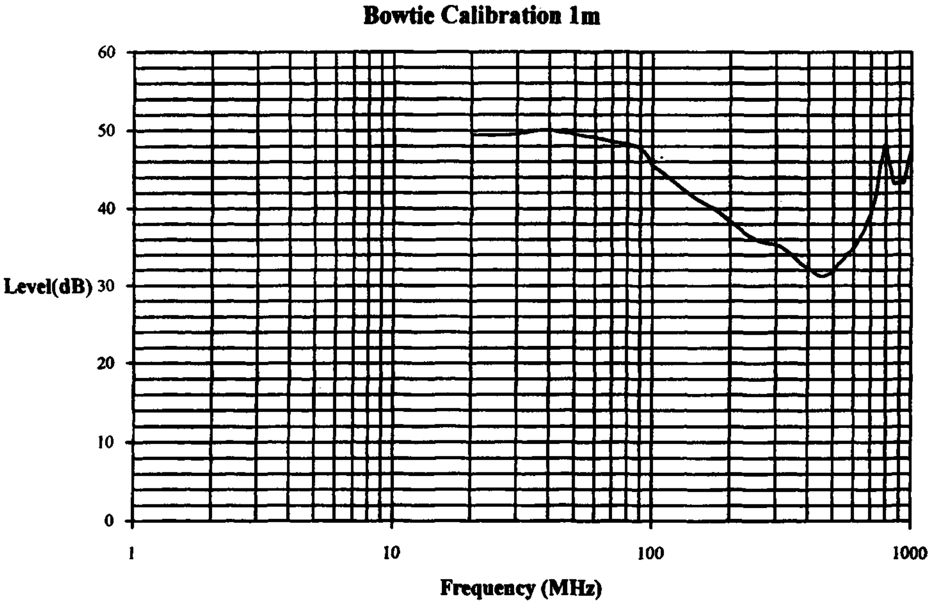

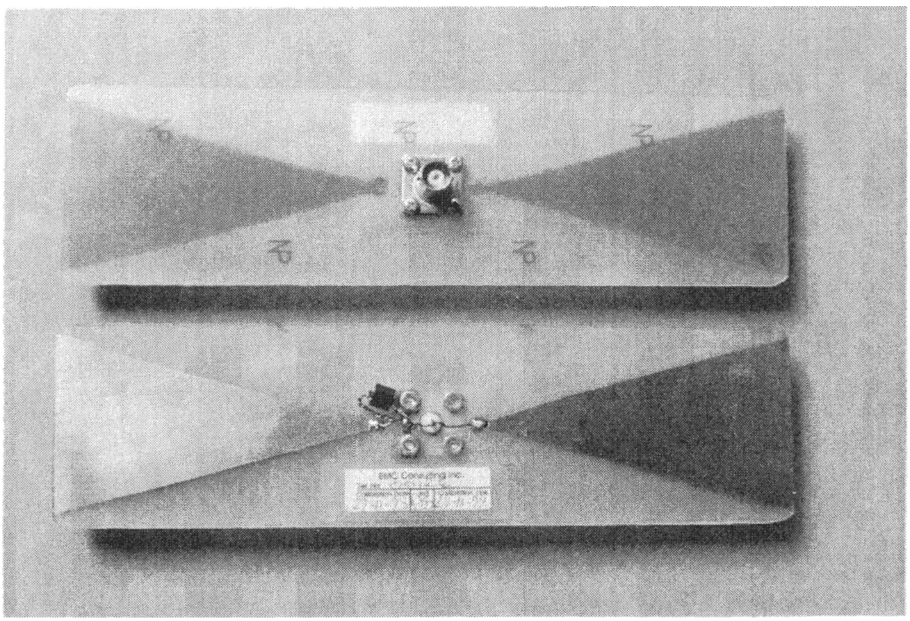

Figure 2.38 Bow tie antenna factor at 1 m and 1 m above a ground plane.

at the base, tapering to 10 cm at the top. The larger antenna is wound as a helical log periodic, with the angle between the base of the antenna and the spiral at approximately 20°. The distances between the windings of the spiral are not critical, and in the larger antenna, shown in Figure 2.42, the ratio of the distance between the windings of the lower spiral and the distance between the windings of the next higher spiral is approximately 1.25. The important criterion is that the